NASA-CR-65139

R-6215

STATISTICAL ANALYSIS FOR 23
THERMOMETRIC SENSORS TEST PROGRAM

FINAL REPORT

ROCKETDYNE
A DIVISION OF NORTH AMERICAN AVIATION, INC.

FACILITY FORM 602

N65-32673 (ACCESSION NUMBER)

(THRU) 1

132 (PAGES)

(CODE) 33

(NASA CR OR TMX OR AD NUMBER)

(CATEGORY)

ROCKETDYNE
A DIVISION OF NORTH AMERICAN AVIATION, INC.
6633 CANOGA AVENUE CANOGA PARK, CALIFORNIA

R-6215

23

STATISTICAL ANALYSIS FOR THERMOMETRIC SENSORS TEST PROGRAM

FINAL REPORT

Contract NAS 9-2599

PREPARED BY

S. R. Webb, H. Kaspar, and J. M. Zimmerman
Mathematics and Statistics Group
Research Department

APPROVED BY

J. E. Witherspoon
J. E. Witherspoon
Chief
Physics, Mathematics and Measurements
Research Department

NO. OF PAGES 129 and iii

REVISIONS

DATE 25 June 1965

DATE	REV. BY	PAGES AFFECTED	REMARKS

FORM R18-G REV. 4-64

FOREWORD

This report was prepared by personnel of the Mathematics and Statistics Group of the Rocketdyne Research Department under Contract NAS 9-2599, "Thermometric Sensors Test Program," which was conducted for NASA/MSC, Houston, Texas. The project manager was Earl W. Hicks, Sr.

The tests conducted at Rocketdyne were performed by R. A. Ayvazian under the direction of H. L. Burge, both of the Propulsion Applications Group, Research Department.

CONTENTS

Summary 1

Conclusions and Recommendations 2

Description of the Data Analyzed 6

Char and Ablation Sensors 11

  Method of Analysis of the Individual Response Curves 11

  Analysis of the Individual Char Data Curves 15

  Analysis of the Individual Ablation Data Curves 20

  Comparisons between the Individual Curves 22

Temperature Sensors 33

References 38

Appendix A - Use of the Rocketdyne Stepwise Regression Computer Program 39

  Input to Rocketdyne Stepwise Regression Computer Program 39

  Output from Rocketdyne Stepwise Regression Computer Program 51

Appendix B - Church Analysis of Radioactive Char Sensors 62

Appendix C - Data and Curve Fits 67

SUMMARY

An extensive statistical evaluation of heat shield thermometric sensor data is presented. The analysis includes tests conducted at the MSC (Houston), Plasmadyne (Los Angeles), and Rocketdyne (Los Angeles). Three types of sensors are evaluated: temperature, ablation, and char. The use of temperature sensors to measure ablation and char was also evaluated. Data from a heat flux sensor were also to have been included in the analysis but could not be made available in time for the present study.

The statistical models used to describe the time responses of the three sensor types are described and the results of the regression analysis presented and discussed. Attempts to determine the effects of several operational variables (such as heat flux and shear) on the sensor responses are reviewed and general conclusions are drawn. Differences between the various facilities at which the testing was conducted are discussed.

Results of a special statistical study of tests of a radioactive char sensor are described. Finally a brief description of how the Rocketdyne Stepwise Regression Computer Program can be used to conduct similar analyses in the future and recommendations for carrying out such analyses are presented. The final appendix is a series of plots containing the data used in the analyses and the best curves fit to the data.

CONCLUSIONS AND RECOMMENDATIONS

A summary of the major conclusions reached on the basis of the statistical evaluation of the thermometric sensor data is given in this section. Recommendations for additional analyses are included. Further details are provided in the body of the report.

1. Reasonably satisfactory mathematical models were found to describe and predict the response of individual temperature, ablation, and char sensors under specified operational conditions.

2. The quantitative aspects of the sensor responses exhibited, in general, considerable variation from test to test even under similar operating conditions. It appears that this lack of repeatability is attributable at least as much to variations in the heat-shield material specimens in which the sensors were embedded as to the sensors themselves.

3. The variability mentioned in 2 prohibited drawing many useful conclusions concerning the effects of such operational variables as heat flux and shear on the sensor responses. In this sense it was not possible to obtain a complete, coupled calibration of all sensors, which is the ultimate goal of the current effort.

4. Despite the exhibited variability, however, it was possible to detect substantial differences among the sensor behavior at the three facilities at which tests were conducted, particularly in regard to the effects of heat flux on the sensor responses.

5. The char and ablation sensors provided more repeatable and apparently more accurate descriptions of these phenomena than were obtained by the use of thermocouples. The use of thermocouples to determine indirectly the extent of charring and ablation is, however, feasible assuming certain systematic errors which were observed can be corrected for.

6. It was possible to distinguish the quality of the two types of char sensors that were evaluated in terms of both their bias and the smoothness of the curve fits of their output versus time.

7. The problem of variations in radioactivity through ablation or char sensor plugs is at the moment not critical in the sense that the effect of such variations are masked by other factors (e.g., heterogeneity in ablative material specimens).

8. Because of the experimental design used to obtain the data (see [1]), it was possible to ascertain that the atmosphere in which the tests were conducted (reducing or oxidizing) had a moderate effect on

the ablation responses, but no effect on char responses.

9. The responses of the radioactive char sensors can be predicted with reasonably small variance, and a comparison of these with the independent measurements of the total char at the conclusion of each test indicated substantial agreement.

10. It should be pointed out that tests of a similar nature to those described here have been carried out more recently at North American Aviation's Space and Information Systems Division. These latter tests benefited from the preliminary knowledge gained from the data studied in this report, and consequently somewhat more satisfactory results were obtained in the statistical analysis of the S+ID data (see [2]). It is anticipated, therefore, that significant improvement can be expected in the quality of the results from future tests of the type treated in this report.

11. Considerable trouble and expense were endured in the testing described in this report in order to obtain data under a wide variety of environmental conditions which could only be made available by testing at several different facilities. Since variability of ablative heat-shield material masked the environmental effects, it seems advisable to limit future testing to one facility until variability is reduced or explained by hitherto unconsidered variables.

12. Despite the inherent variability in the data mentioned above, it would be profitable to expand the statistical analyses already conducted in several basic directions:

(a) Attempt to find even better models to describe the sensor time responses.

(b) Attempt to uncover more effects of operational and facility variables that may exist and obtain quantitative descriptions of these effects.

(c) Attempt to cross calibrate the thermocouples when used as ablation and char sensors with direct ablation and char devices in a comprehensive and quantitative manner.

DESCRIPTION OF THE DATA ANALYZED

The data analyzed in this report were obtained at a number of different times, from three types of sensors, and at three types of testing facilities. In the course of this program several different schemes have been used to identify the tests. In order to eliminate any confusion, the relationship between these identification schemes is reviewed in Table I. The first column, "Test Number," gives numerals by which the tests will be identified throughout this report. Any other previous designation for a test is given in the second column. The location column indicating where the test was conducted contains the entry "MSC-1" for tests run with that oxygen-acetylene torch at the NASA Manned Spacecraft Center; the entry "PLAS." for tests run with the Plasmadyne arc jet facility; the entry "ROCK." for tests run with a Rocketdyne oxygen-hydrogen rocket engine; and the entry "MSC-2" for tests run on that oxygen-acetylene torch at the Manned Spacecraft Center. The sensors which have been analyzed include temperature gradient (ΔT) sensors of three types (I, IA, and II), radioactive char sensors, and radioactive ablation sensors.

Test conditions for each of the tests in Table I are given in Table II. Included are the levels of the independent variables: heat flux, enthalpy, shear, source gas, chamber pressure, mixture ratio,

Table I

Identification of the Tests

Test Number	Other Designation	Test Data	Location	Sensor Type	Sensor Designation	Char Data	Ablation Data	Temperature Data
1-26		3/16/64	MSC-1	ΔT-II	B	Yes	Yes	No
1-27		3/18/64	MSC-1	ΔT-II	A	Yes	Yes	No
1-28		3/21/64	MSC-1	ΔT-II		Yes	Yes	No
1-29		8/3/64	MSC-1	ΔT-II		Yes	Yes	No
1-30		8/20/64	MSC-1	ΔT-II		Yes	Yes	No
1-31		8/27/64	MSC-1	ΔT-IA		Yes	Yes	No
1-34	1	5/14/64	MSC-2	Char	8	Yes	No	No
1-35	2	5/14/64	MSC-2	Char	1	Yes	No	No
1-36	4	5/14/64	MSC-2	Char	9	Yes	No	No
1-37	7	5/14/64	MSC-2	Char	3-A	Yes	No	No
1-38	18	5/28/64	MSC-2	Char	2	Yes	No	No
1-39	8	5/28/64	MSC-2	Char	10	Yes	No	No
1-40	22	5/28/64	MSC-2	Char	6	Yes	No	No
1-41	9	5/28/64	MSC-2	Char	5	Yes	No	No
1-42	10-4A	5/28/64	MSC-2	Char	4-A	Yes	No	No
1-43	10-4	5/28/64	MSC-2	Char	4	Yes	No	No
1-44	12-7A	5/28/64	MSC-2	Char	7-A	Yes	No	No
1-45	12-7	5/28/64	MSC-2	Char	7	Yes	No	No
1-50	H-2	9/3/64	MSC-2	Ablation		No	Yes	No
1-51	H-4	9/3/64	MSC-2	Ablation		No	Yes	No
1-52	H-6	9/3/64	MSC-2	Ablation		No	Yes	No
2-14	Test 8-10	5/5/64	Plas.	ΔT-I	#3-1	Yes	Yes	No
2-15	Test 8-6	5/5/64	Plas.	ΔT-I	#2-8	Yes	No	No
2-21	P 11	7/22/64	Plas.	ΔT-IA	AF	Yes	Yes	Yes
2-22	P 9	7/22/64	Plas.	ΔT-1A	AK	Yes	Yes	Yes
2-23	P 6	7/22/64	Plas.	ΔT-IA	AH	Yes	Yes	Yes
2-24	P 3	7/22/64	Plas.	ΔT-IA	AA	Yes	Yes	Yes
2-25	P 12	7/22/64	Plas.	ΔT-II	P	Yes	Yes	Yes
2-26	P 4	7/22/64	Plas.	ΔT-II	O	Yes	Yes	Yes
2-27	P 2	7/22/64	Plas.	ΔT-II	O	Yes	Yes	Yes
2-28	P 10	7/22/64	Plas.	ΔT-II	G	Yes	Yes	Yes
3-13	3, Block 2	7/23/64	Rock.	ΔT-IA	AE	Yes	Yes	No
3-14	Block 3	7/23/64	Rock.	ΔT-IA	AC	Yes	Yes	No
3-15	Block 4	7/23/64	Rock.	ΔT-IA	AG or AD	Yes	Yes	No
3-16	2, Block 1	7/23/64	Rock.	ΔT-II	M	Yes	Yes	No
3-17	3, Block 2	7/23/64	Rock.	ΔT-II	L	Yes	Yes	No
3-18	Block 3	7/23/64	Rock.	ΔT-II	N	Yes	Yes	No
3-19	Block 4	7/23/64	Rock.	ΔT-II	R	Yes	Yes	No
3-20	Block 5	7/23/64	Rock.	ΔT-II	E	Yes	Yes	No

Table II

Test Conditions

Test Number	Heat Flux BTU/ft^{2}sec	Enthalpy BTU/lbx10^3	Model Distance Inches	Shear psf	Test Duration sec
1-26	200	.93	2	.2	214
1-27	200	.93	2	.2	230
1-28	200	.93	2	.2	255
1-29	250	1.21	3	.3	310
1-20	250	1.21	3	.3	384
1-31	250	1.21	3	.3	346
1-34	85	1.40	3	<.1	240
1-35	110	1.40	3	<.1	180
1-36	190	1.36	1	<.1	120
1-37	210	1.20	1	<.1	120
1-38	85	1.40	3	<.1	120
1-39	85	1.40	3	<.1	240
1-40	110	1.40	3	<.1	120
1-41	110	1.40	3	<.1	180
1-42	190	1.36	1	<.1	90
1-43	190	1.36	1	<.1	120
1-44	210	1.20	1	<.1	60
1-45	210	1.20	1	<.1	90
1-50	250	1.21	3	.3	50
1-51	250	1.21	3	.3	72
1-52	250	1.21	3	.3	48
			Source Gas		
2-14	50	5.08	N_2	<.5	870
2-15	570	25.0	N_2	<.5	409
2-21	293	21.2	N_2	<.5	155
2-22	146	10.2	Air	<.5	170
2-23	565	25.2	Air	<.5	170
2-24	261	13.1	N_2	<.5	180
2-25	294	20.8	Air	<.5	170
2-26	568	24.9	N_2	<.5	170
2-27	260	13.1	Air	<.5	170
2-28	145	10.1	N_2	<.5	170

Table II (continued)

Test Number	Heat Flux BTU/ft^2sec	Chamber Pressure psig	Mixture Ratio	Shear psf	Test Duration sec	Incidence Angle
3-13	300	275	9.7	3.75	31	$12\frac{1}{2}^{\circ}$
3-14	98	165	25.9	1.1	40	$12\frac{1}{2}^{\circ}$
3-15	150	230	21.0	1.75	76	0°
3-16	60	160	12.6	.75	89	0°
3-17	300	275	9.7	3.75	31	$12\frac{1}{2}^{\circ}$
3-18	98	165	25.9	1.1	40	$12\frac{1}{2}^{\circ}$
3-19	150	230	21.0	1.75	76	0°
3-20	400	310	11.3	5.00	36	$12\frac{1}{2}^{\circ}$

insertion distance, incidence angle, and test duration.

The char data analyzed are of two varieties. These are (a) data obtained directly from radioactive char sensors, and (b) char data inferred from tests of temperature sensors. The radioactive char sensor is a plug of radioactive material which is subject to pyrolysis at the temperature of char formation in the heat-shield material. Because the heat conduction of char is higher than that of virgin heat-shield material, the output of a thermocouple exhibits a change of slope when the char front moves through the location of the thermocouple. The time at which a thermocouple registers this change of slope is therefore the time at which the char front is at the known depth of the thermocouple. Char data were analyzed from all the char and temperature gradient sensor tests given in Table I.

Similarly, ablation data have been obtained directly from radioactive ablation sensors and indirectly from temperature sensors. The latter are obtained by noting the time at which a thermocouple is exposed, hence the time the surface has receded to the known depth of the thermocouple, which can be determined exactly from motion pictures taken during the tests. Table I indicates from which tests ablation data were analyzed in this manner.

In the following sections the methods used to perform the statistical analyses are presented. In subsequent sections the results are discussed, compared, and interpreted.

CHAR AND ABLATION SENSORS

METHOD OF ANALYSIS OF THE INDIVIDUAL RESPONSE CURVES

The same type of analysis was used for all char and ablation data. It was found that for each individual test the data could be represented by a curve of the following form:

$$Y = -A + Bt + AD^{t} \quad , \qquad (1)$$

where for char sensors Y is the distance (in inches) as a function of time t, from the original surface to the char-virgin interface, and for ablation sensors is the amount of material ablated as a function of time. Note that when $t = 0$, $Y = 0$. The constant D is to be taken between zero and one, so that as t (in seconds) gets larger, D^{t} approaches zero. Thus, the curves asymptotically approach the straight line $A + Bt$. The magnitude of D determines how rapid is the approach. If A is negative (that is, the intercept $-A$ is positive) the curve (1) is convex, which is the typical shape of the char curves.

For A positive (-A negative) the curve is concave which is the typical shape of ablation curves. Examples of curves of the form (1) for various values of the parameters A, B, and D are given in Appendix C.

The model (1) is a linear function in the parameters A and B. Because of this linearity, if the value of the parameter D were known, the values of the parameters A and B could be determined easily by means of ordinary least-squares procedures. In this case the necessary computations may be conducted using the Rocketdyne Stepwise Regression Program, previously supplied to NASA, or by any other least-squares computer program. While computer codes do exist for obtaining least-squares estimates of nonlinear parameters such as D, they are both expensive and difficult to use. For the present data a simple and more convenient iterative technique was employed. Linear regressions using various assumed values for D were run and that one selected for which the residual standard deviation (standard error of estimate) was smallest. Since the residual standard deviation is proportional to the sum of squared deviations about the fitted line, the estimate of D obtained in this way is in fact the least-squares estimate of those tried. By successively refining the grid of trial values for D, it is easy to obtain the least-squares estimate accurate to several decimal places.

One additional device was used with the model (1) in order to ensure numerical stability. If a model contains two identical terms, as for example $Y = A + Bx + Cx$, it is obviously impossible to obtain unique estimates of the parameters B and C. This indeterminacy may be explained mathematically as being due to the singularity of the matrix of the normal equations used in calculating least-squares estimates. If, on the other hand, a model contains terms which are almost the same, the matrix of the normal equations is nearly singular. Many of the numerical steps performed in solving a system of equations whose matrix is nearly singular involve finding a small difference of very large numbers. Because the number of bits assigned to each number is a fixed number, many significant figures may be lost in performing such a subtraction. Often the results obtained by a computer in this case are meaningless.

To see how this problem arises in the present case we note first that the model (1) may be rewritten in the following form:

$$Y = Bt + A(D^t-1) \quad .$$

The factor associated with A may be expanded in a Taylor series in t about $t = 0$ as follows:

$$D^t-1 = \Sigma_{n=0}^{\infty} (t\log D)^n/n! - 1 = \Sigma_{n=1}^{\infty} (t\log D)^n/n! \quad .$$

Suppose D is nearly 1 as is the case here. Then all the terms in the summation are practically negligible except the first, so that (1) becomes

$$Y = Bt + A(t\log D + \text{negligible terms}) \quad ,$$

from which it is obvious that the equation contains two nearly identical terms. This difficulty was resolved as follows. Model (1) may be rewritten in the form

$$Y = (B + A\log D)t + A(D^t - t\log D - 1) \quad , \tag{2}$$

from which estimates of A and $B' = B + A\log D$ may be obtained by least squares. Use of the new variable $(D^t - t\log D - 1)$, having the linear part subtracted out, gives increased numerical stability. From the estimated coefficients A and B' it is easy to recover B. Note that, while B is the slope of the asymptote line, B' is the slope of the curve for $t = 0$.

For those sets of data for which the least-squares estimate of D was very large (near 1) or very small (near 0), the data were also fitted using the simplified model

$$Y = Bt \quad . \tag{3}$$

Under the provision that Y must be zero at time zero, it is easy to see that (3) is the limiting model for (1) as D approaches both 0 and 1.

ANALYSIS OF THE INDIVIDUAL CHAR DATA CURVES

Data from the temperature and char sensors given in Table I were analyzed using the model (2). Char data (Y) were in inches, and time was in seconds × 10 (so that $t = 1$ is 10 seconds). Results of the individual least-squares analyses are given in Table III. In each case the fit is given which gives the smallest value of σ, the residual standard deviation. Note that for several of the tests the best fit is obtained using model (3) in which D does not appear. The values of D are accurate to two decimal places, except in a few cases where three places are given. The value $D = .999$ is the largest value of this parameter used; it is possible that the fits could be improved, but only very slightly, by obtaining additional decimal places. The value of B was calculated by the formula $B = B' - A \log D$. As can be seen in Table III, B generally had a small positive value. For large values of D, however, there is a tendency for B to have negative values and A to have very large negative values (so that the intercept-A is large and positive). For two of the tests A has a positive value and the slope B of the asymptote is very large. These two apparently "pathological" cases are presented in Figures 1 and 2. Note that in both figures the actual data, represented by the solid part of the curve, are very close to a straight line.

Table III

Best Char Data Curve Fits

Test Number	Number of Observations	D	A	B	B'	σ
1-26	6	.78	-.158	.037	.0766	.0069
1-27	4	.999	-4340	< 0	.0833	.0122
1-28	7	.35	-.111	.038	.1549	.0247
1-29	7	.35	-.129	.031	.1662	.0630
1-30	8	.71	-.258	.026	.1144	.0187
1-31	9	.71	-.259	.027	.1161	.0183
1-34	24	.999	-713	< 0	.0252	.0143
1-35	18	.75	-.220	.020	.0830	.0100
1-36	12	.11	-.133	.027	.3200	.0140
1-37	12	.999	-3180	< 0	.0550	.0129
1-38	12	.88	-.139	.018	.0359	.0045
1-39	24	.91	-.396	.008	.0450	.0064
1-40	12	.71	-.228	.025	.1033	.0063
1-41	18	.71	-.177	.034	.0949	.0051
1-42	9	.96	-4.62	< 0	.0861	.0077
1-43	12	.98	-6.81	< 0	.0639	.0079
1-44	6	.997	-1370	< 0	.1030	.0074
1-45	9	.91	-1.47	< 0	.0958	.0074
2-14	7	.999	-201	< 0	.0167	.0372
2-15	11	.999	.587	> 1	.0390	.1494
2-21	7	.92	-1.21	< 0	.0836	.0129
2-22	7	.20	-.062	.031	.1318	.0122
2-23	8	.78	-.319	.031	.1108	.0189
2-24	7	.78	-.308	.018	.0947	.0161
2-25	7	.67	-.187	.029	.1033	.0106
2-26	7	.50	-.165	.035	.1490	.0220
2-27	7	.67	-.162	.034	.0988	.0141
2-28	5		0	.0312		.0119
3-13	5		0	.0988		.0203
3-14	6	.005	-.023	.0869	.2114	.0182
3-15	7		0	.0785		.0170
3-16	7		0	.0532		.0250
3-17	5		0	.1030		.0088
3-18	4	.005	-.0163	.0634	.1498	.0138
3-19	7		0	.0851		.0164
3-20	7	.999	68200	> 1	.1176	.0289

Figure 1

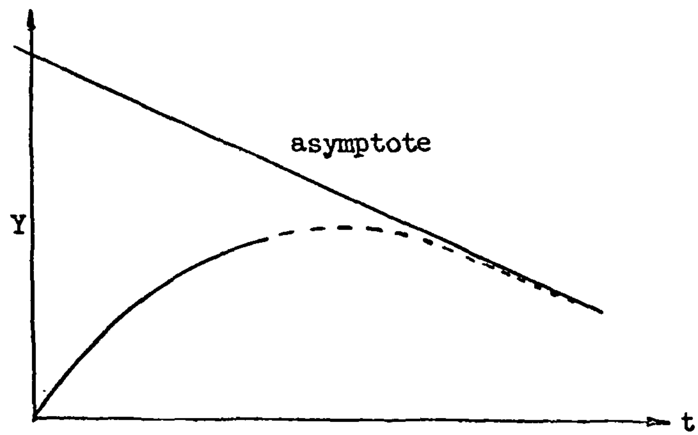

Interpretation of negative slopes (B < 0)
for large D

Figure 2

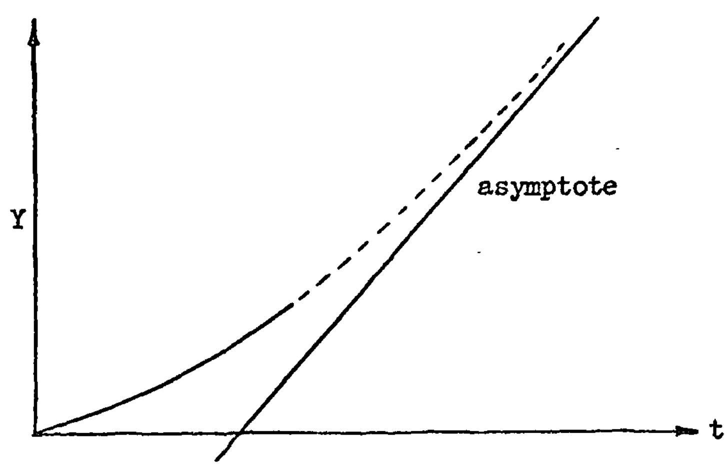

Interpretation of negative intercept (-A < 0)
and large slope B for large D

Apart from tests 2-15 and 3-20 mentioned above (Figure 2), it should be noted that the values of A are consistently negative, so that the curves are concave. The two exceptions have comparatively large standard errors and are therefore suspect. They could be due to a single bad datum for each curve.

Several other observations may be made from Table III. Tests 1-34 through 1-45 are the radioactive char sensor tests (see Table I). The first four used a slightly different type of sensor from the last eight. Examination of the residual standard deviations (σ) indicates the superiority of the second design. It should be noted, however, that the standard deviations of the curves obtained from the temperature sensors (tests 2-14 through 3-20) are only a little larger. This indicates that the use of the inflection points of temperature curves is a consistent indication of char.

The last eight tests, 3-13 through 3-20, were performed at Rocketdyne. Apart from the large slopes, which will be discussed in the next section, these tests are distinguished by the fact that they are all eight very nearly linear (i.e., model (3)), without any appreciable transient effect.

For completeness of this discussion several slight inconsistencies should be noted in the way in which σ was calculated. The values of

σ given in Table III were read directly from computer printouts. Since D was fixed for each individual regression, the tests in which D appeared (model (2)) were treated as having two degrees of freedom removed for effects. Technically, three degrees of freedom should be taken out since D is also estimated. Similarly, the regressions using the linear model (3) had one degree of freedom removed, but two is the correct number since A is estimated to be zero. Thus from this viewpoint the values of σ given in Table III should each be slightly increased. Since in almost all cases the numerical effect of this change is small (and in the same direction) this question need not concern us further.

Another minor inconsistency is that for the char sensor tests the initial observation was at $t = 1$ (10 seconds). The "observation" at $t = 0$, however, was included in the remaining analyses. Actually this is not a data point with the same statistical features as the others, and strictly speaking should not appear in the analysis. It was included primarily so that it would appear on the plots of the individual curves. Its effect can be removed by adjusting (i.e., increasing) σ^2 to correspond to one fewer datum.

In addition to these analyses an independent analysis of the radioactive char sensor data was conducted using a different approach. This is described in a subsequent section entitled "Church Analysis."

ANALYSIS OF THE INDIVIDUAL ABLATION DATA CURVES

The ablation data from the ablation sensors and temperature sensors were analyzed in exactly the same way as were the char data. The response was in inches and time in seconds X 10. The better of models (2) or (3) was used to fit the individual curves as in the analysis of the char data; the results are given in Table IV. In all cases but one (test 1-50) the value of A was found to be non-negative, indicating a negative intercept. Since the slope values B were positive in all cases, this means that as expected the ablation curves are concave. In the single case where A was negative the slope was very small and the ablation curve was convex. D is given correct to the nearest .05.

As can be seen from Table IV in the case of the ablation data, the optimum D values were with only two exceptions (tests 1-28 and 2-27) either near zero or unity. In particular on more than half the tests the optimum D value was .95. Because of this all the data were also fit by means of the linear model (3), but in general the nonlinear curves gave smaller values of σ even though D was either near zero or unity. In five cases the linear curves gave smaller values of σ than the model (2), these values being consistent with those obtained from the nonlinear curve-fits on the other runs.

Table IV

Ablation Data Curve Fits

Test Number	Number of Observations	D	A	B	B'	σ
1-26	5	.95	2.491862	.1211	-.006682	.0256
1-27	5	.95	.752920	.0428	.004193	.0221
1-28	7	.70	.150222	.0356	-.017861	.0205
1-29	6	.95	.513154	.0316	.005281	.0140
1-30	8		0	.026146		.1640
1-31	7	.95	.910107	.0264	-.002028	.0386
1-50	14	.10	-.013278	.0011	.031638	.0014
1-51	18		0	.012140		.0068
1-52	13	.95	.516751	.0379	.011347	.0030
2-14	3		0	.0007		.0175
2-21	4	.95	1.629604	.0768	-.006826	.0006
2-22	6	.95	1.028631	.0465	-.006252	.0250
2-23	5	.05	.141065	.0434	-.379211	.0191
2-24	5	.95	.944992	.0450	-.003424	.0179
2-25	5	.95	1.499955	.0756	-.001368	.0192
2-26	5	.95	.278557	.0239	.009594	.0077
2-27	5	.75	.204055	.0442	-.014510	.0142
2-28	3		0	.0049		.0076
3-13	4	.95	19.084652	.9627	-.016163	.0144
3-14	5		0	.069284		.0157
3-15	7	.05	.111082	.0900	-.242795	.0285
3-16	7	.10	.207216	.0753	-.401849	.0242
3-17	4	.95	25.565976	> 1	.038534	.0021
3-18	5	.95	6.404054	.3521	.023633	.0057
3-19	7	.10	.104073	.0956	-.144084	.0315
3-20	7	.95	21.134874	> 1	.112820	.0223

It can be seen from Table IV that in general larger values of A are associated with larger slopes B, which indicates a more significant transient portion in the response in those cases where more rapid ablation is observed.

It appears reasonable to conclude from Table IV that the ablation sensors (tests 1-50, 1-51, 1-52) give a more repeatable measure of the ablation than generally obtained by means of the temperature sensors. It should be emphasized, however, that the temperature sensors give useful results, their standard deviations being only a little larger in many cases.

COMPARISONS BETWEEN THE INDIVIDUAL CURVES

There is no systematic variation of the values of D, A, or B which is apparent from Tables III and IV. For example, tests 1-26, 1-27, and 1-28 were run under identical conditions, yet the values of these three parameters vary considerably over these tests. If, however, the tests for extreme values of D are excluded, the values of the remaining estimates, particularly B, exhibit much more stability. It was decided to make an analysis of the curve fits using B as the dependent variable. So that those tests with extreme values of D could be included in the analysis, a separate curve fit was performed for these tests using model (3). These curves, of course, do not fit as well as the best curves given in Tables III and IV, but their fits are adequate for the present analyis. Those char tests with newly computed values are marked with an asterisk in Table V. The remaining entries are the same (apart from rounding) as those given in Tables III and IV.

A comparison of the char slopes with heat flux shows that for a given facility, an approximate linear relationship exists between these quantities (see Figure 3). These least-square linear relationships (obtained from the Rocketdyne Stepwise Regression Program) for the four facilities are as follows:

MSC-1	$b = -.000240\,\dot{Q} + .039$	$(\sigma = .050)$
MSC-2	$b = +.000314\,\dot{Q} - .010$	$(\sigma = .037$
PLAS	$b = +.000038\,\dot{Q} + .006$	$(\sigma = .034)$
ROCK	$b = +.000328\,\dot{Q} + .036$	$(\sigma = .028)$

As can been seen from Figure 3, the slopes are all positive, with the exception of MSC-1. The standard deviation (σ) indicate that the fits are rather poor, as one would expect.

A plot of ablation slopes versus heat flux is given in Figure 4. Curve fits to these points could be made, but due to the scatter it is unlikely they would indicate anything not apparent from the plot.

Table V

Char and Ablation Slopes

Test Number	Char Slope	Ablation Slope	Heat Flux	Facility
1-26	.037	.037*	200	MSC-1
1-27	.045*	.021*	200	MSC-1
1-28	.038	.036	200	MSC-1
1-29	.031	.016*	250	MSC-1
1-30	.026	.026	250	MSC-1
1-31	.027	.020*	250	MSC-1
1-34	.019*	-	85	MSC-2
1-35	.020	-	110	MSC-2
1-36	.027	-	190	MSC-2
1-37	.040*	-	210	MSC-2
1-38	.018	-	85	MSC-2
1-39	.008	-	85	MSC-2
1-40	.025	-	110	MSC-2
1-41	.034	-	110	MSC-2
1-42	.061*	-	190	MSC-2
1-43	.052*	-	190	MSC-2
1-44	.073*	-	210	MSC-2
1-45	.059*	-	210	MSC-2
1-50	-	.005*	250	MSC-2
1-51	-	.012	250	MSC-2
1-52	-	.014*	250	MSC-2
2-14	.010*	.001	50	Plas.
2-15	.049*	-	570	Plas.
2-21	.045*	.016*	293	Plas.
2-22	.031	.009*	146	Plas.
2-23	.031	.033*	565	Plas.
2-24	.018	.011*	261	Plas.
2-25	.029	.020*	294	Plas.
2-26	.035	.014*	568	Plas.
2-27	.034	.044	260	Plas.
2-28	.031	.005	145	Plas.
3-13	.099	.049*	300	Rock.
3-14	.094*	.069	98	Rock.
3-15	.079	.068*	150	Rock.
3-16	.053	.045*	60	Rock.
3-17	.103	.049*	300	Rock.
3-18	.073*	.052*	98	Rock.
3-19	.085	.075*	150	Rock.
3-20	.213*	.186*	400	Rock.

*Values different from those given in Tables III and IV.

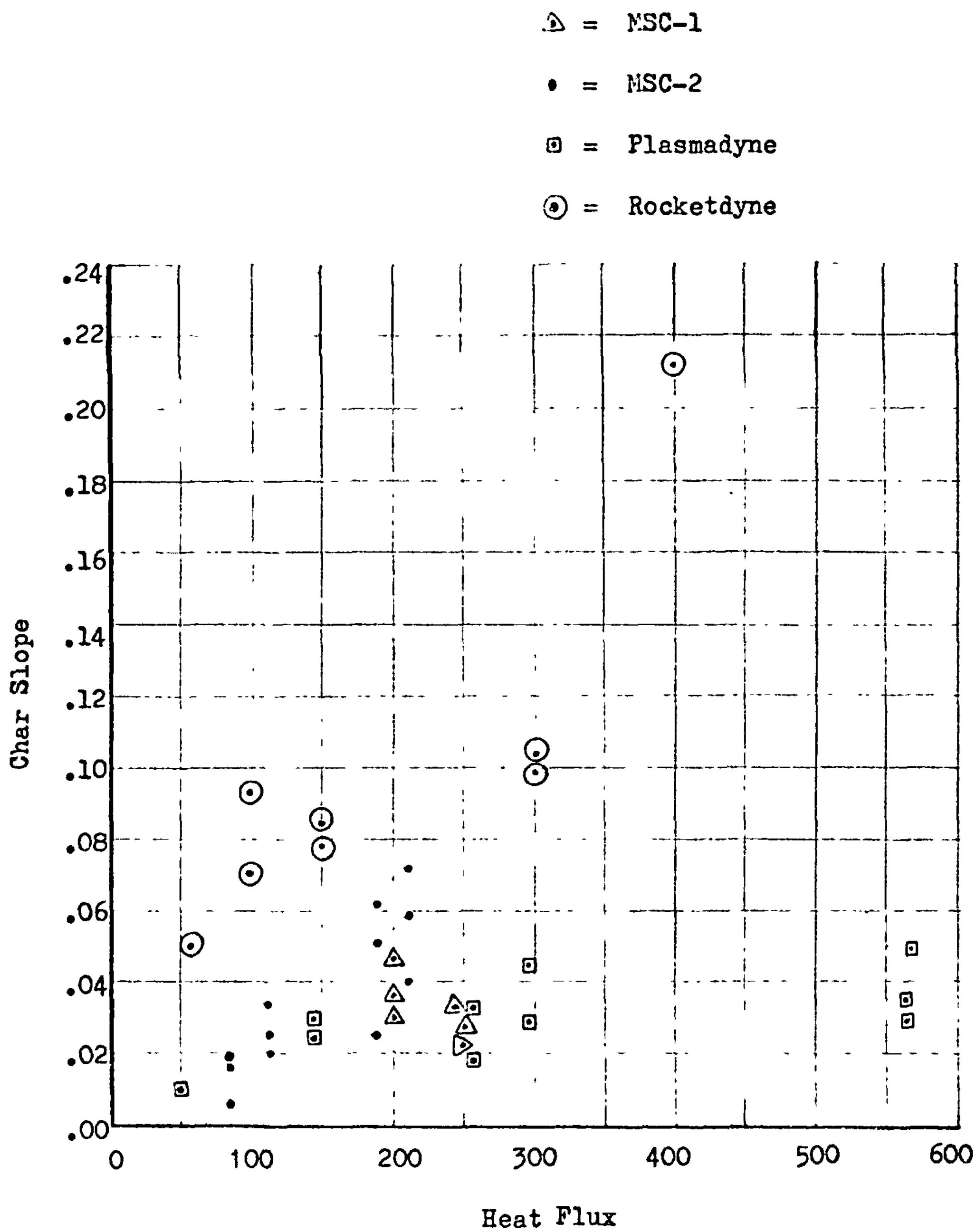

△ = MSC-1
• = MSC-2
⊡ = Plasmadyne
⊙ = Rocketdyne
Char Slope
.24
.22
.20
.18
.16
.14
.12
.10
.08
.06
.04
.02
.00
0
100
200
300
400
500
600
Heat Flux

Fig. 3

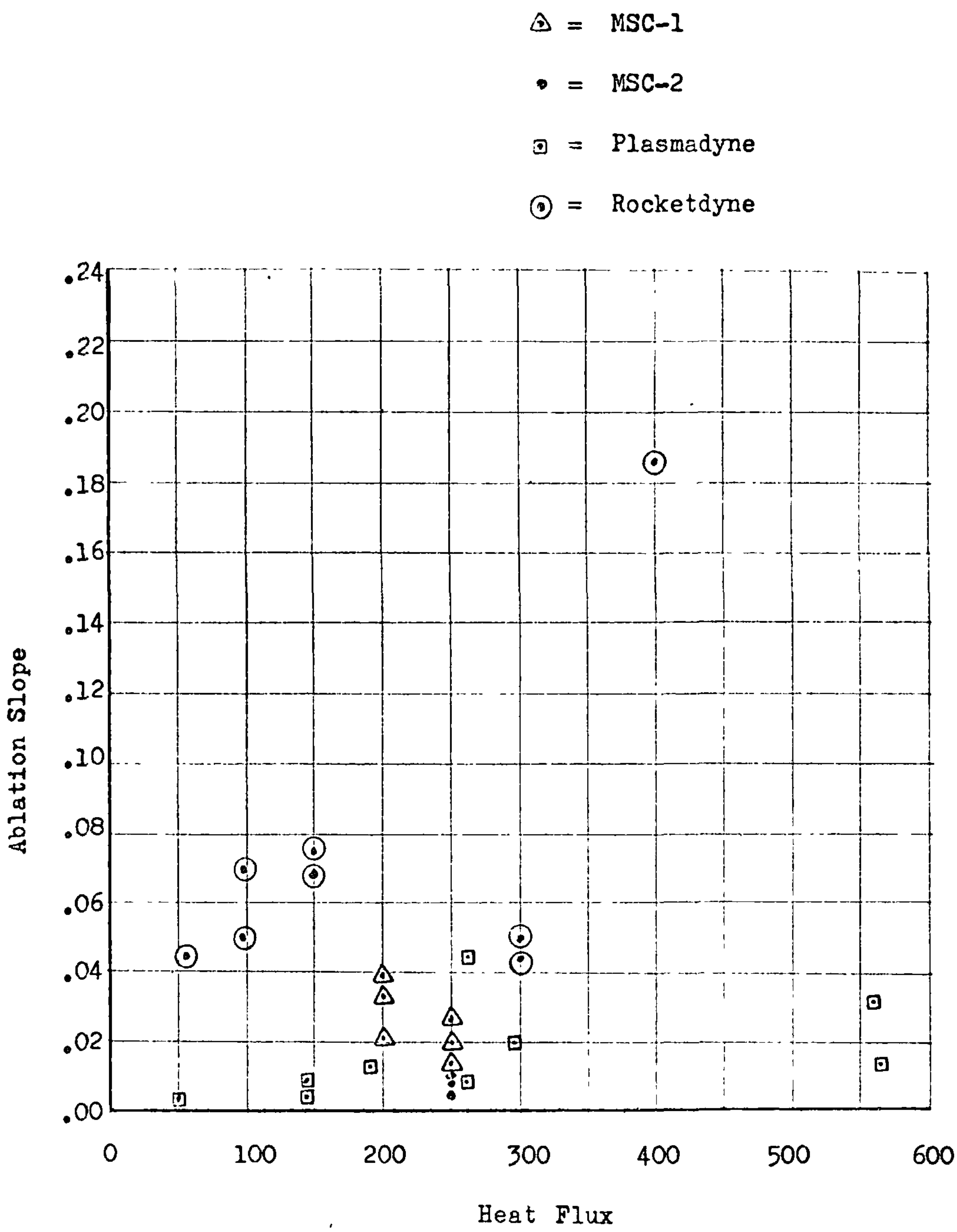
= MSC-1
= MSC-2
= Plasmadyne
= Rocketdyne
.24
.22
.20
.18
.16
.14
.12
.10
.08
.06
.04
.02
.00
Ablation Slope
0
100
200
300
400
500
600
Heat Flux

Fig. 4

From Figures 3 and 4 it is clear that there is a systematic difference in the behavior of the sensors at the four facilities. Particularly surprising is the difference between MSC-1 and MSC-2, since these are nearly identical facilities. The gross differences between the results at the facilities do not appear to be correlated with any of the testing variables (shear, enthalpy, etc.) given in Table II, except that the generally higher values of the slopes from Rocketdyne may be due to the relatively high shear condition of a rocket exhaust. It seems more likely that the facility differences are due to a very complex combination of a large number of facility variables.

One important observation may be made by an intercomparison of the char and ablation slopes obtained from the same tests. For an individual test the variation of the char slope from the average tends to be uncorrelated with the variation of the ablation slope from the average. This fact gives a strong indication that the major source of variability is the inhomogeneity of the heat-shield material. If the variability were due to lack of reproducibility of testing condition, the char and ablation deviation would be highly correlated. Since the char and ablation data are obtained from the same sensing element, a high correlation would also result if the sensors themselves were the source of error.

One deviation from this lack of coherence between the apparent errors in the char and ablation data is the Rocketdyne firing which gave a heat flux of 300 BTU/ft^2sec. There were two "tests" (ΔT sensors) incorporated into the same firing. For both sensors the char slopes are nearly identical, the ablation slopes are nearly identical, and the slopes are considerably below the best line drawn through the other data points. The reason for this discrepeancy is not at all clear. The mixture ratio of 9.7 for this firing was the lowest of the five firings (see Table II), so the unexpectedly low slopes could be due to the fact that the exhaust gas provided a less oxidizing atmosphere than during the other tests. If this is in fact the correct explanation, however, it means that the influence of mixture ratio on char or ablation slope is highly nonlinear. The tests with heat fluxes of 60 and 400 also had relatively low mixture ratios (12.6 and 11.3) but do not appear to deviate from the best straight line to any significant degree. The mixture ratio explanation is not inconsistent with the results given in the following section.

Effect of Source Gas on Char and Ablation Slopes

In order to determine the effect of testing atmosphere on the results, the experimental design included the tests run at Plasmadyne with an inert N_2 atmosphere and with an oxidizing simulated air atmosphere.

In order to obtain a close comparison, an air and an N_2 test was performed at each of four heat rates. The results, somewhat rearranged from Table V, are given in Table VI.

TABLE VI

Nitrogen Atmosphere				Air Atmosphere			
Test Number	Char Slope	Ablation Slope	Heat Flux	Test Number	Char Slope	Ablation Slope	Heat Flux
2-28	.031	.005	145	2-22	.031	.009	146
2-24	.018	.011	261	2-27	.034	.044	260
2-21	.045	.016	293	2-25	.029	.020	294
2-26	.035	.014	568	2-23	.031	.033	565

It is apparent even from a cursory examination of Table VI that the variability in char slopes is sufficient to mask any dependence of slope on test atmosphere. Looking across the rows of Table VI, one can see that the char slopes are essentially the same for two of the four heat fluxes, in one case the slope for nitrogen is higher, and in the other the slope for air is higher.

The ablation slopes observed in air are consistently higher than those observed in a nitrogenous atmosphere. The following statistical t-test (two-sided) of the differences in the logarithms of the four pairs of slopes indicates that the slopes are significantly higher for air at the 5% level of significance. The (rescaled) logarithms of the slopes and their differences are:

N_2	Air	Difference
16	22	6
24	38	14
26	30	4
28	35	7

The mean difference in 7.75, and the standard deviation of the mean difference is 2.18, so that the value of the t statstic is 3.55. This is greater than the 5% value of 3.18, so the difference is significant at this level.

Sensor Outputs Versus Physical Measurements

After a test is completed, the amount of ablation and char thickness of the plug are measured physically to check the accuracy of the sensor output observed at or near the end of the test. For the twelve MSC-2 char sensors the errors (sensor output minus measurement) were as follows:

Test	Error (inches)
1-34	-.01
1-35	-.01
1-36	-.02
1-37	-.06
1-38	.03
1-39	.02
1-40	.03
1-41	.04
1-42	.03
1-43	.04
1-44	.03
1-45	.02

The first four tests were done earlier and with a slightly different sensor than the last eight. The average bias for the first four is -.025 inches, and the standard deviation around the average bias is .024 inches. The average bias for the second set is .03 inches and the standard deviation is .007 inches. For the second set the magnitude of the bias is quite large when compared with the standard error about the curve fits as given in Table III. It is still not large enough to cause an error of practical consequence, however.

The char data inferred from temperature measurements can also be checked for bias. The last point on the curves given in Appendix C is the physical measurement of char taken at the end of the test. If a systematic bias is present, this point will appear to deviate from the remaining data in the plots. Such a phenomena may be observed on the following tests: 1-28, 1-29, 1-31, 2-15, 3-13, and 3-14, but is not noticable on other char tests. In all six cases the measured value was higher (more char formation) than indicated by the sensor output. The cause of this systematic error is not known; it may be important, since its magnitude is as much as .1 inches. For the most part there are not enough data on each ablation curve to detect a possible bias. On test 1-51 there seems to be a bias, which, however, is small compared with the variability exhibited by the data.

TEMPERATURE SENSORS

The model used to describe the temperature response was similar to that employed in previous temperature sensor analyses [2] and has the following form

$$T = T_s\{1-\exp[P(t,x,T_s)]\} \quad .$$

Here x is a thermocouple insertion depth measured in inches from the surface; $T_s = T_s(t;\dot{q},p)$ is the measured surface temperature in degrees Fahrenheit at specific points in time (t) which depends on the test input values of total pressure (p) and heat flux $(\dot{q})$; and $P(t,x,T_s)$ is a polynomial to be discussed below. Although the effects of heat flux and total pressure could have been introduced directly in the regression model, it was felt that it would be more satisfactory to incorporate their effect through the inclusion of experimentally measured values of T_s. The polynomial $P(t,x,T_s)$ contains all the unknown coefficients which are to be estimated by least-squares procedures and was taken generally to be of the form

$$P(t,x,T_s) = B_0 + \frac{T_s}{x}(B_1+B_2t+B_3t^2) + \frac{T_s^2}{x}(B_4+B_5t+B_6t^2) \quad .$$

In Table VII, the input conditions or independent variables for each test specimen considered in the analysis are listed. Each specimen contained up to seven thermocouples inserted at various depths, although only three or sometimes four functioned properly and were included in the analysis. As can be seen from Table VII, apart from differences in testing gas, close similarities in input conditions existed for tests 1 and 2, 3 and 4, 5 and 6, and 7 and 8. In Table VIII, the estimated coefficients B_0 - B_6 of the polynomial $P(t,x,T_s)$ are given in those cases where the coefficients were significantly different from zero on the 95 percent confidence level. Absence of an entry in Table VIII indicates a lack of such significance. Actual plots of the predicted temperature response curves analogous to those given in Appendix C for ablation and char were not obtained due to limitations in computer time. They may of course be easily constructed from Table VIII.

It is apparent from Table VIII that little similarity exists between the coefficients of the polynomial P under similar input conditions. In fact, unless the effect of the test gas is highly significant the results given in Table VIII demonstrate a considerable lack in coefficient repeatability under similar test conditions. Unfortunately this question cannot be completely resolved at this time since there is insufficient data to substantiate the effect of the testing gas.

In Table VIII, the standard deviations about each regression line are given in degrees Fahrenheit. Again we note that the dispersion of the

Table VII

Test Conditions for Temperature Sensor Evaluation

Test Input Conditions	Test Specimen Number 2-27	2-24	2-26	2-23	2-22	2-28	2-21	2-25
Total Pressure(atm)	.0217	.0218	.0274	.0270	.0121	.0121	.0122	.0118
Heat Flux (Btu/ft^2/sec)	260	261	568	565	146	145	293	294
Enthalpy Btu/lb	13,106	13,125	24,908	25,218	10,249	10,141	21,235	20,821
Testing Gas	air	N_2	N_2	air	air	N_2	N_2	air

Table VIII

Statistical Analysis of Temperature Sensor Data

Part A - Regression Coefficients

Test Specimen Number	Estimated Coefficients B_0	B_1	B_2	B_3	B_4	B_5
2-27	.9551	-5.226×10^{-4}	-1.028×10^{-3}			2.123×10^{7}
2-24	.3995		-8.692×10^{-4}		-1.826×10^{-7}	1.944×10^{-7}
2-26	.8038		-1.475×10^{-4}	3.297×10^{-7}	-2.095×10^{-7}	
2-23	1.1890	1.07×10^{-2}	-1.239×10^{-4}		3.305×10^{-6}	
2-22	.1504	-7.8×10^{-4}	-4.797×10^{-5}	-1.809×10^{-7}		
2-28	-.1316		6.898×10^{-5}		-3.148×10^{-8}	
2-21	1.1970	4.038×10^{-3}	-9.446×10^{-5}		-2.509×10^{-6}	
2-25	.8049	-4.075×10^{-4}	-6.588×10^{-4}			1.237×10^{-7}

Part B - Variability

	Test Specimen Number 2-27	2-24	2-26	2-23	2-22	2-28	2-21	2-25
Standard Deviation in $^{\circ}F$	147	225	241	120	269	220	54	115

experimental data about its regression line is in most cases rather large, particularly if one considers the relatively large number of data points present in each data set and the considerable number of terms in the polynomial. From these preliminary results one must conclude that (1) the non-repeatability of tests must be further understood and explained first before any improvement can be made in estimating temperature responses, and (2) a more sophisticated regression model must be developed in order to be able to predict other experimental results such as ablation rates and material charring rates.

In addition to those described above, other analyses were performed in order to gain more information as to the behavior of the temperature responses. For example, numerical derivatives of a set of response curves were correlated with surface temperature and varying thermocouple insertion depths using a regression model with surface recession as one of its independent variables. The results were successful in the sense that it was possible to estimate the ablation slope (previously discussed) in terms of the thermocouple data. The estimated value fell well within the confidence interval of the previously estimated ablation slope (see Table IV, Test 2-14).

Also, an attempt was made to predict thermocouple response by a regression model based only on the initial temperature, the measured surface temperature, surface recession, position, and the coefficient of diffusivity. The quality of these predictions was not satisfactory. However, the approach appears promising and should be pursued in future analyses.

REFERENCES

[1] WEBB, S. R. (1964). Experimental design for sensor evaluation program directed by NASA Manned Spacecraft Center, Houston, Texas. Research Memorandum 1024-251, Rocketdyne, Canoga Park.

[2] KASPAR, H. (1965). Analysis of high-temperature thermocouples for the Apollo heat shield. Research Memorandum 1146-351, Rocketdyne, Canoga Park.

[3] WILDEN, C. W. (1964). Revised stepwise regression program (deck 6R-001). Report STD 4185-122, Rocketdyne, Canoga Park.

[4] CHURCH, A., Jr. (1965). Analysis of data when the response is a curve. Presented at the Nineteenth Annual Technical Conference, American Society for Quality Control, May 3, 1965.

APPENDIX A

USE OF THE ROCKETDYNE STEPWISE REGRESSION COMPUTER PROGRAM

The data in this investigation were analyzed using the Rocketdyne Stepwise Regression Computer Program [3] previously supplied to the Manned Spacecraft Center. This program is an extremely useful and flexible program with many available options which are described in the program writeup. This appendix gives detailed instructions of its use for analyzing char and ablation data using models (2) and (3). Included are the cards which must be keypunched for program input of a sample problem, and a partial output obtained with this program.

INPUT TO ROCKETDYNE STEPWISE REGRESSION COMPUTER PROGRAM

A sample of data deck setup for program input for $D = .60, .65, \cdots, .80$ in model (2) is given in this appendix. This description emphasizes card entries likely to be changed for different tests.

Each data point of a char or ablation test is entered on a separate card. For example, card 240 contains the sixth point of the test and the char recession entry of 1000 in columns 3 through 6 is interpreted as 1.000 inches while the time entry of 240 in columns 10 through 12 is interpreted as 240 seconds. To facilitate computations, the value of t is automatically scaled by dividing by 10.

The number of points in the test is entered farthest to the right in the block of columns 13 through 24 of card 10. Test identification is entered in columns 37 through 72 of card 10. Card 20 is a specification of the input form of the data points (cards 90 through 150). This card is a standard IBM FORTRAN format specification which can be changed by anyone familiar with the FORTRAN system.

Cards 30 through 60 are transformation cards generating variables x_3, x_4, ••• , x_7. Consider the generation of x_3. Transformation 18 (card 30) generates $x_3 = D^{x_2}$, where x_2 = time and D = .60. Transformation 25 (card 40) generates $x_8 = \log_e x_3 = \log_e D^{x_2}$. Transformation 13 (card 40) generates $x_3 = x_3 - x_8 = D^{x_2} - \log_e D^{x_2}$. Transformation 11 (card 60) generates $x_3 = x_3 - 1 = D^{x_2} - \log_e D^{x_2} - 1$. Variables x_4, x_5, x_6, x_7 are similarly generated. The number of variables to be generated can be extended beyond x_7 to a maximum of x_{59} to include more values of D.

Cards 70 and 80 identify each variable.

The three cards 160, 170, and 180 cause the program to (1) print results at the end to the current analysis; (2) perform a regression analysis using the first, second, and third variables; and (3) plot the estimate $\hat{y}$ and the residual $(y-\hat{y})$. Cards 190 and 210 have the same entries as cards 160 and 180. Card 200 differs from 170 in specifying the use of the first, second, and fourth variable in the analysis. A similar procedure continues through cards 280, 290, and 300. Card 310 ends analyses of all problems on the computer run. Using the preceding dec for the linear model (3) requires the removal of cards 30 through 80, 190 through 300, and 170 and the insertion of cards 70B and 170B.

FORTRAN FIXED 10 DIGIT DECIMAL DATA

DECK NO. 2 PROGRAMMER ________ DATE ________ PAGE 1 of 9 JOB NO. ________

Col	NUMBER	IDENTIFICATION	DESCRIPTION DO NOT KEY PUNCH
1	M P 3 2 32		
13	7		Data Deck Setup for input to
25			Rocketdyne Stepwise Computer Program.
37	TEST 1-28 PT		Nonlinear Model.
49	. 3 DESIGN I	73 80	
61	I	10	
1	VF(F6.3,F6.1		
13	)		
25			
37			
49		73 80	
61		20	
1	TR181818181818		
13	3 2 .60		
25	4 2 .65		
37	5 2 .70		
49	6 2 .75	73 80	
61	7 2 .80	30	
1	TR251325132513 25		
13	8 3		
25	3 3 8		
37	8 4		
49	4 4 8	73 80	
61	8 5	40	

114-C-17 VELLUM

FORTRAN FIXED 10 DIGIT DECIMAL DATA

DECK NO. ______ PROGRAMMER ______ DATE ______ PAGE 2 of 9 JOB NO. ______

	NUMBER	IDENTIFICATION 73–80	DESCRIPTION DO NOT KEY PUNCH
1	T R1325132513		
13	5 5 8		
25	8 6		
37	6 6 8		
49	8 7		
61	7 7 8	50	
1	T R1111111111		
13	3 3 -1		
25	4 4 -1		
37	5 5 -1		
49	6 6 -1		
61	7 7 -1	60	
1	V N 1CHAR		
13	2TIME		
25	3D=.60		
37	4D=.65		
49	5D=.70		
61	6D=.75	70	
1	V N 7D=.80		
13			
25			
37			
49			
61		80	

114-C-17 VELLUM

FORTRAN FIXED 10 DIGIT DECIMAL DATA

DECK NO. ______ PROGRAMMER ______ DATE ______ PAGE 3 of 9 JOB NO. ______

Col	NUMBER		IDENTIFICATION	DESCRIPTION DO NOT KEY PUNCH
1	0.0.0	0.0.0		
13				
25				
37				
49			73 80	
61			90	
1	050	005		
13				
25				
37				
49			73 80	
61			100	
1	100	008		
13				
25				
37				
49			73 80	
61			110	
1	200	023		
13				
25				
37				
49			73 80	
61			120	

414-C-17 VELLUM

FORTRAN FIXED 10 DIGIT DECIMAL DATA

DECK NO. ______ PROGRAMMER ______ DATE ______ PAGE 4 of 9 JOB NO. ______

	NUMBER		IDENTIFICATION	DESCRIPTION DO NOT KEY PUNCH
1	800	185		
13				
25				
37				
49			73 80	
61			130	
1	1000	240		
13				
25				
37				
49			73 80	
61			140	
1	1125	255		
13				
25				
37				
49			73 80	
61			150	
1	AN	2		
13				
25				
37				
49			73 80	
61			160	

114-C-17 VELLUM

FORTRAN FIXED 10 DIGIT DECIMAL DATA

DECK NO. ______ PROGRAMMER ______ DATE ______ PAGE 5 of 9 JOB NO. ______

Col.	NUMBER	IDENTIFICATION	DESCRIPTION DO NOT KEY PUNCH
1	A C 1 1 -1 -1		
13	-1 -1 -1		
25			
37			
49		73 80	
61		170	
1	P L 0 2		
13	1 -1		
25			
37			
49		73 80	
61		180	
1	A N 2		
13			
25			
37			
49		73 80	
61		190	
1	A C 1 -1 1 -1		
13	-1 -1 -1		
25			
37			
49		73 80	
61		200	

T4-C-17 VELLUM

R-6215

FORTRAN FIXED 10 DIGIT DECIMAL DATA

DECK NO. ______ PROGRAMMER ______ DATE ______ PAGE 6 of 9 JOB NO. ______

	NUMBER	IDENTIFICATION	DESCRIPTION DO NOT KEY PUNCH
1	PL 0 2	73	
13	1-1		
25			
37			
49		80	
61		210	
1	AN 2	73	
13			
25			
37			
49		80	
61		220	
1	AC 1-1-1 1	73	
13	-1-1-1		
25			
37			
49		80	
61		230	
1	PL 0 2	73	
13	1-1		
25			
37			
49		80	
61		240	

114-C-17 VELLUM

FORTRAN FIXED 10 DIGIT DECIMAL DATA

DECK NO. ______ PROGRAMMER ______ DATE ______ PAGE 7 of 9 JOB NO. ______

Col.	NUMBER	IDENTIFICATION (73–80)	DESCRIPTION DO NOT KEY PUNCH
1	AN 2		
13			
25			
37			
49			
61		250	
1	AC 1-1-1-1		
13	1-1-1		
25			
37			
49			
61		260	
1	PL 0 2		
13	1-1		
25			
37			
49			
61		270	
1	AN 2		
13			
25			
37			
49			
61		280	

114-C-17 VELLUM

FORTRAN FIXED 10 DIGIT DECIMAL DATA

DECK NO. 2 PROGRAMMER ______ DATE ______ PAGE 8 of 9 JOB NO. ______

	NUMBER	IDENTIFICATION	DESCRIPTION DO NOT KEY PUNCH
1	AC 1-1-1-1	73 80	
13	-1 1-1		
25			
37			
49			
61		290	
1	PL 0 2	73 80	
13	1-1		
25			
37			
49			
61		300	
1	END	73 80	
13			
25			
37			
49			
61		310	
1		73 80	
13			
25			
37			
49			
61			

FORTRAN FIXED 10 DIGIT DECIMAL DATA

DECK NO. ______ PROGRAMMER ______ DATE ______ PAGE 9 of 9 JOB NO. ______

Col.	NUMBER	IDENTIFICATION	DESCRIPTION DO NOT KEY PUNCH
1	Y N. ICHAR.		
13	2TIME		Card changes to setup for
25			input to Rocketdyne Stepwise
37			Computer Program. Linear Model.
49		73 … 80	
61		70	← B
1	A C 1		
13			
25			
37			
49		73 … 80	
61		170	← B
1			
13			
25			
37			
49		73 … 80	
61			
1			
13			
25			
37			
49		73 … 80	
61			

114-C-17 VELLUM

OUTPUT FROM ROCKETDYNE STEPWISE REGRESSION COMPUTER PROGRAM

Sample output from the program is shown on the following pages. This output was obtained from the sample input data previously described.

Page 1 of the output contains information pertaining to the test being analyzed and confirms variable format and transformations specified on input. Page 2 gives values of variables at each point, including variables generated by transformations. Page 3 associates with each variable its name, mean, variance, and standard deviation. Page 4 contains the information matrix. Pages 5, 6, 7, and 8 contain the results of the first analysis, using x_1, x_2, and x_3 in regression model (2). Page 6 gives the standard error of estimate and $\hat{y} = Bx_2 + Ax_3$. Page 8 tabulates actual Y (observed char recession), predicted Y, and the residual for each point. In addition to this tabulation the program constructs a graph, in the form of a CRT plot, plotting X_2 (time) versus actual Y (shown by the character ◻) and X_2 versus predicted Y (shown by the character *). For the test problem given earlier the output continues, repeating pages analogous to 5 through 8, giving the results of analyses 2 through 5.

The most important part of the output for purposes of analyzing char and ablation data is that on page 6. The quantity labeled "std error of estimate," whose value is .02759843, is the number which determines which value of D gives the best fit. The value of D = .60, used in this analysis, is inferior to the optimum value D = .35, given in Table III, for which the value of the standard error of the estimate is .0247, a minimum value. The following line gives the equation

YHAT = +(0.116999)X2 + (-0.158198)X3 ,

which is of the form of model (2) with B' equal to .1170 and A equal to -.1582. Note that these values differ from the values given in Table III of B' = .1549 and A = -.111, which are associated with the optimum D = .35.

PROBLEM NUMBER	3
NO OF OBSERVATIONS	7
NO OF VARIABLES (IN DATA)	2
NO OF VAR GENERATED	6
NO OF VARIABLES (IN PRCR)	8

DATA FORMAT USED
(F6.3,F6.1)

TRANSFORMATION OPERATIONS

NO	VAR	XA	XB	CODE
1	3	2	0.6000000	18
2	4	2	0.6500000	18
3	5	2	0.7000000	18
4	6	2	0.7500000	18
5	7	2	0.8000000	18
6	8	3	-0.	25
7	3	3	8.0000000	13
8	8	4	-0.	25
9	4	4	8.0000000	13
10	8	5	-0.	25
11	5	5	8.0000000	13
12	6	6	-0.	25
13	6	6	8.0000000	13
14	8	7	-0.	25
15	7	7	8.0000000	13
16	3	3	-1.0000000	11
17	4	4	-1.0000000	11
18	5	5	-1.0000000	11
19	6	6	-1.0000000	11
20	7	7	-1.0000000	11

RA 1	0.	0.	0.	0.	0.	0.	0.	0.
RA 2	0.050	0.500	0.030	0.022	0.015	0.010	0.006	-0.112
RA 3	0.100	0.800	0.073	0.053	0.037	0.025	0.015	-0.179
RA 4	0.200	2.300	0.484	0.362	0.261	0.178	0.112	-0.513
RA 5	0.800	18.500	8.450	6.970	5.600	4.327	3.144	-4.128
RA 6	1.000	24.000	11.260	9.339	7.560	5.905	4.360	-5.355
RA 7	1.125	25.500	12.026	9.985	8.095	6.337	4.694	-5.690

VARIABLE		MEAN	VARIANCE	STANDARD DEVIATION
1	DEPTH	0.46786	0.23765	0.48749
2	TIME	10.22857	140.38572	11.84845
3	D=.60	4.61760	32.30046	5.68335
4	D=.65	3.81863	22.25876	4.71792
5	D=.70	3.08118	14.61095	3.82243
6	D=.75	2.39729	8.92526	2.98752
7	D=.80	1.76154	4.86973	2.20675
8		-2.28244	6.99023	2.64390

INFORMATION MATRIX

		1	2	3	4	5	6	7	8
DEPTH	X 1	2.9581							
TIME	X 2	68.0525	1574.6800						
D=.60	X 3	31.6550	734.4178	343.0583					
D=.65	X 4	26.2266	608.5767	284.3106	235.6264				
D=.70	X 5	21.2041	492.1139	229.9334	190.5634	154.1216			
D=.75	X 6	16.5341	383.7935	179.3498	148.6438	120.2212	93.7804		
D=.80	X 7	12.1800	282.7704	132.1650	109.5401	88.5975	69.1148	50.9396	
	X 8	-15.1855	-351.3797	-163.8806	-135.8000	-109.8120	-85.6410	-63.0984	78.4081

PROBLEM NUMBER	3
ANALYSIS NUMBER	1
CONF TO INCLUDE	.9000
CONF TO RETAIN	.9000
MAXIMUM NO OF STEPS	16
DEPENDENT VARIABLE	1

THE FOLLOWING VARIABLES ARE DELETED IN THIS ANALYSIS

4 5 6 7 8

THE FOLLOWING VARIABLES ARE FORCED INTO THE REGRESSION IN THIS ANALYSIS

2 3

STD ERROR OF DEP VAR	0.487492E-00
VARIANCE	0.237649E-00
DEGREES OF FREEDOM	6.

ALL FORCED VARIABLES ARE NOW IN THE REGRESSION

VARIABLES IN REGRESSION

VARIABLE	CONTR TO SS	F RATIO	CONFIDENCE	COEFFICIENT	VARIANCE	CORRELATION
2 TIME	0.035419	43.8761	0.998379	0.11700E-00	0.4096E-00	0.947471
3 D=.60	0.013311	17.4760	0.990789	-0.15820E-00	0.1880E 01	0.881783

CONFIDENCE NECESSARY TO RETAIN VARIABLE 0.900000

STEP NUMBER 3
REGRESSION IS THE SAME AS PREVIOUS

MULTIPLE CORRELATION COEFF 0.99866367
RESIDUAL VARIANCE 0.00076167
STD ERROR OF ESTIMATE 0.02759843

YHAT = +(0.116999)X 2 +(-0.158198)X 3

OEFFICIENT VARIANCE-COVARIANCE MATRIX

		2	3
ME	X 2	0.409608	
.60	X 3	0.876888	1.880152

NUMBER	ACTUAL Y	PREDICTED Y	RESIDUAL
1	0.	-0.	0.
2	0.05000	0.05375	-0.00375
3	0.10000	0.08202	0.01798
4	0.20000	0.19257	0.00743
5	0.80000	0.82765	-0.02765
6	1.00000	1.02669	-0.02669
7	1.12500	1.08098	0.04402

1-CRT PLOT OF 0 VS 2 ERROR COUNT = 0
2-CRT PLOT OF 1 VS -1 ERROR COUNT = 0

END OF ANALYSIS - ALL SIGNIFICANT VARS INCLUDED

8311-26
006 000

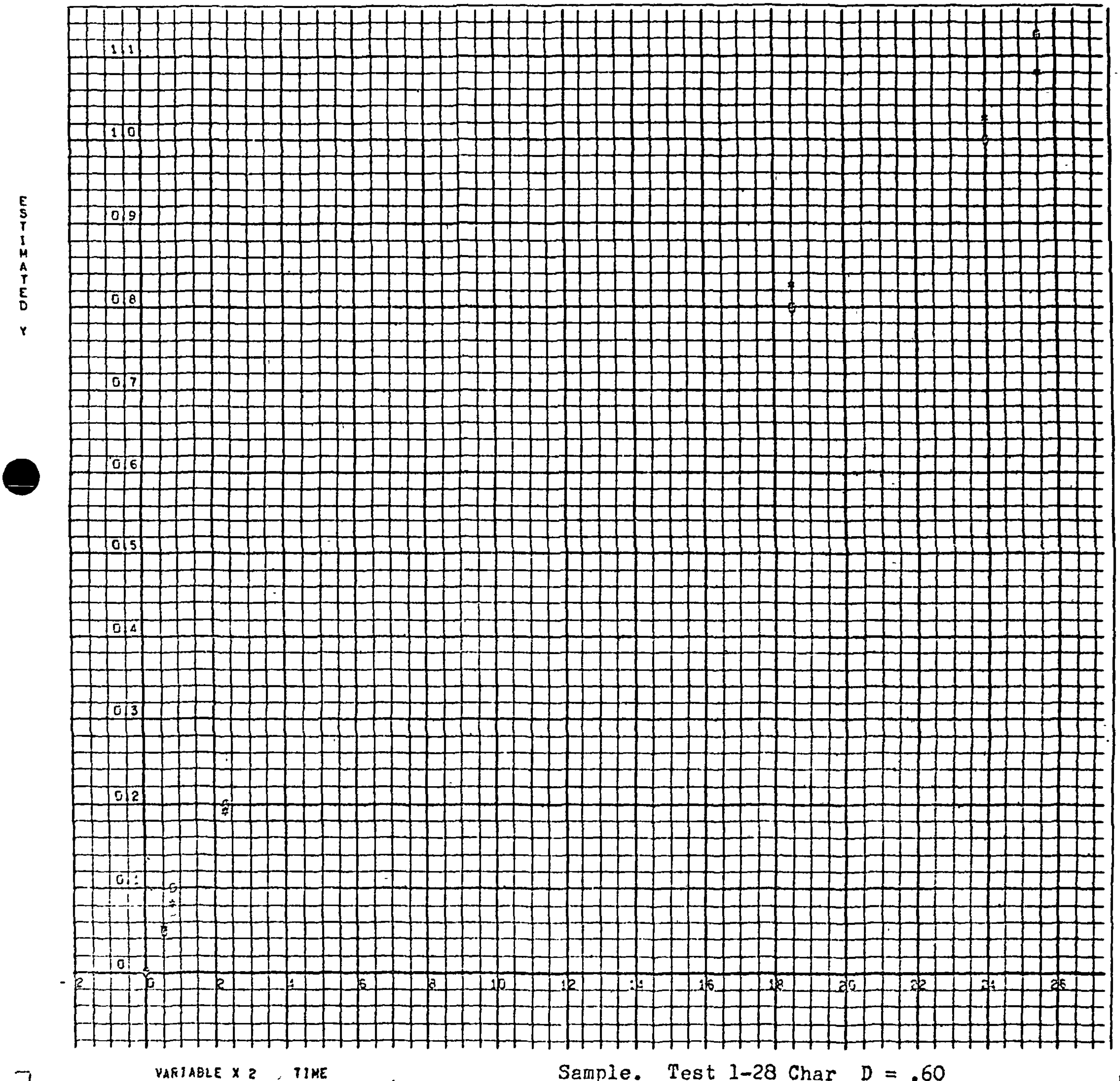

Sample. Test 1-28 Char D = .60

APPENDIX B

CHURCH ANALYSIS OF RADIOACTIVE CHAR SENSORS

The analyses described earlier in this report depend rather significantly on the models chosen to describe the responses. A different type of analysis was performed on the data from the radioactive char sensors (tests 1-34 through 1-45). The technique used, a form of principal components analysis, was developed by Alonzo Church, Jr. [4]. This analysis attempts to explain differences between output curves on the basis of the independent variables selected (in this case effects of heat flux were studied), without first fitting a model to the original data. By eliminating the necessity for choosing a particular functional form (say, of the type (2) or (3)) to describe the individual response curves, one more or less arbitrary element in the analysis is obviated.

The first step in a Church analysis is to select a set of time points at which the curves will be represented. Since the shortest test of the 12 had a duration of 60 seconds, it was decided to use six time points equally spaced at 10, 20, 30, 40, 50, and 60 seconds. For each time point, the average response is computed from the 12 tests. Subsequent steps of the analysis use the deviations from the averages. These deviations are given in Table IX, Part A.

Table IX, Part A

Radioactive Char Data Used in Church Analysis
(Deviations in thousandths of an inch)

Test	Time in Seconds 10	20	30	40	50	60
1-34	-38	-72	-95	-111	-148	-179
1-35	-15	21	5	9	- 8	- 9
1-36	85	31	45	19	- 8	- 19
1-37	-35	-39	-35	- 41	- 18	- 19
1-38	-41	-59	-87	-100	-108	-119
1-39	-25	-44	-55	- 81	- 68	- 77
1-40	25	24	41	49	47	53
1-41	17	31	26	42	43	65
1-42	3	29	45	59	72	96
1-43	-15	- 9	-15	9	34	35
1-44	20	59	73	81	90	100
1-45	15	31	55	69	72	71
average curve	65	129	177	231	268	299

Table IX, Part B

Principal Components from Church Analysis

Test	Value of z_1	Value of z_2	Heat Flux
1-34	-.29	.019	85
1-38	-.22	-.011	85
1-39	-.15	-.010	85
1-35	0	.004	110
1-40	.10	.011	110
1-41	.10	-.003	110
1-36	.03	.099	190
1-42	.14	-.026	190
1-43	.03	-.042	190
1-37	-.07	-.041	210
1-44	.18	.001	210
1-45	.14	-.001	210

Let X_{ij} represent the value given in row i and column j of the above table. Let $Q_{jk} = \Sigma_{i=1}^{12} X_{ij}X_{ik}$. The next step in the analysis deals with the square matrix Q which contains Q_{jk} as the entry in the j-th row and k-th column. The matrix Q is as follows (the entries have been multiplied by 10^6):

$$Q = \begin{bmatrix} 14197 & 12935 & 17640 & 17895 & 16314 & 18048 \\ 12935 & 20424 & 26499 & 30858 & 32091 & 37117 \\ 17640 & 26499 & 35854 & 41363 & 43731 & 50221 \\ 17895 & 30858 & 41363 & 50053 & 54171 & 62649 \\ 16314 & 32091 & 43731 & 54171 & 62326 & 72646 \\ 18048 & 37117 & 50221 & 62649 & 72646 & 85450 \end{bmatrix} .$$

The j-th eigenvector L_j of the matrix Q is a column of six numbers $L_{1j}, \cdots, L_{6j}$, such that $\Sigma_{n=1}^{6} Q_{in}L_{nj} = \lambda_j L_{ij}$, for $i = 1, \cdots, 6$. The number λ_j is called the eigenvalue associated with the eigenvector L_j. The principle on which the Church analysis is based is that the percentage of the variation in the data "explained" by the eigenvector associated with the largest eigenvalue is greater than that for any other variable. That is, the best possible one-variable regression is obtained using this eigenvector. The total variation in the data is the sum of the diagonal elements of Q; that is, $\Sigma_{i=1}^{6} Q_{ii}$. The percentage of this variation explained by an eigenvector is the associated eigenvalue divided by $\Sigma_{i=1}^{6} Q_{ii}$. For the matrix Q the eigenvalues are:

$\lambda_1 = .25069$

$\lambda_2 = .01465$

$\lambda_3 = .00184$

$\lambda_4 = .00061$

$\lambda_5 = .00037$

$\lambda_6 = .00014$

The sum of the Q_{ii} is .26830, and the percentage of this total variation explained by L_1 is 93%. The percentage explained by L_1 and L_2 is $\lambda_1+\lambda_2/.26830 = 99\%$. The marginal increase with λ_3 is small, so that only L_1 and L_2 will be used subsequently. These vectors are given explicitly as follows:

$$L_1 = \begin{bmatrix} .153 \\ .271 \\ .366 \\ .443 \\ .493 \\ .574 \end{bmatrix}, \qquad L_2 = \begin{bmatrix} .717 \\ .289 \\ .367 \\ .123 \\ -.276 \\ -.420 \end{bmatrix}$$

The analysis is done in terms of vectors Z_1 and Z_2 defined by

$$Z_{i1} = \Sigma_{n=1}^{6} X_{in} L_{n1}$$

$$Z_{i2} = \Sigma_{n=1}^{6} X_{in} L_{n2} \quad .$$

The variables Z_1 and Z_2, the principal components of the variation, should correlate with the values of the independent variable, which for these data is heat flux. The Z's and the heat-flux values are given in Table IX, Part B. Comparing Tables IX-B and II it appears that the value of Z_1 is smaller for the lowest heat flux, but that there is no other systematic variation with heat flux in either Z_1 or Z_2.

A method called a one-way analysis of variance was used to determine the statistical significance of the dependence of Z_1 and Z_2 on heat flux. An exposition of this method can be found in many statistical texts. The idea is to compare the variability of the values of the Z's for fixed heat flux with the variation in the average Z's between heat flux. Computational details will not be reproduced here. The variance in Z_1 for fixed heat flux was found to be .00757, and the variance between the average values of Z_1 was .0214. The ratio is not statistically significant at the .1 level. This means that the inherent variability in the values of Z_1 is such that, even with no dependence of Z_1 on heat flux, this difference in variation would be observed by chance at least 10% of the time. The dependence of Z_2 on heat flux is completely insignificant. Thus heat flux is only "mildly" significant in affecting the sensor response.

APPENDIX C

DATA AND CURVE FITS

This appendix gives plots resulting from the optimum curve-fits for char and ablation data as given in Tables III and IV. The vertical axis, labeled "ESTIMATED Y," is the char or ablation depth in inches. The horizontal axis, labeled "VARIABLE X2 TIME," gives time in seconds/10 (so that $t = 2$ is 20 seconds). Each plot contains the original data used in the analysis, plotted with a small square, and the best curve fit, plotted with an asterisk. A legend identifying the plot has been typed in at the bottom.

8311-36
001 000

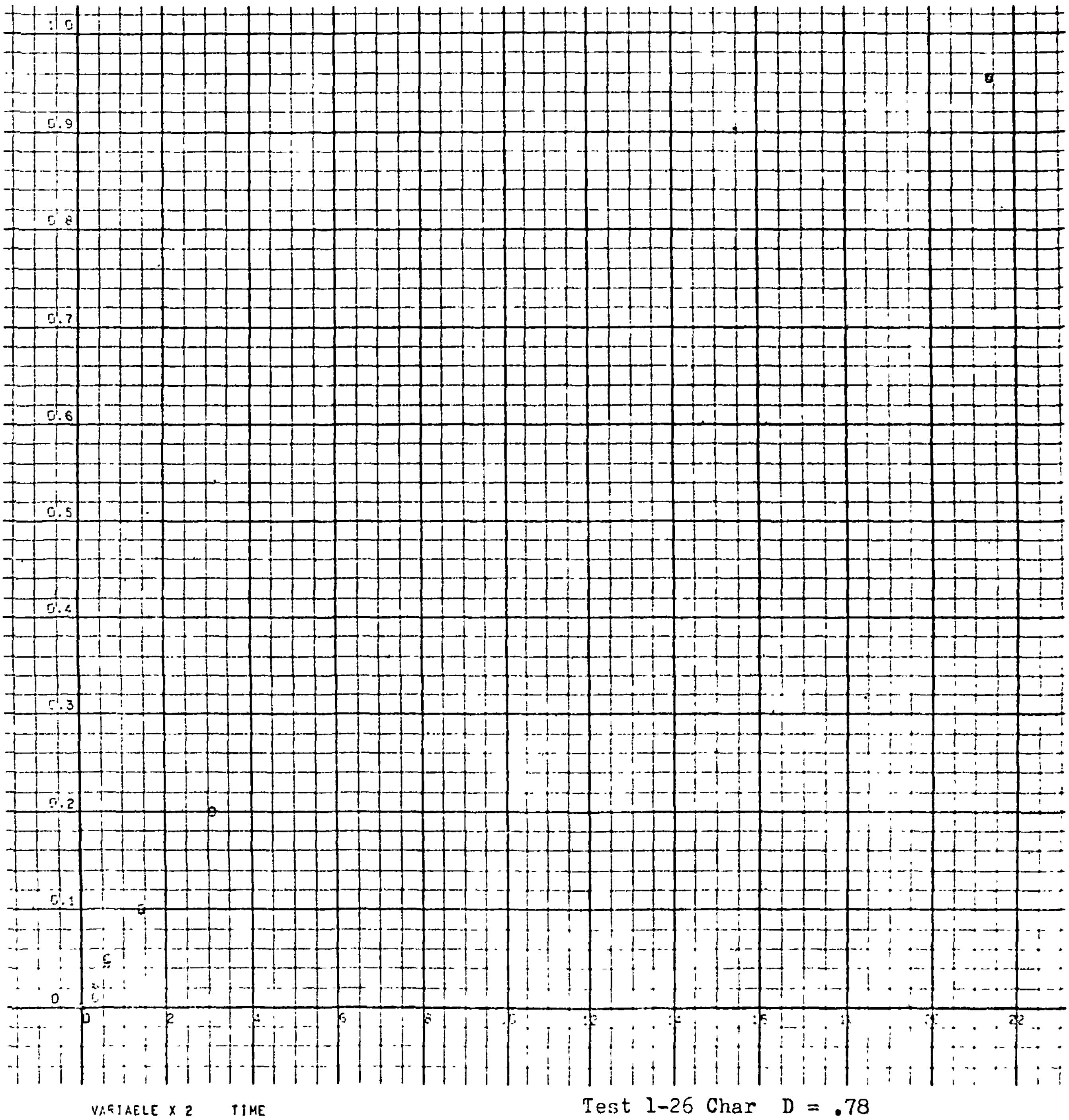

Test 1-26 Char D = .78

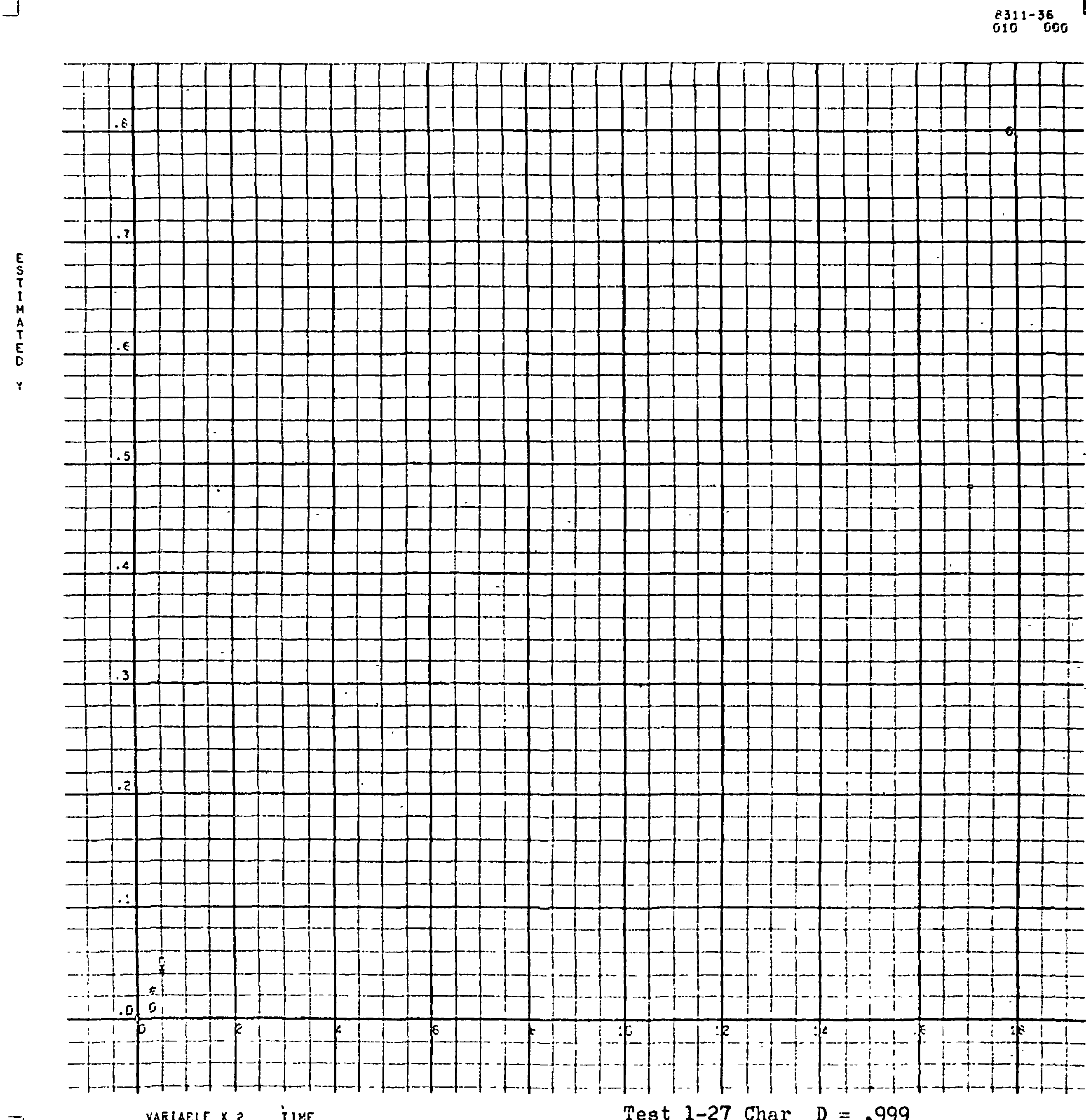

Test 1-27 Char D = .999

8311-32
011 000

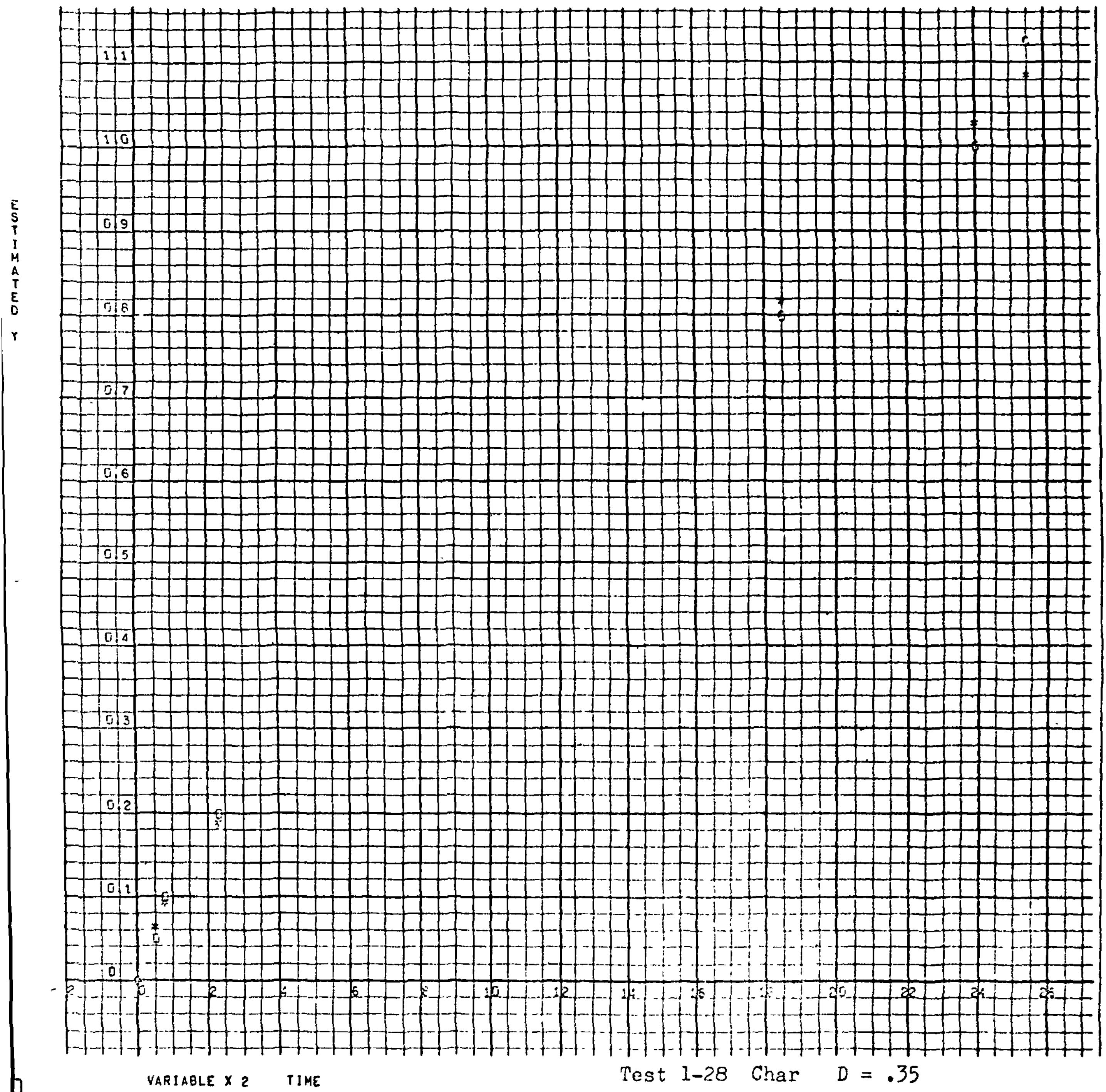

Test 1-28 Char D = .35

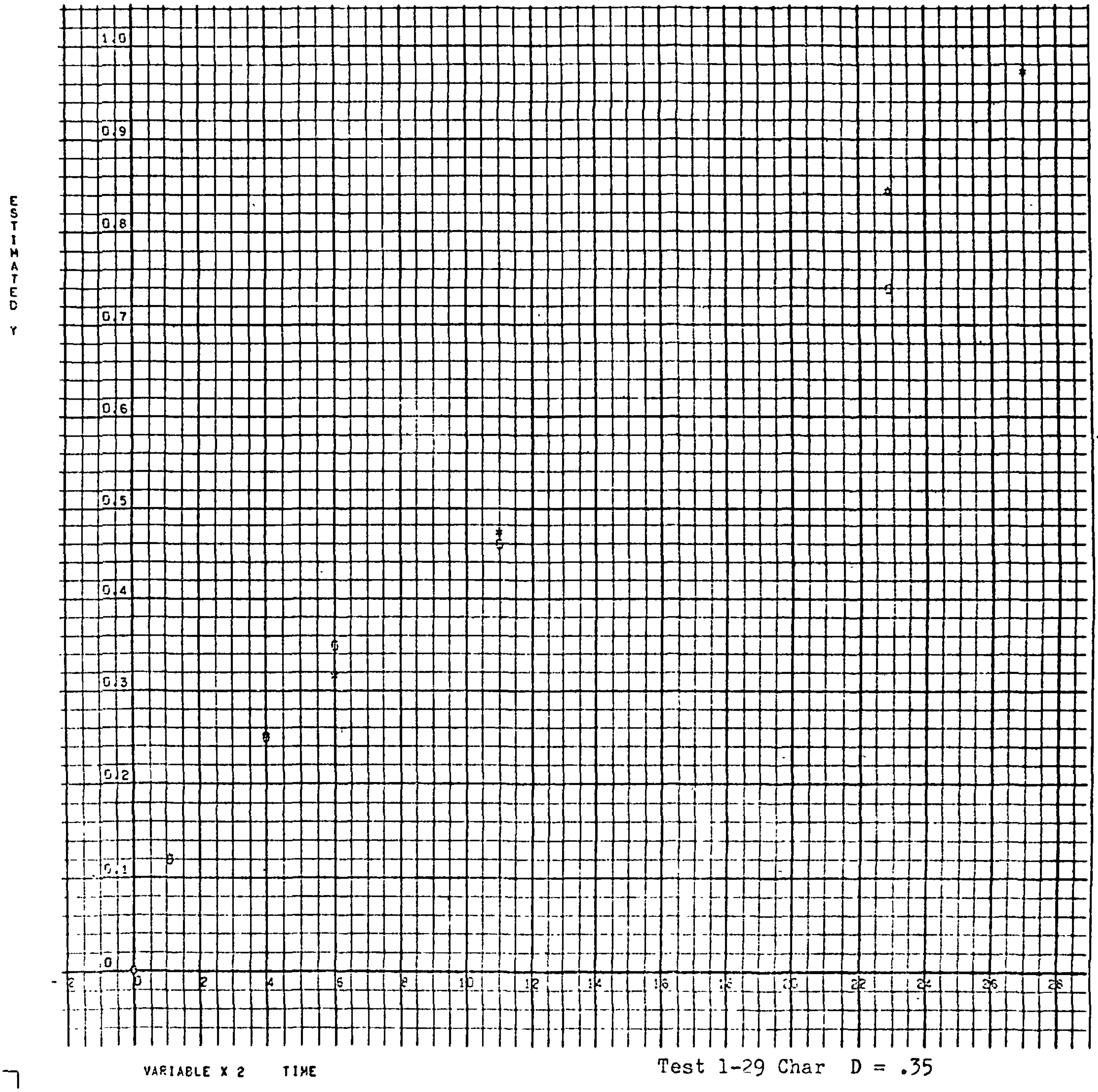

Test 1-29 Char D = .35

8311-32
023 000

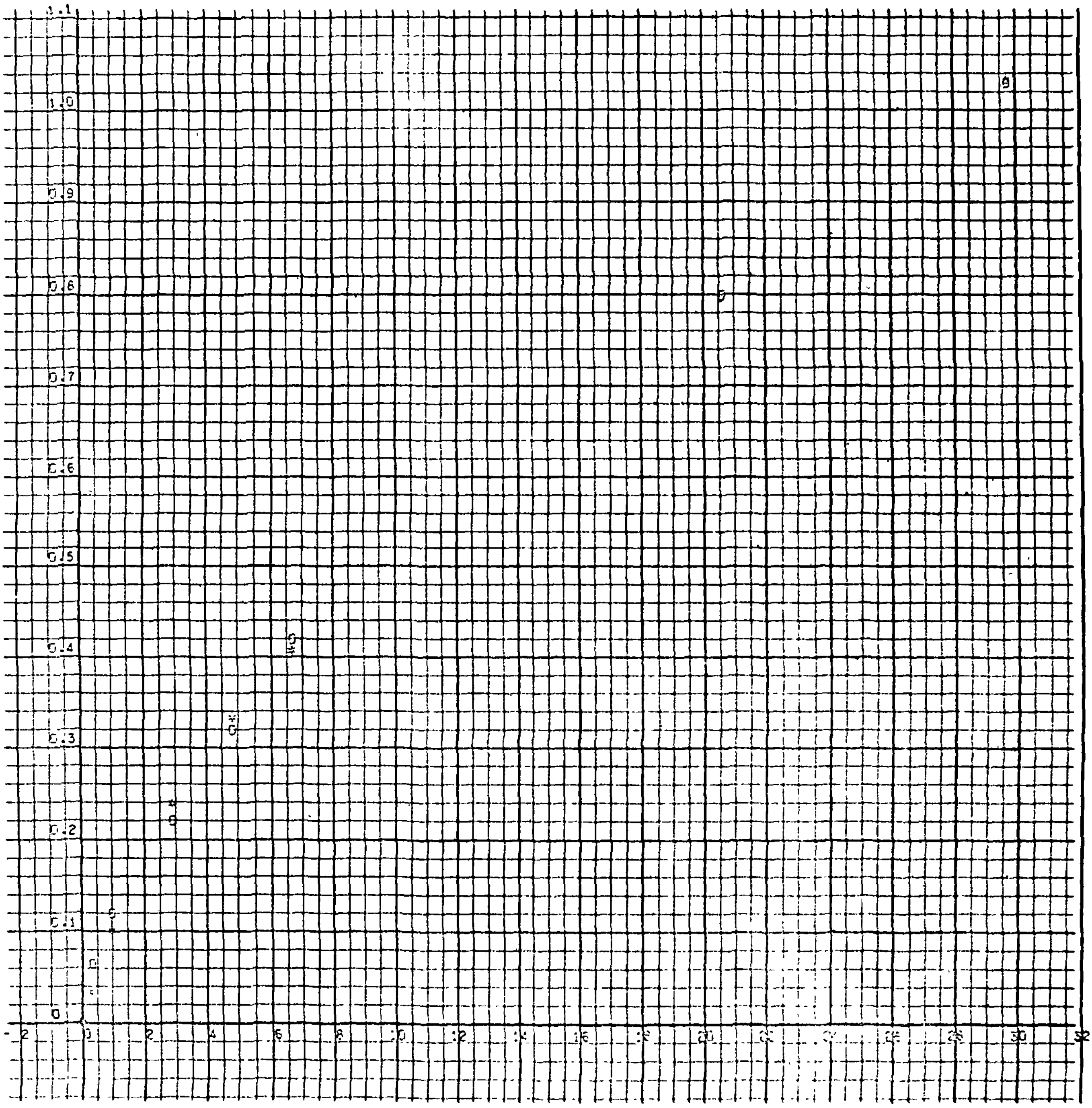

VARIABLE X 2 TIME

Test 1-30 Char D = .71

8311-32
028 000

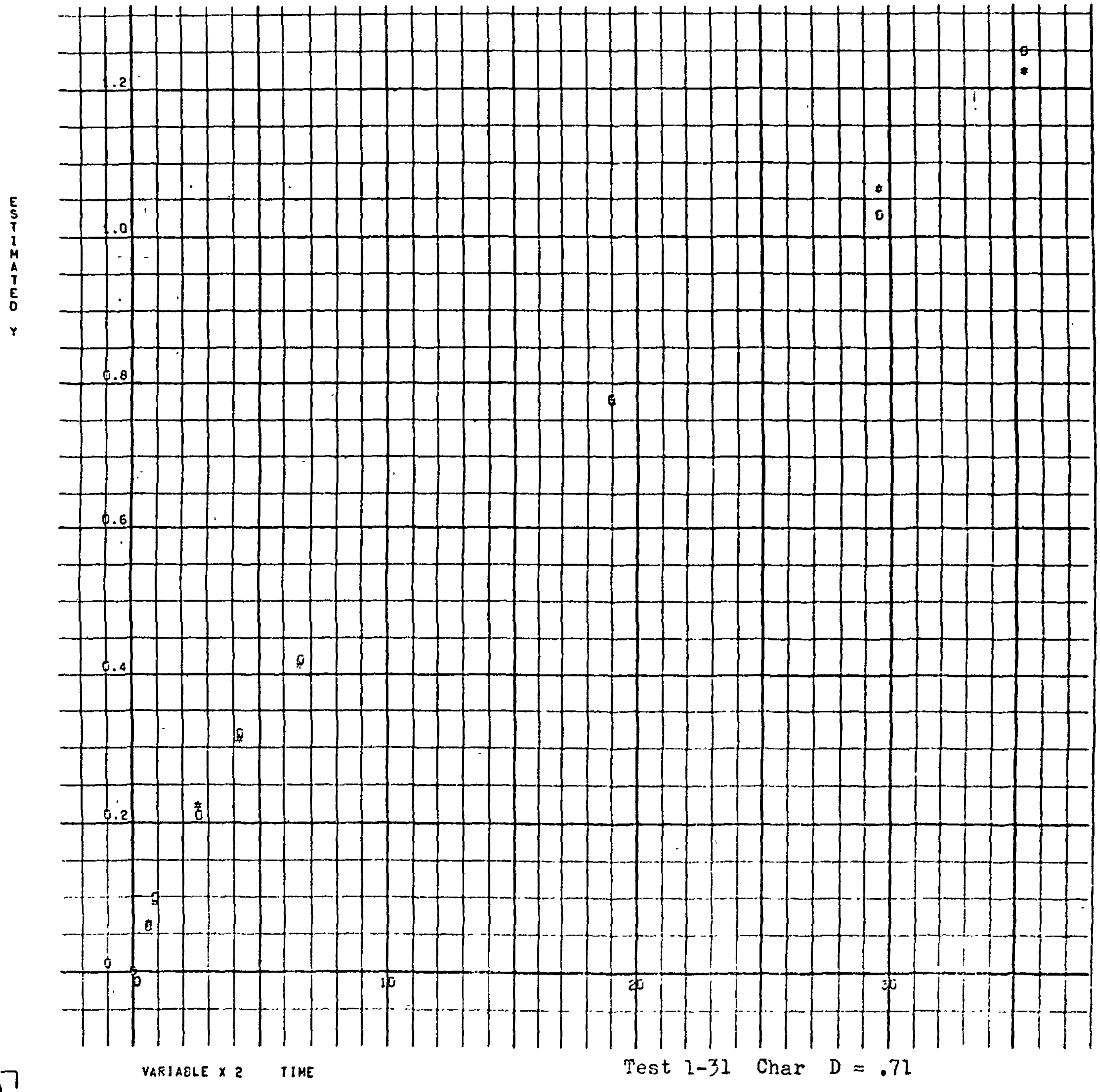

Test 1-31 Char D = .71

8311-31
005 000

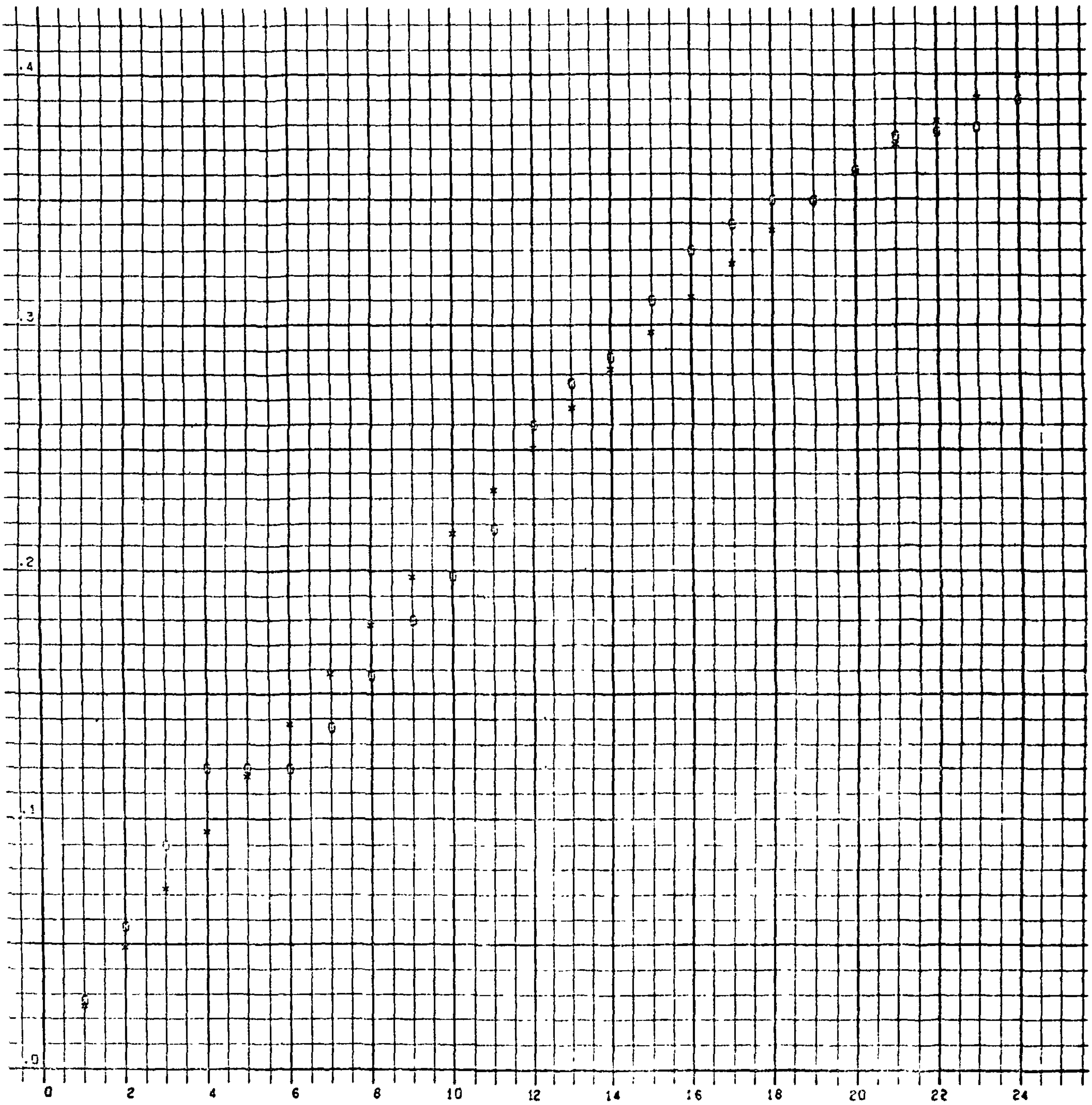

VARIABLE X 2 TIME

Test 1-34 Char D = .999

8311-35
001 000

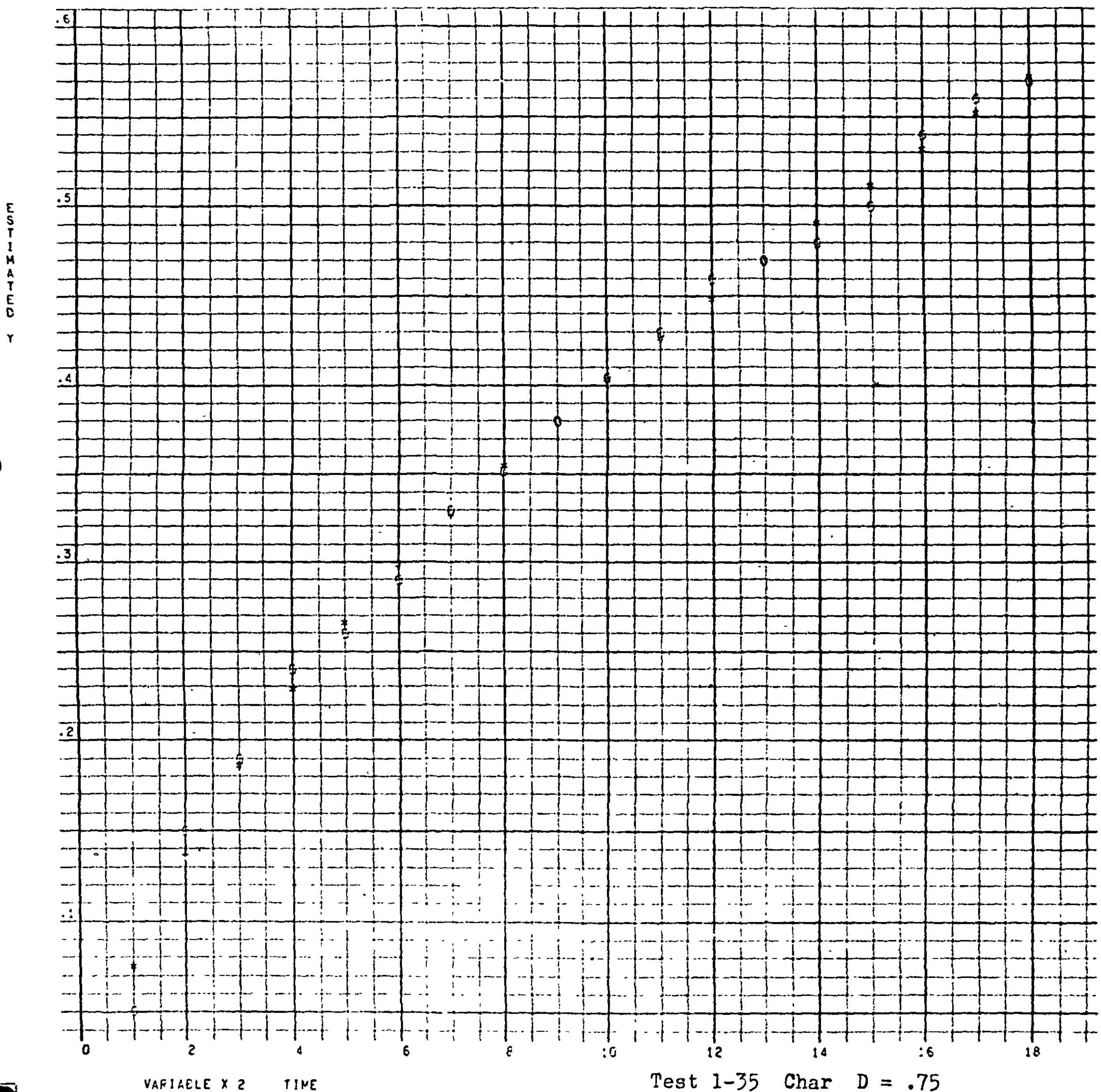

Test 1-35 Char D = .75

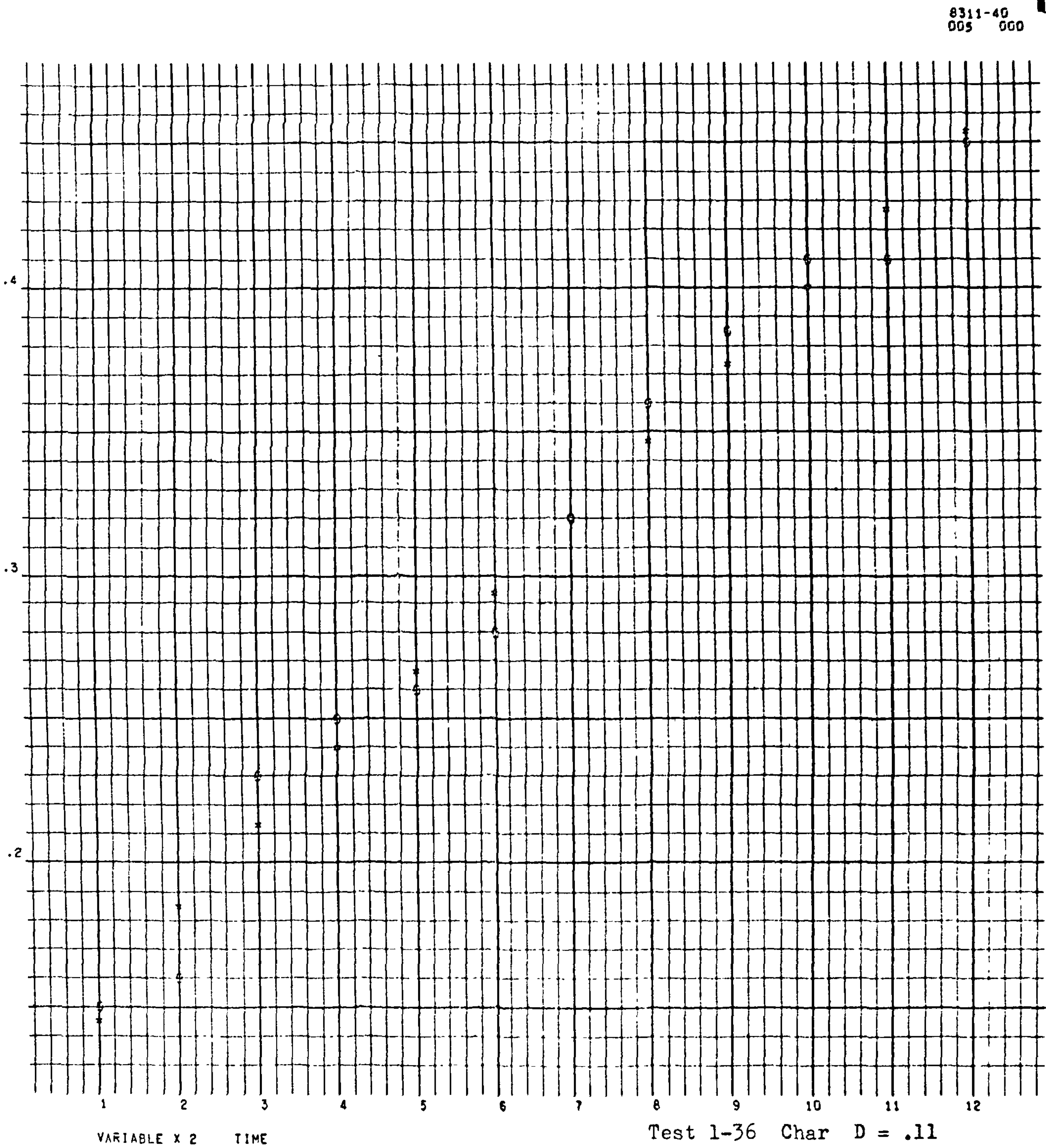

Test 1-36 Char D = .11

8311-35
015 000

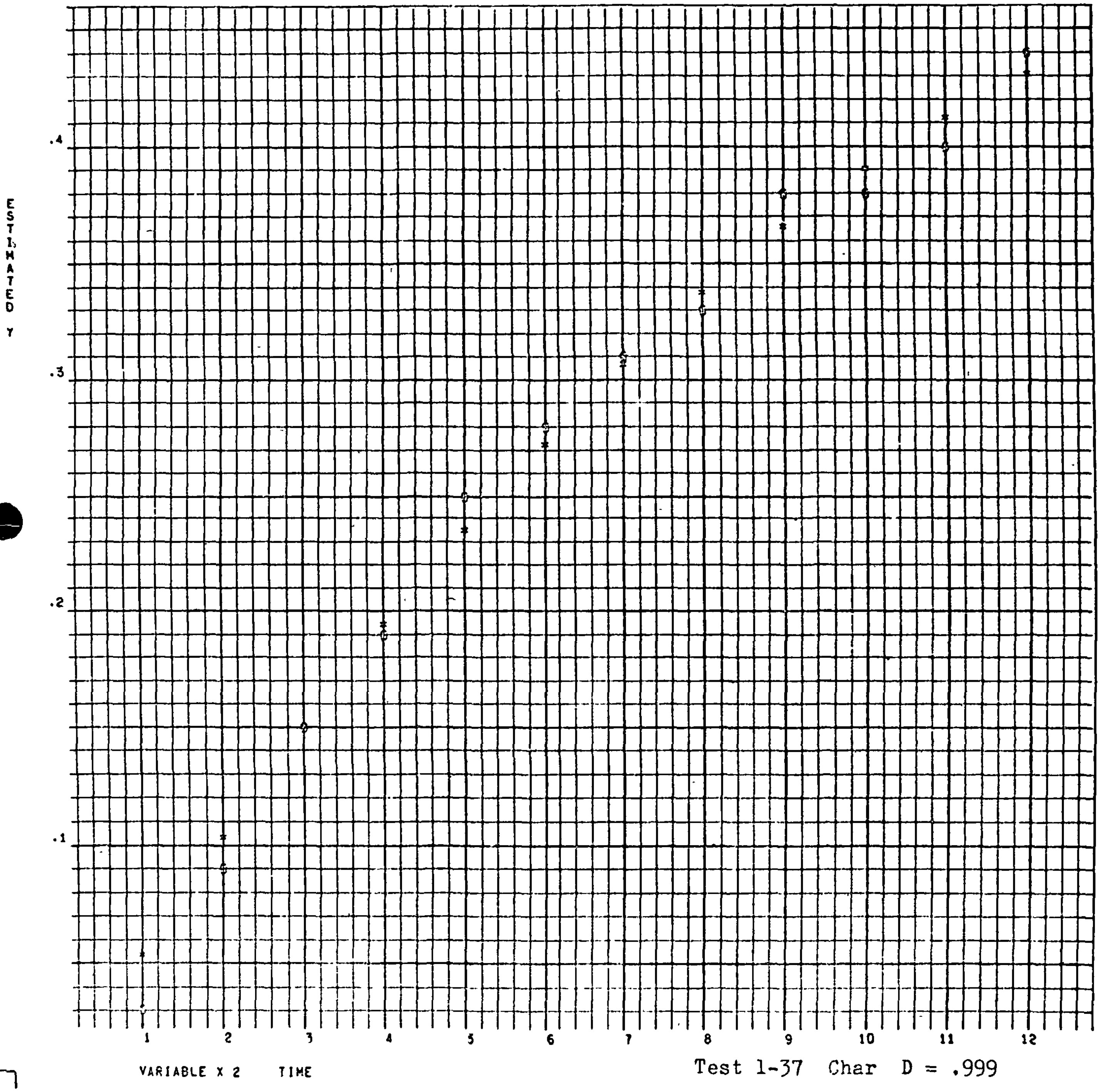

Test 1-37 Char D = .999

8311-38
019 000

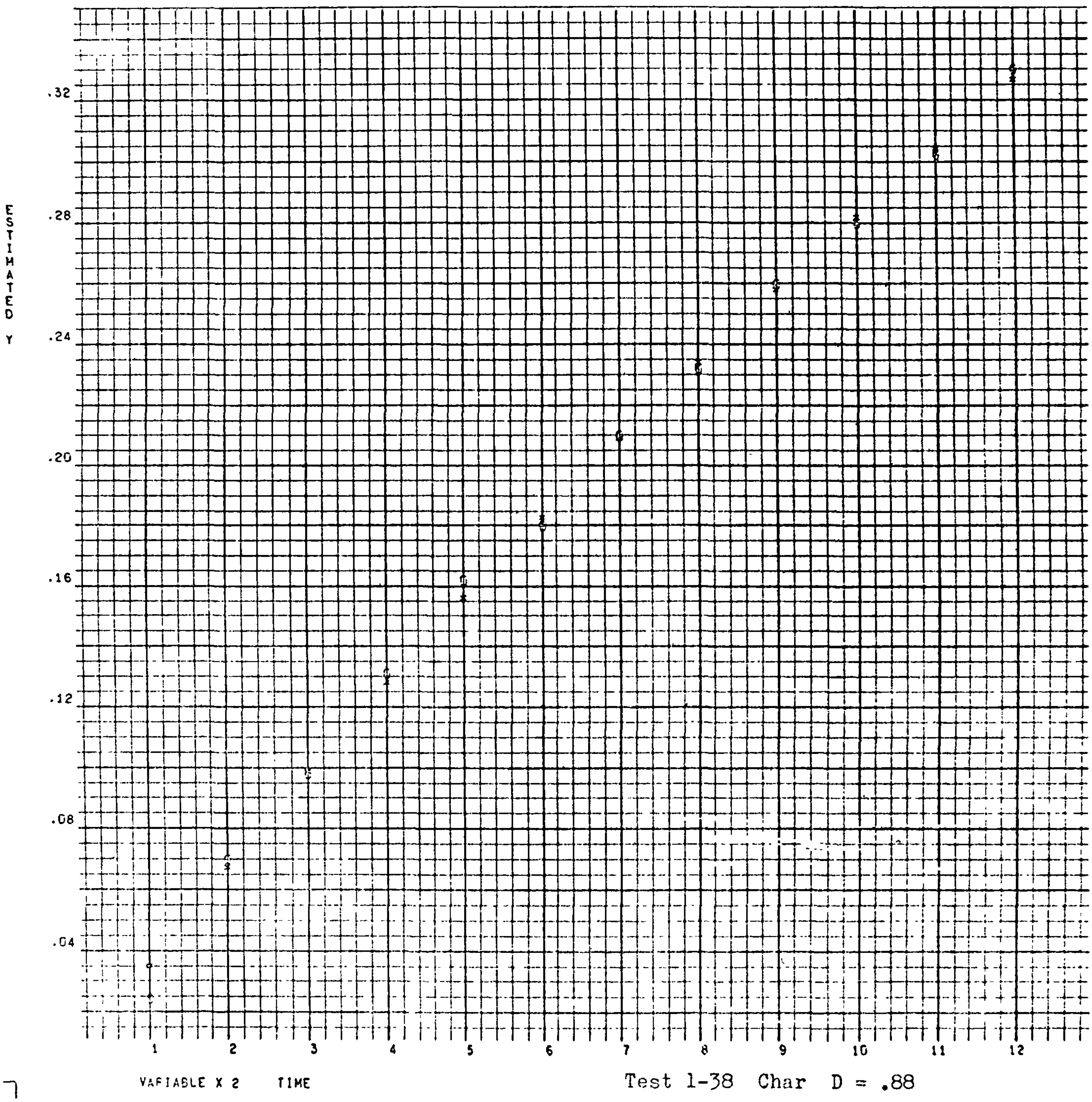

Test 1-38 Char D = .88

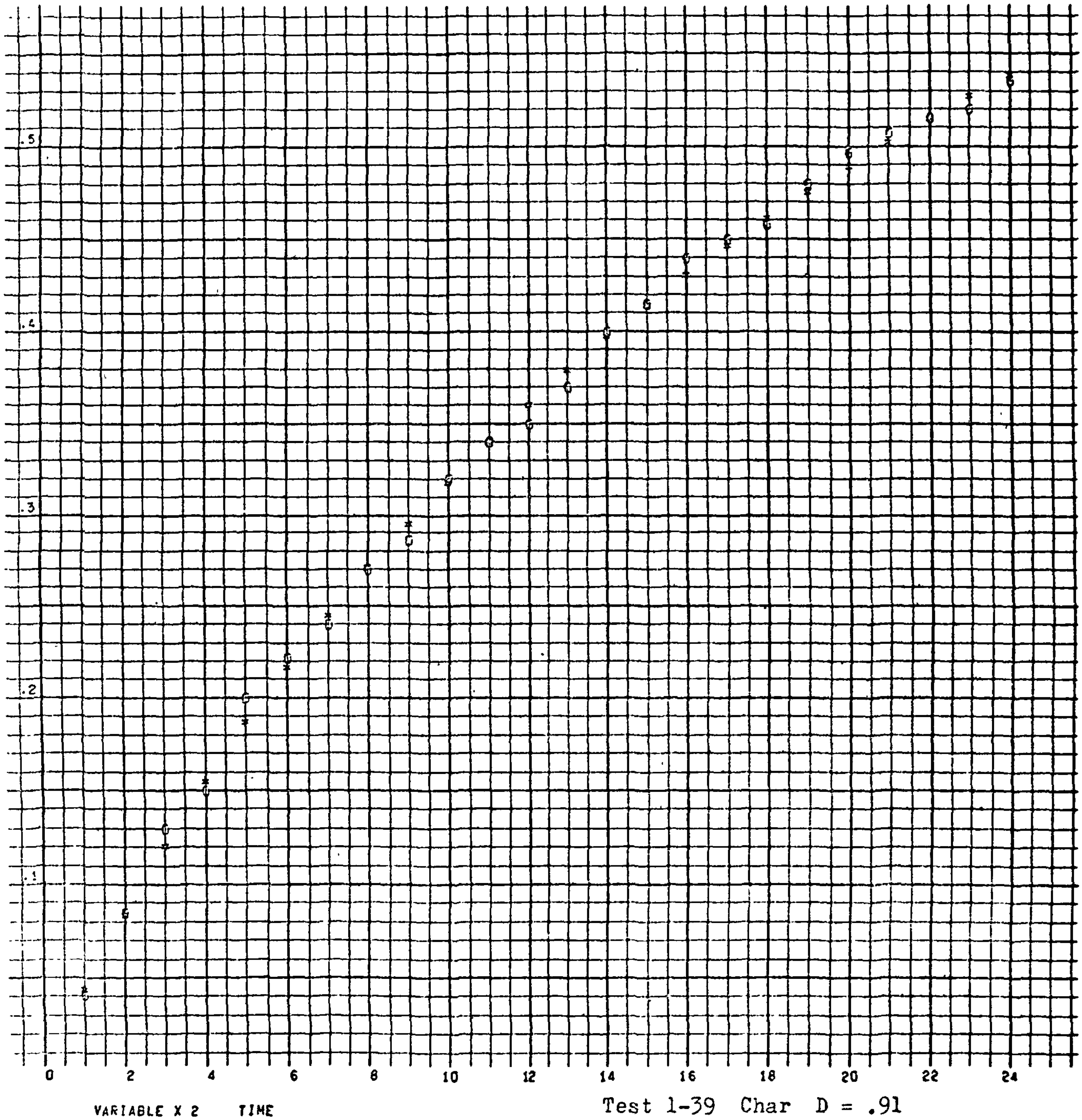

Test 1-39 Char D = .91

8311-35
042 000

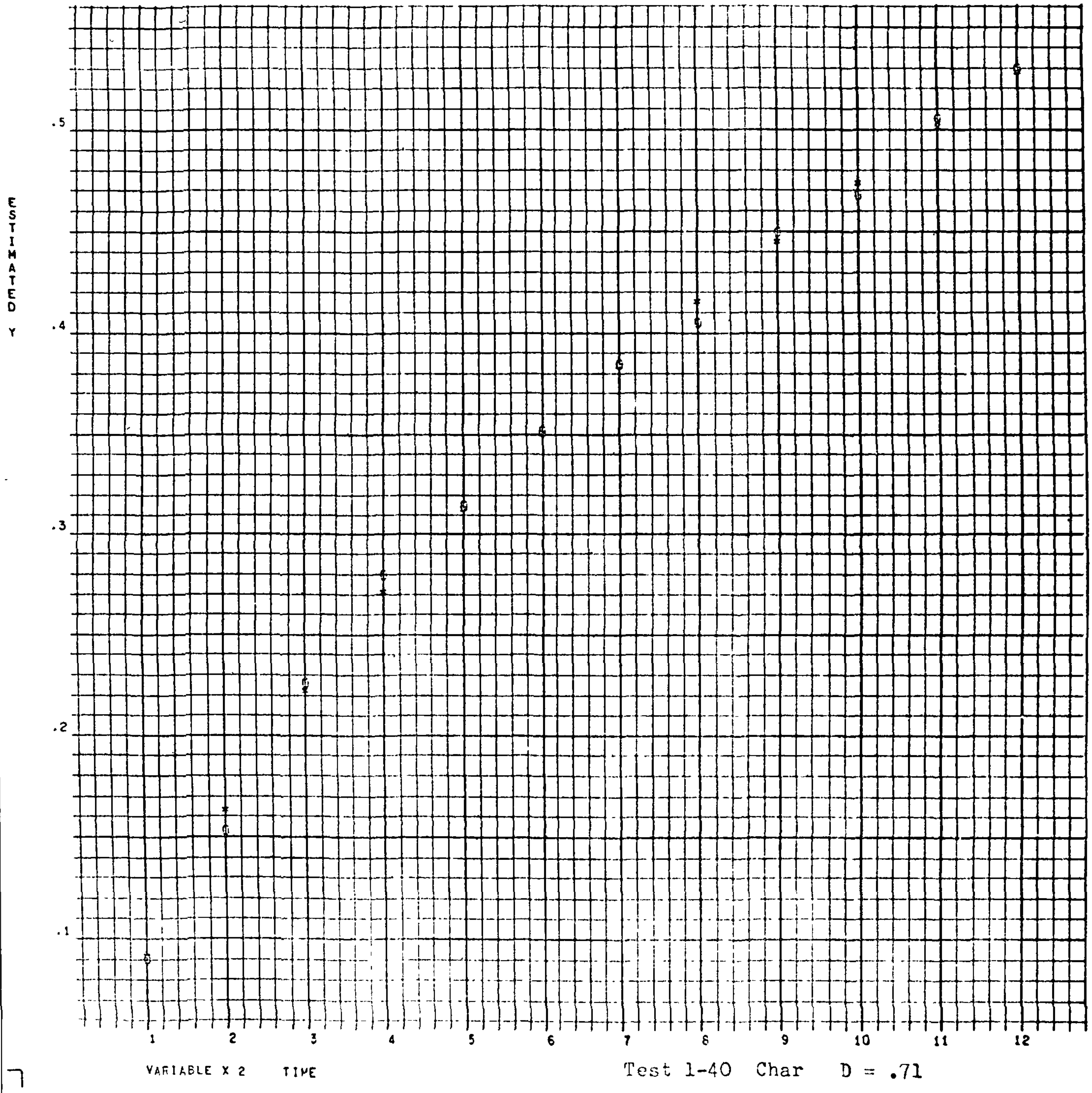

Test 1-40 Char D = .71

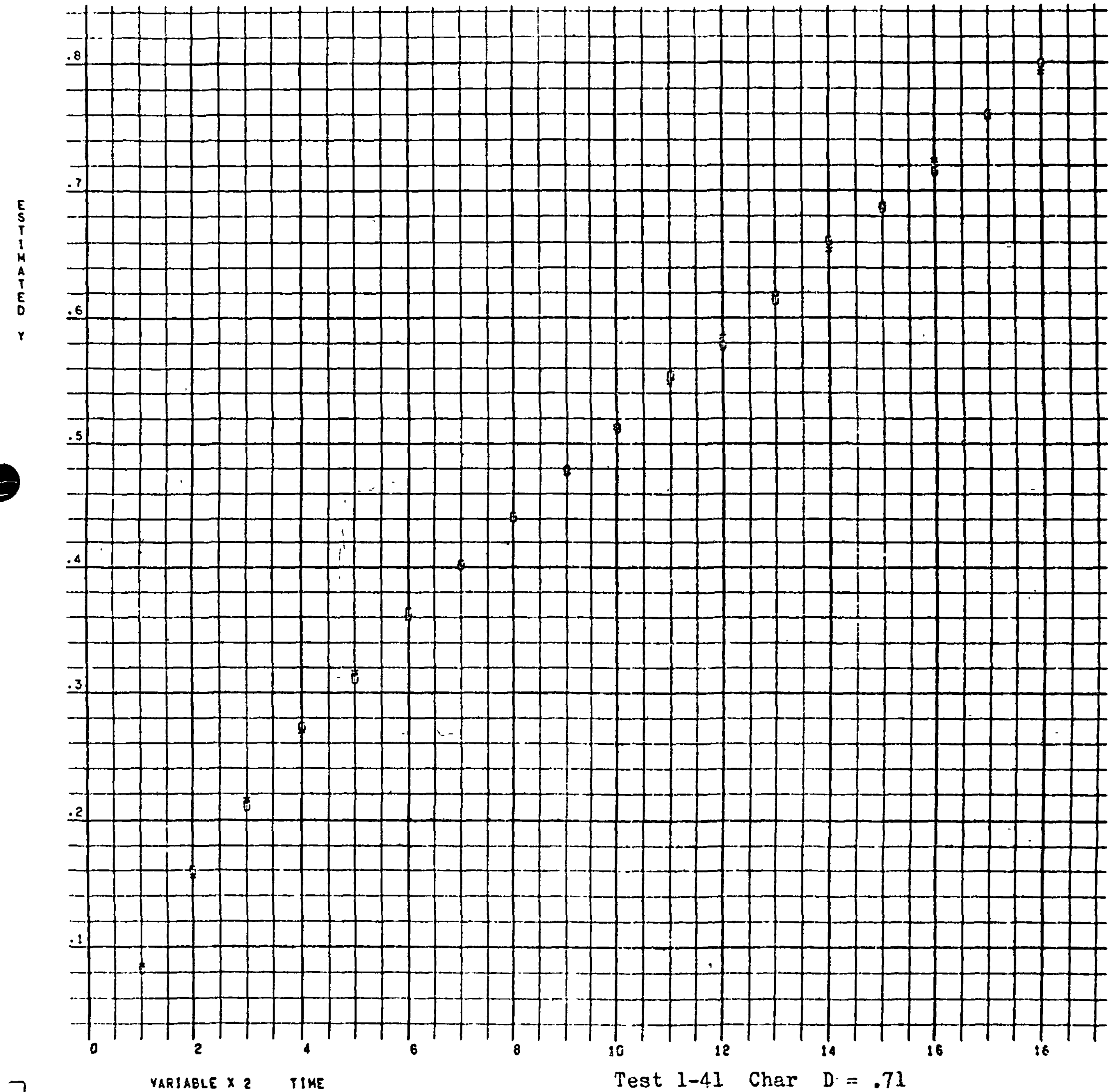

Test 1-41 Char D = .71

8311-31
038 000

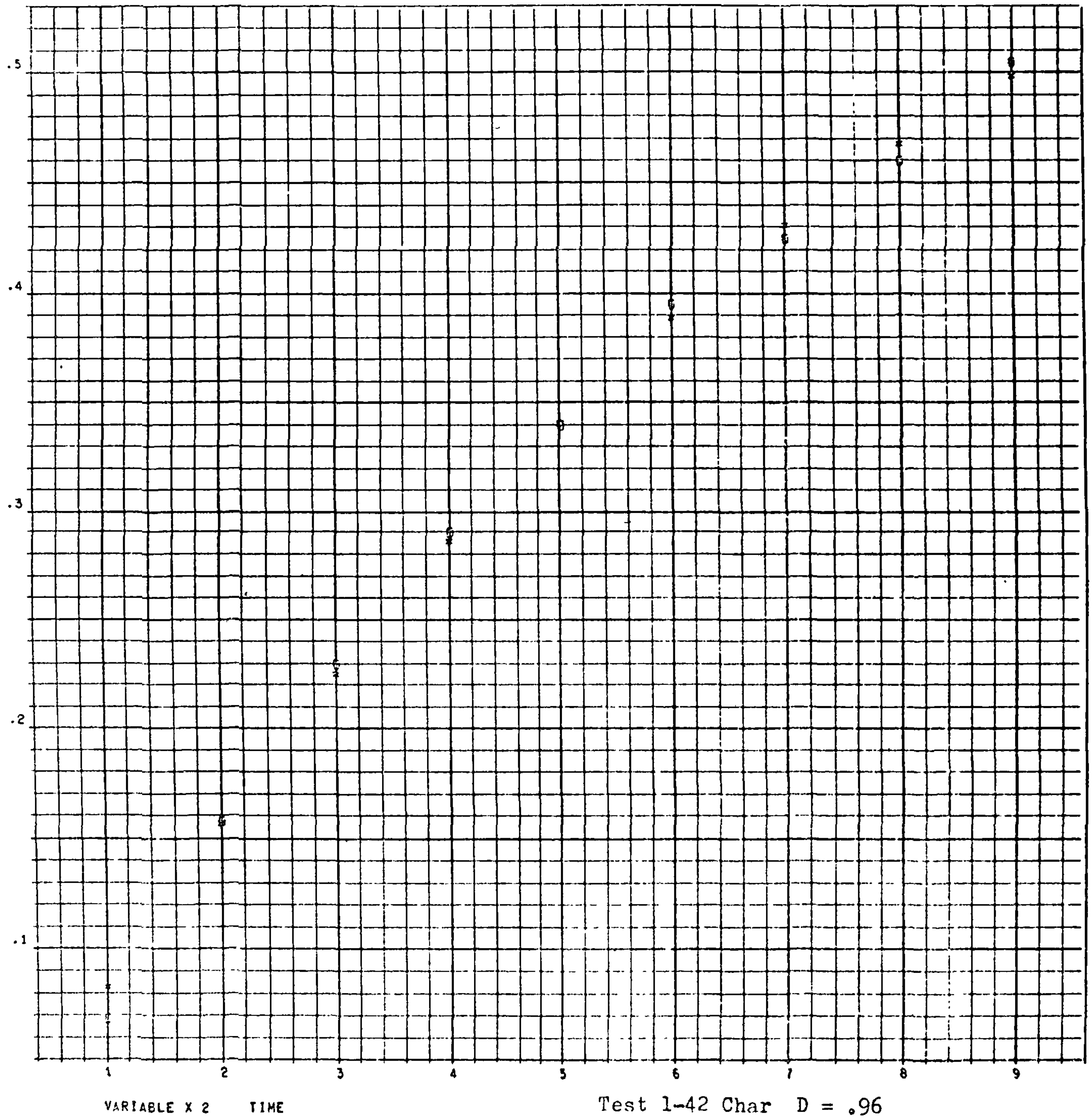

Test 1-42 Char D = .96

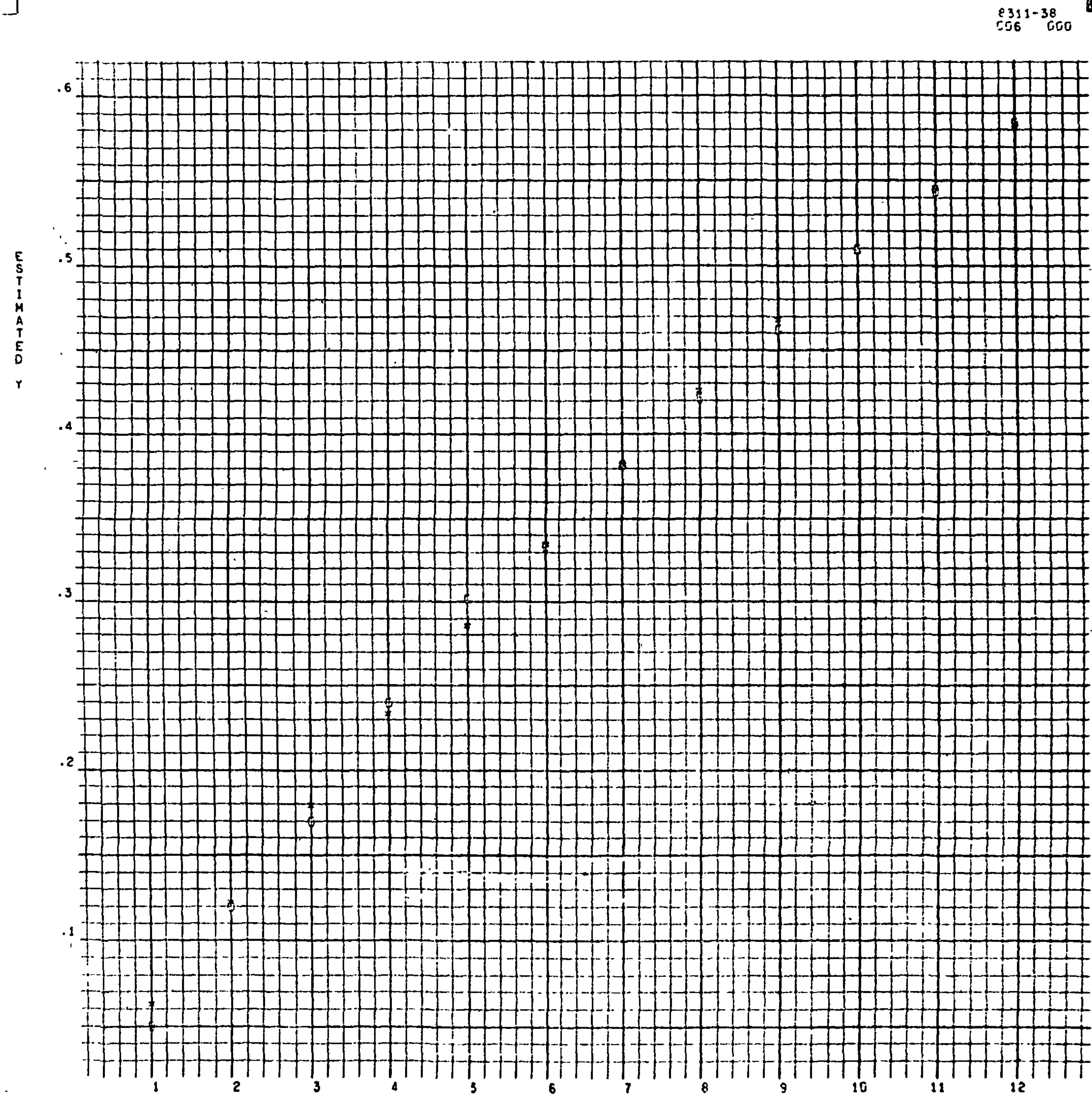

Test 1-43 Char D = .98

8311-35
035 000

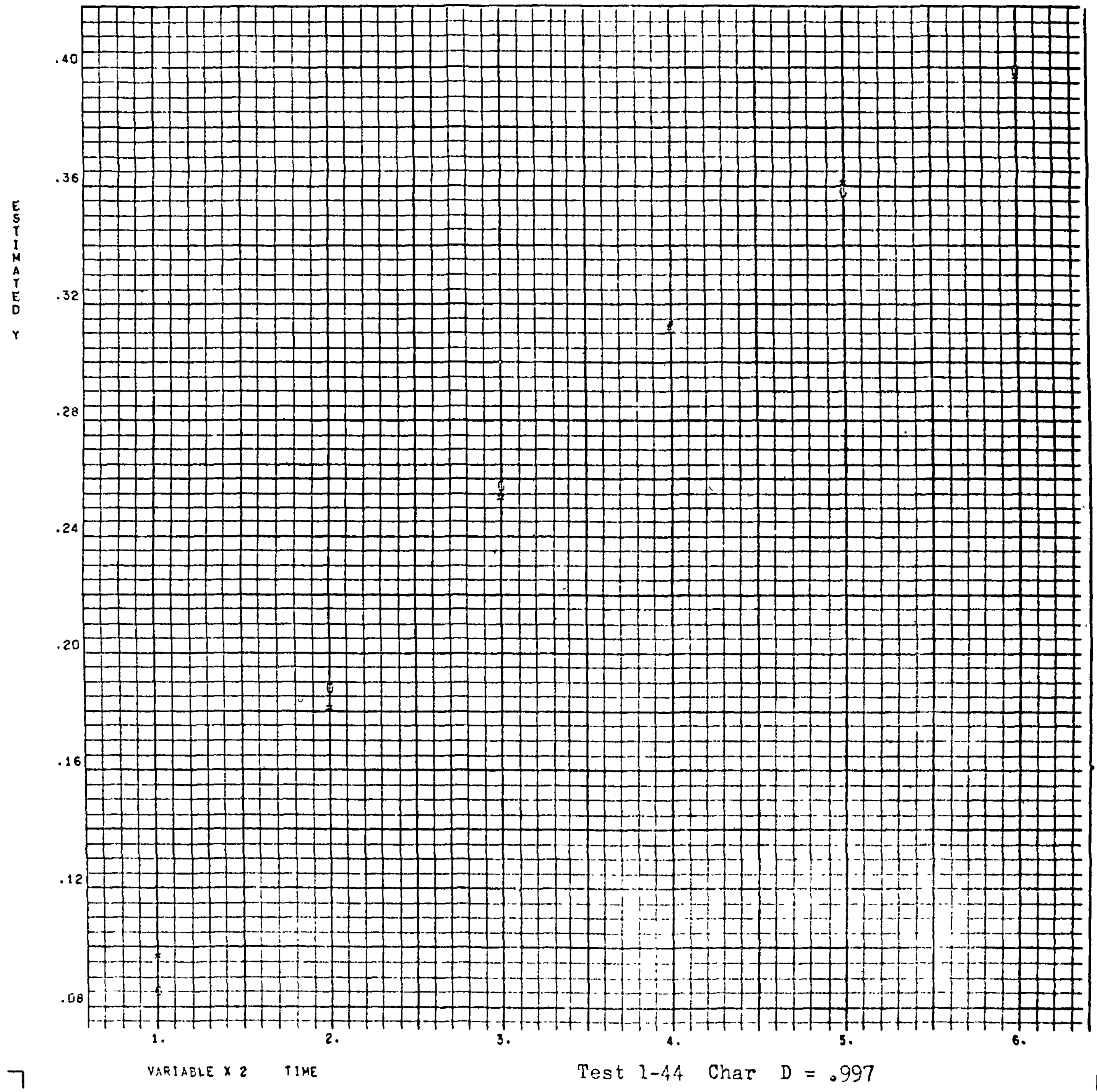

Test 1-44 Char D = .997

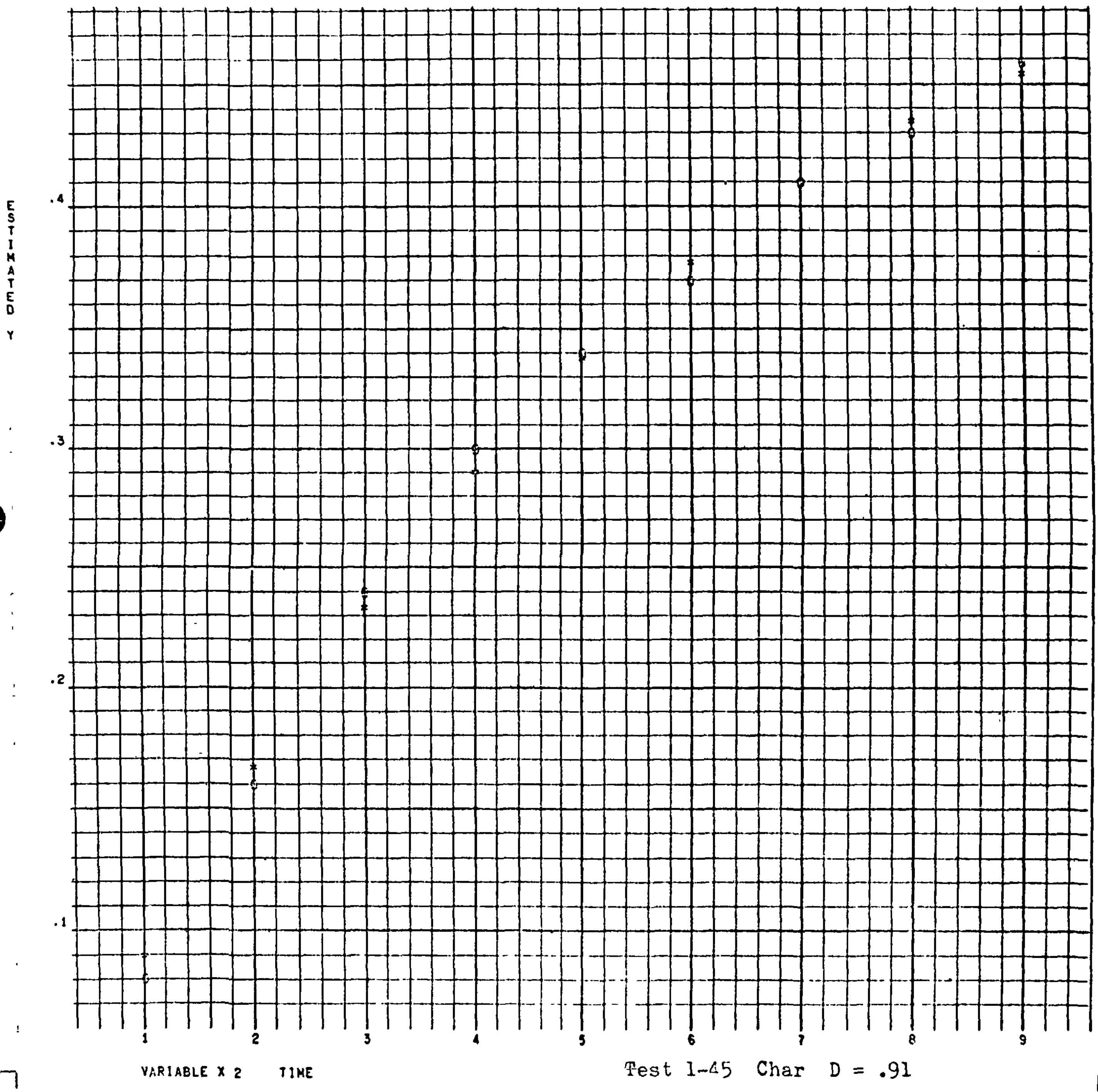

Test 1-45 Char D = .91

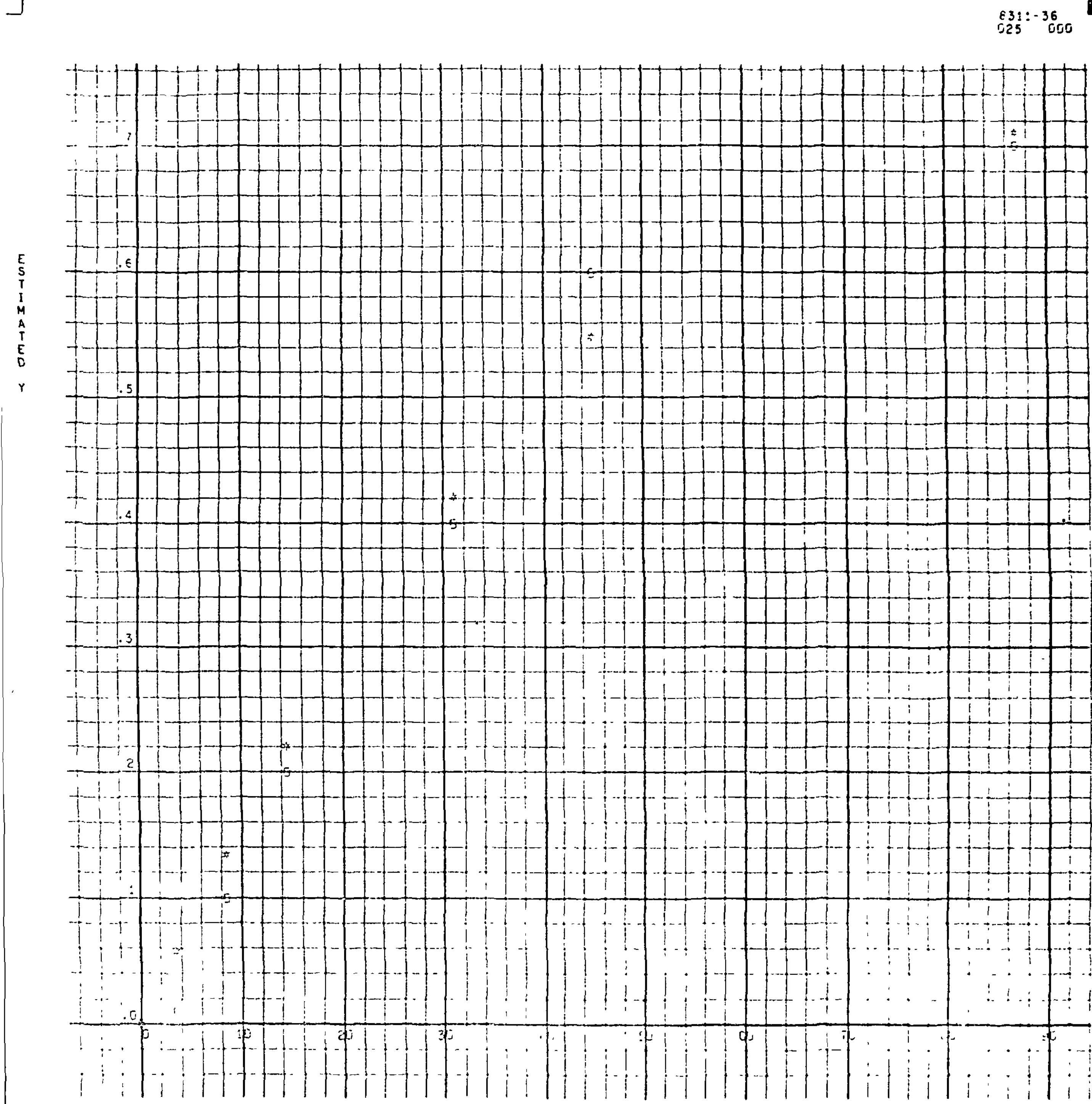

Test 2-14 Char D = .999

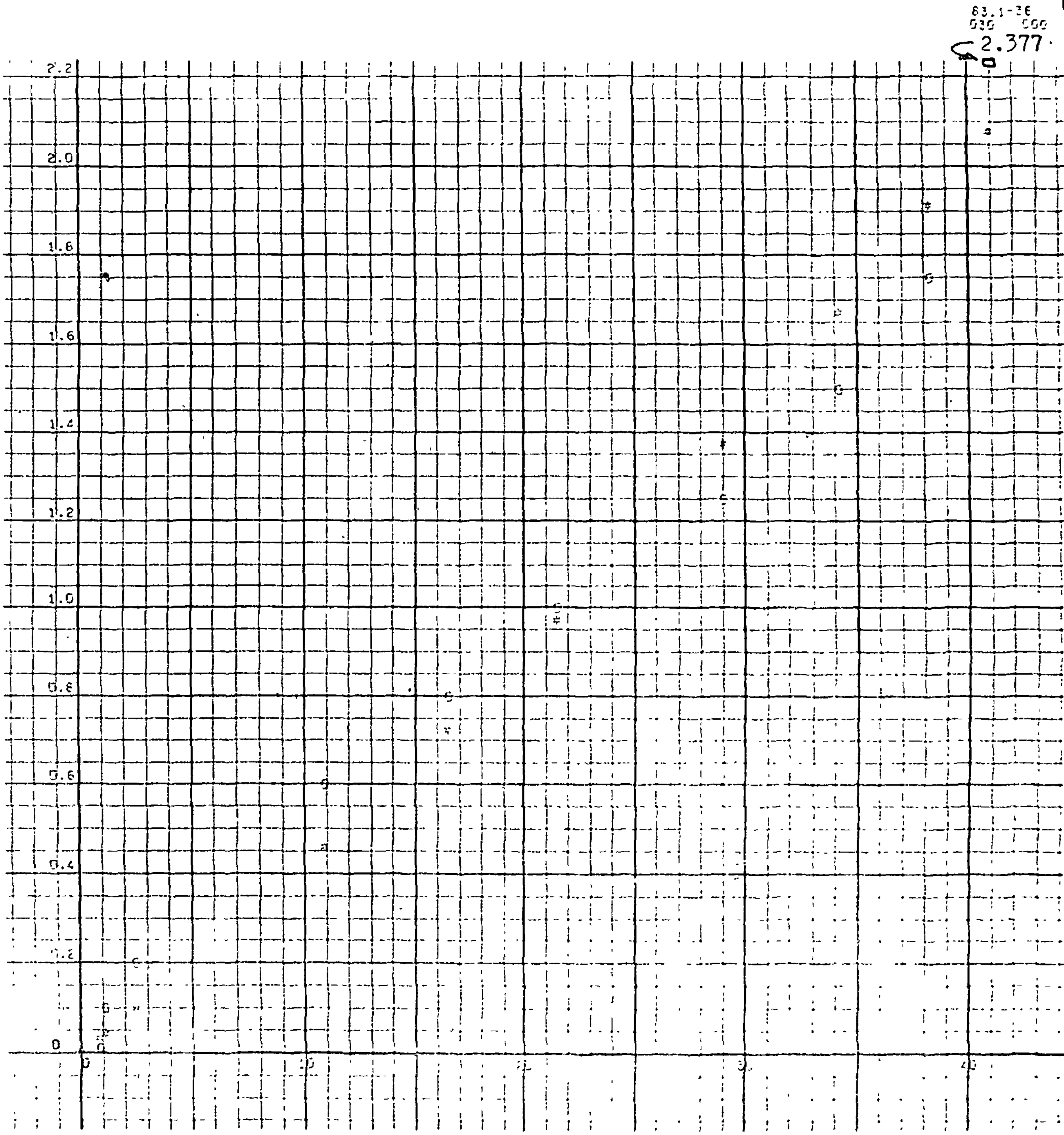

Test 2-15 Char D = .999

8311-32
043 000

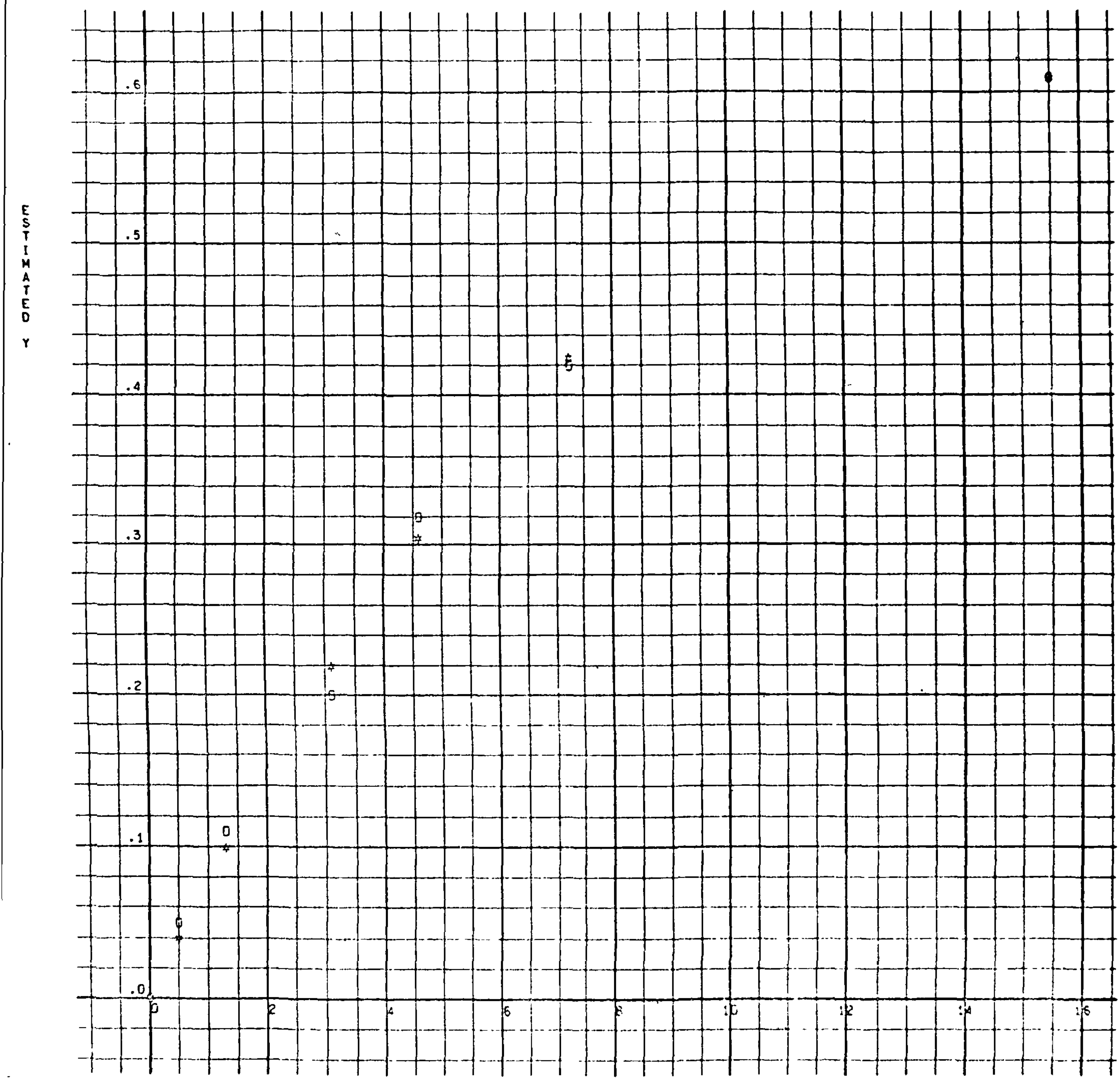

Test 2-21 Char D = .92

8311-36
038 000

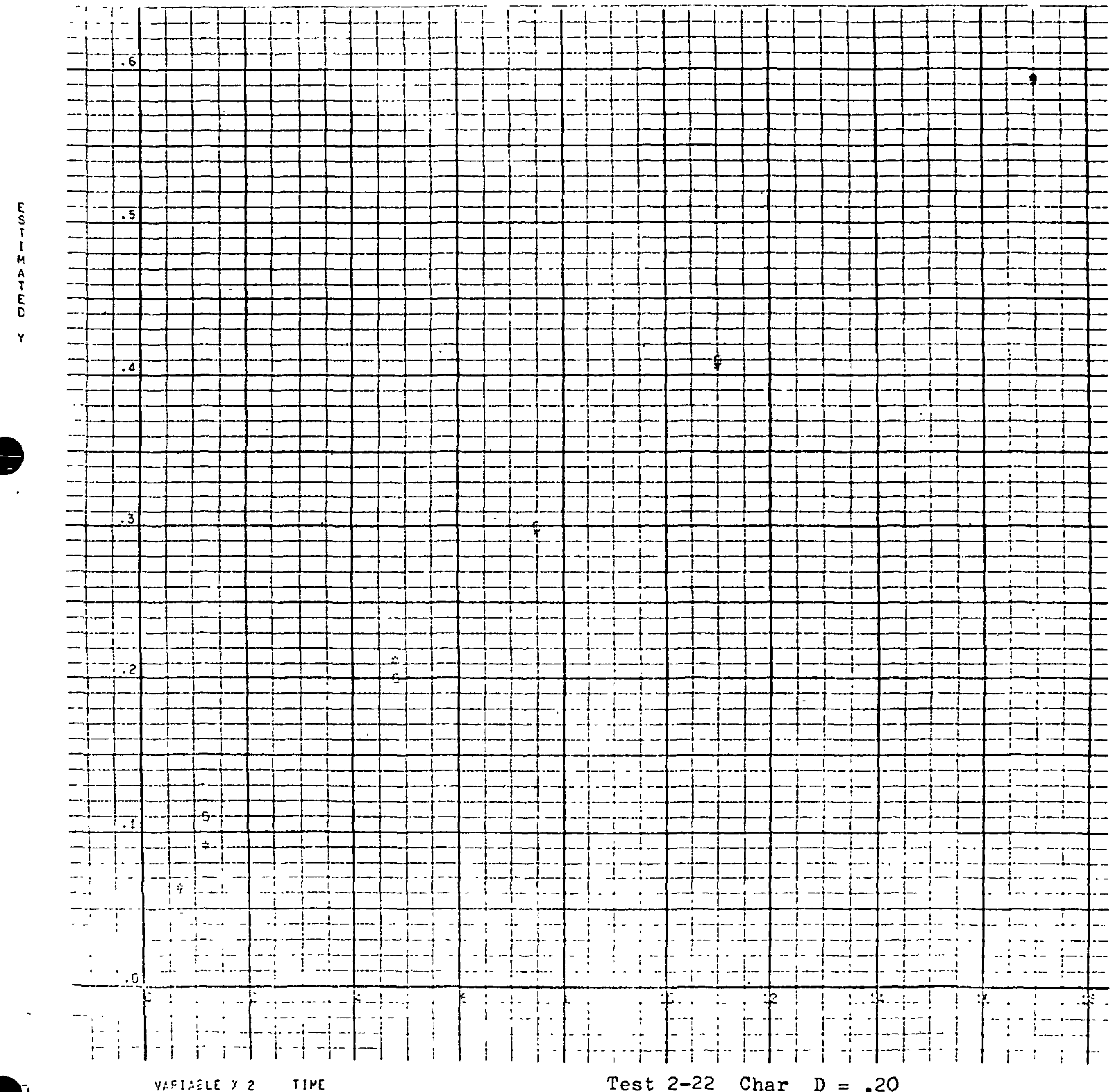

Test 2-22 Char D = .20

8311-36
041 000

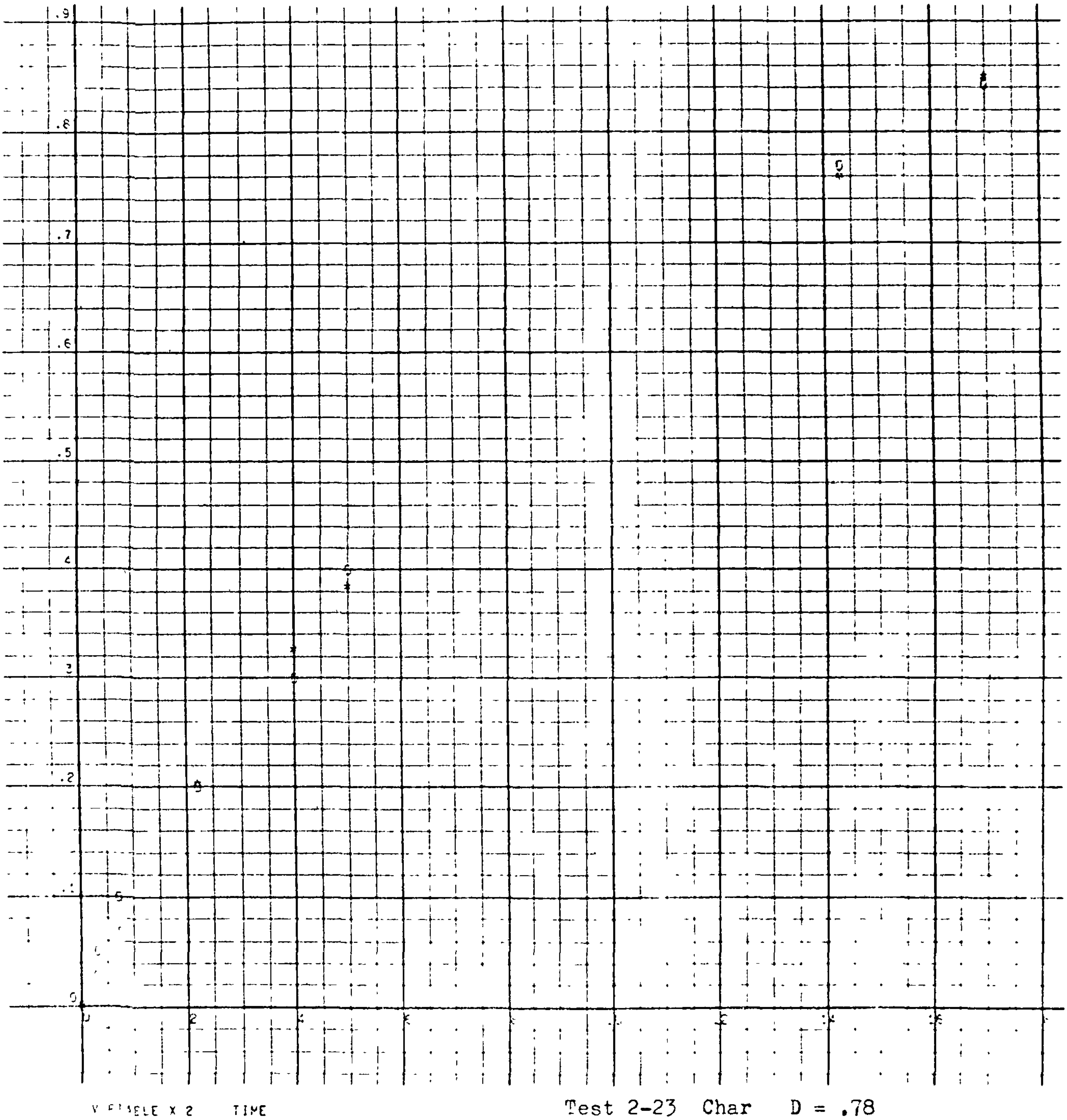

Test 2-23 Char D = .78

P-6215

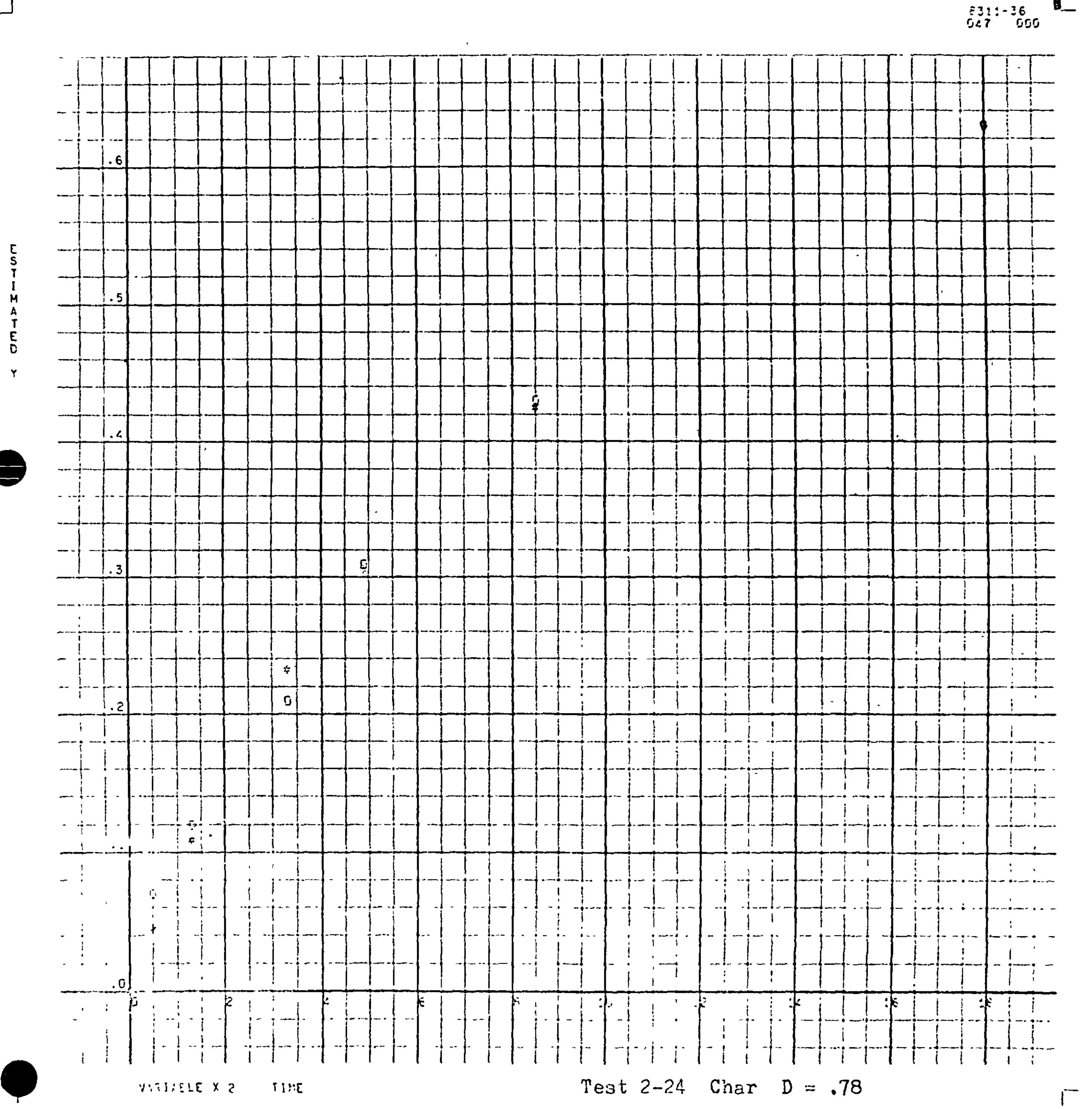

Test 2-24 Char D = .78

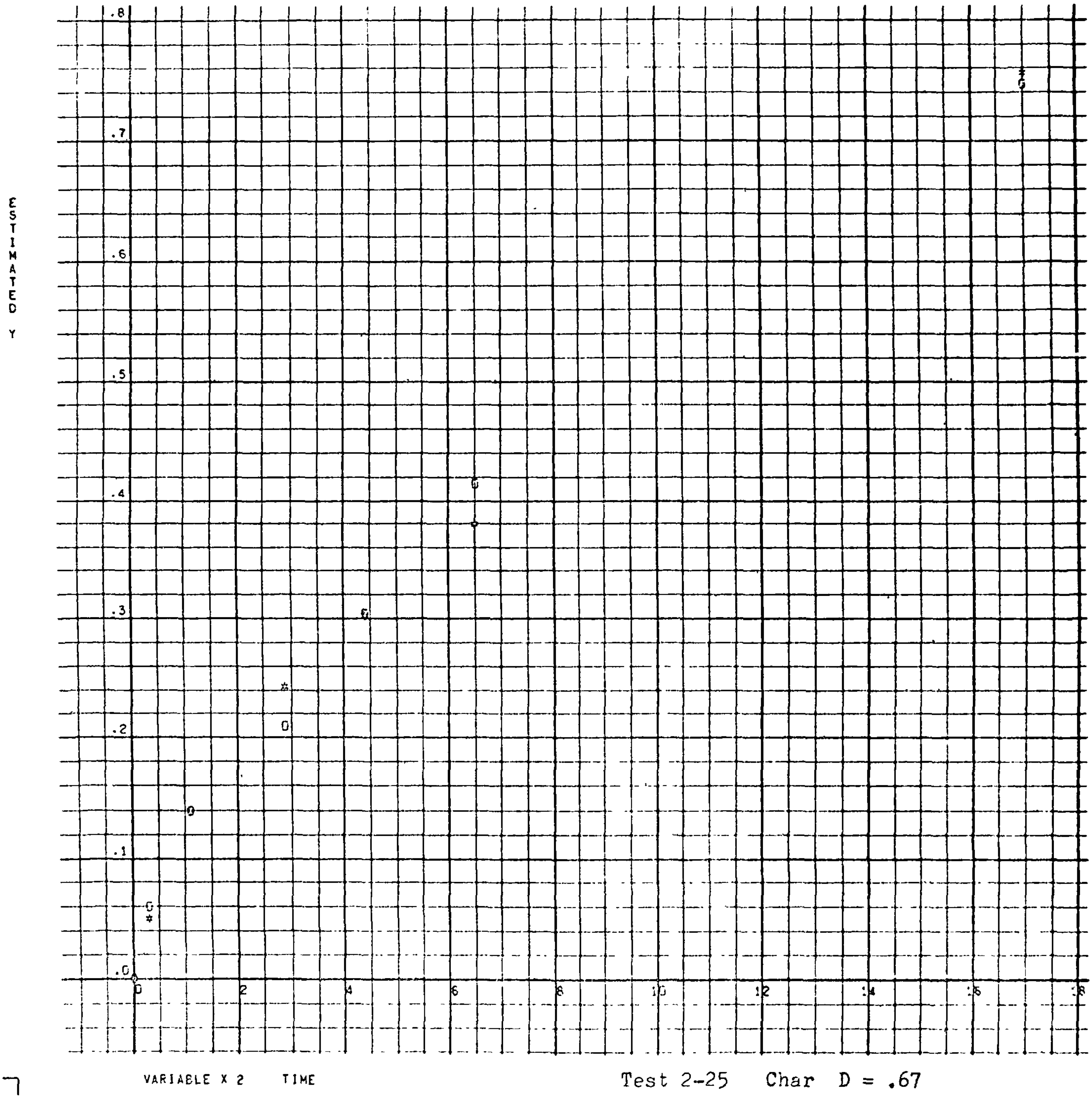

Test 2-25 Char D = .67

8311-32
070 000

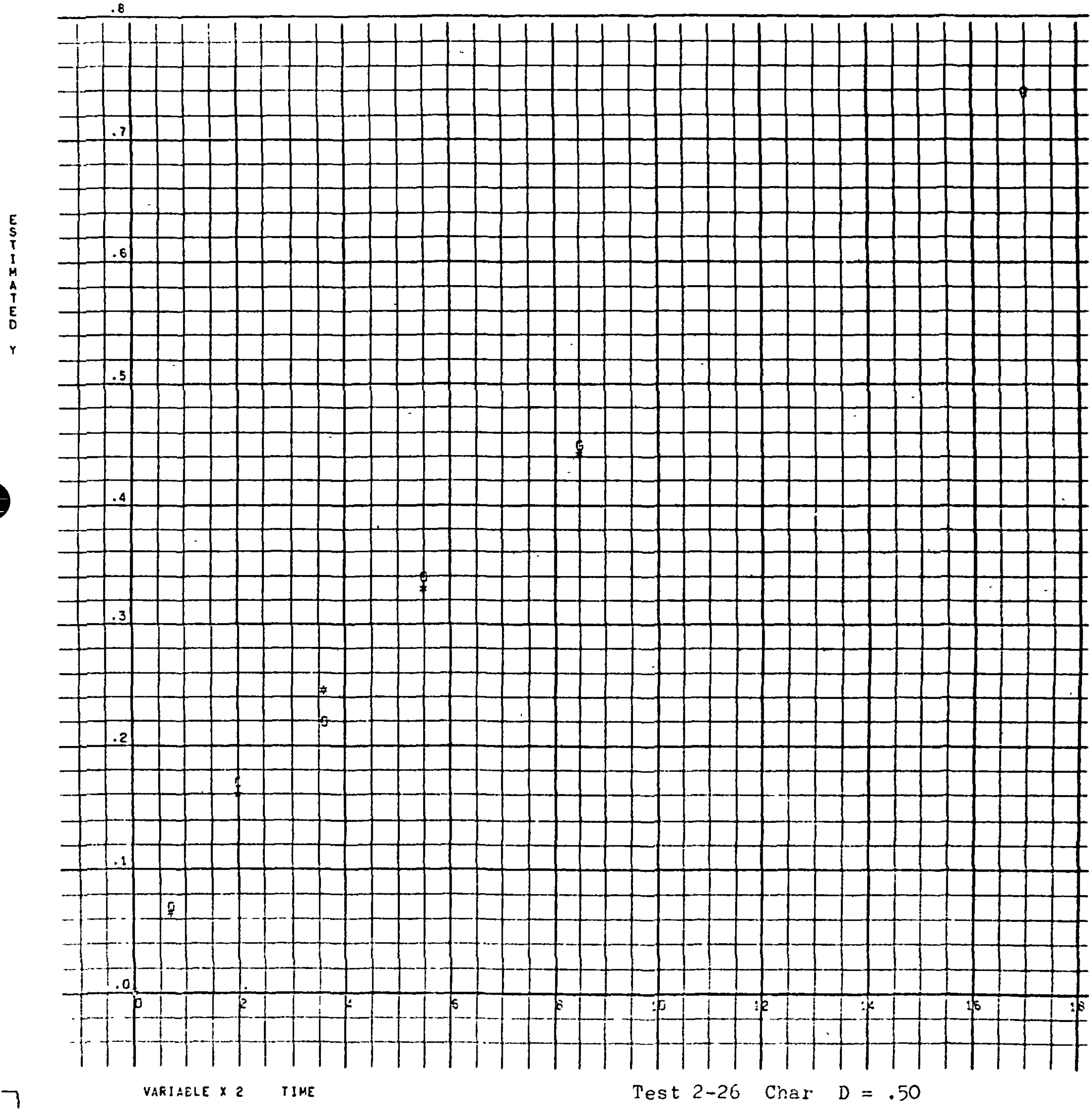

Test 2-26 Char D = .50

8311-32
075 000

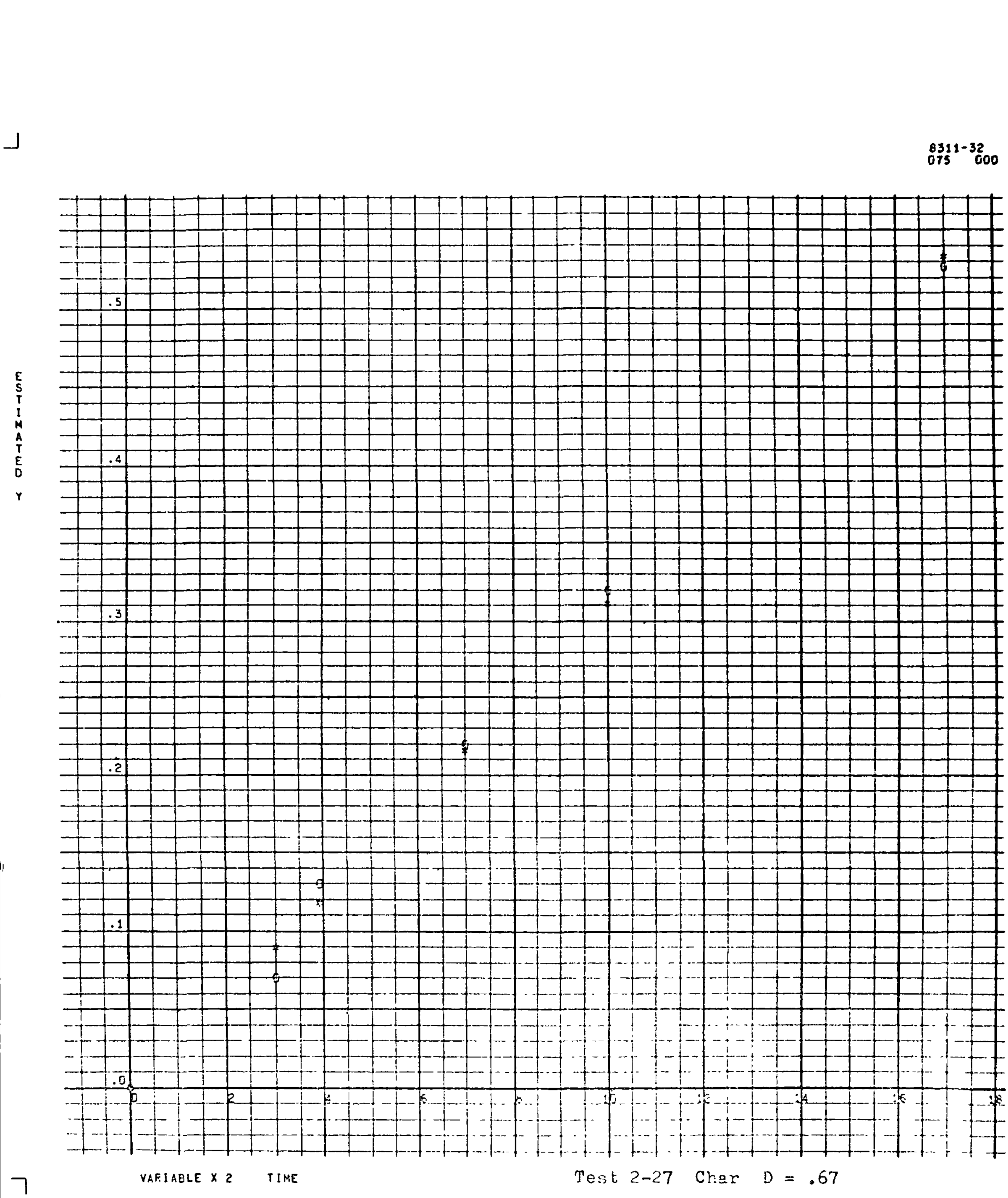

Test 2-27 Char D = .67

8311-46
001 000

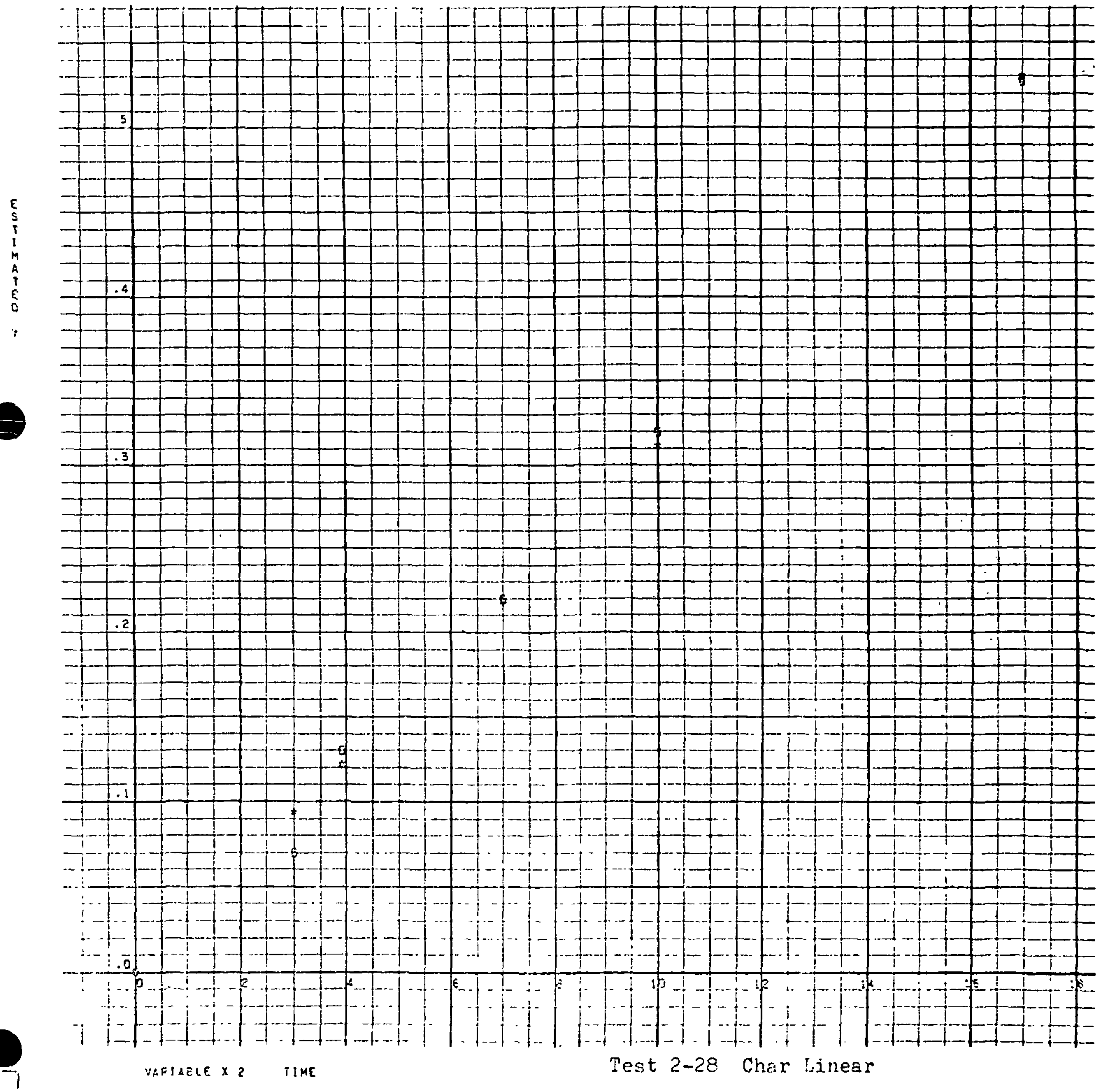

Test 2-28 Char Linear

8311-46
002 000

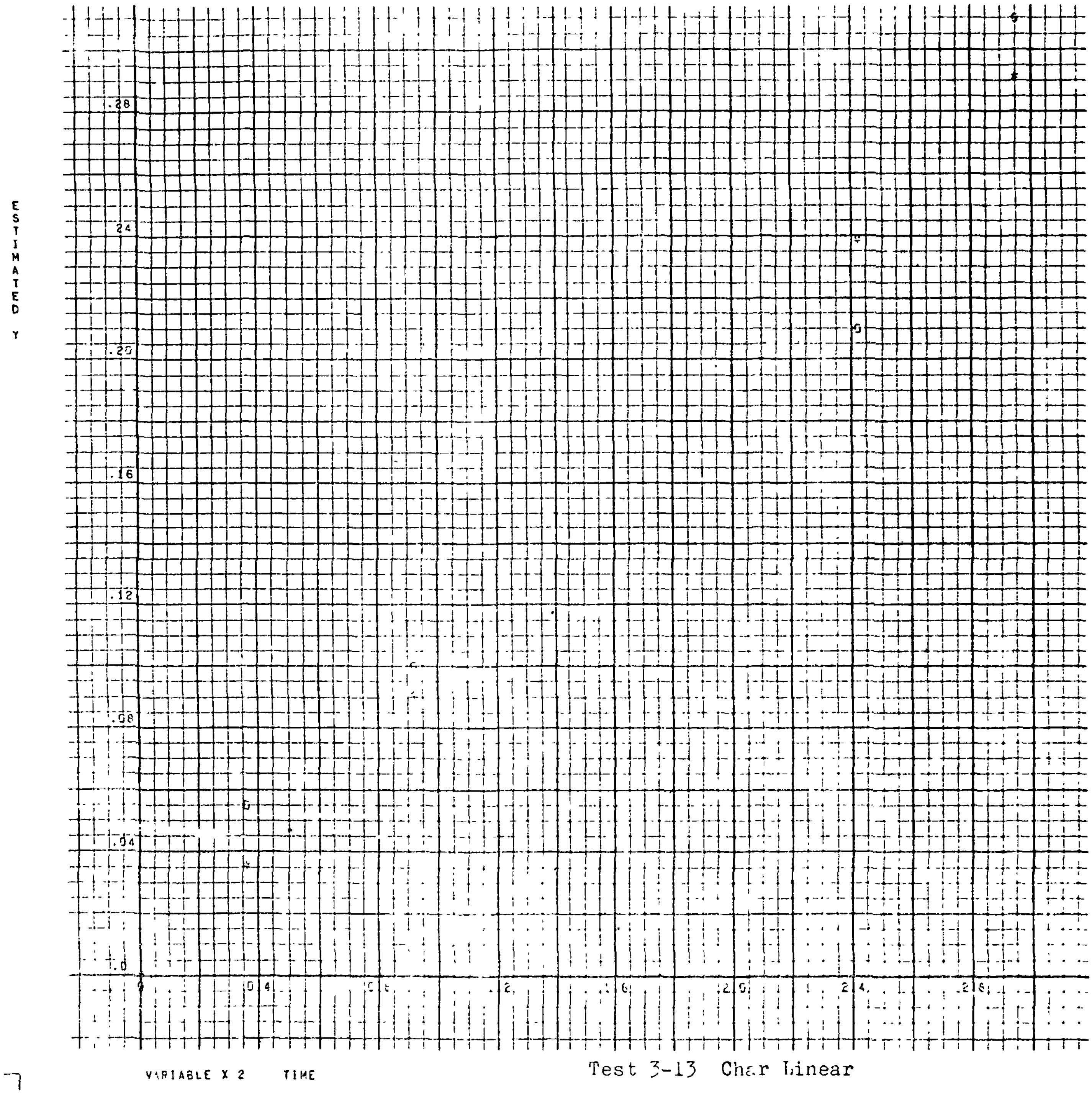

Test 3-13 Char Linear

8311-42
011 000

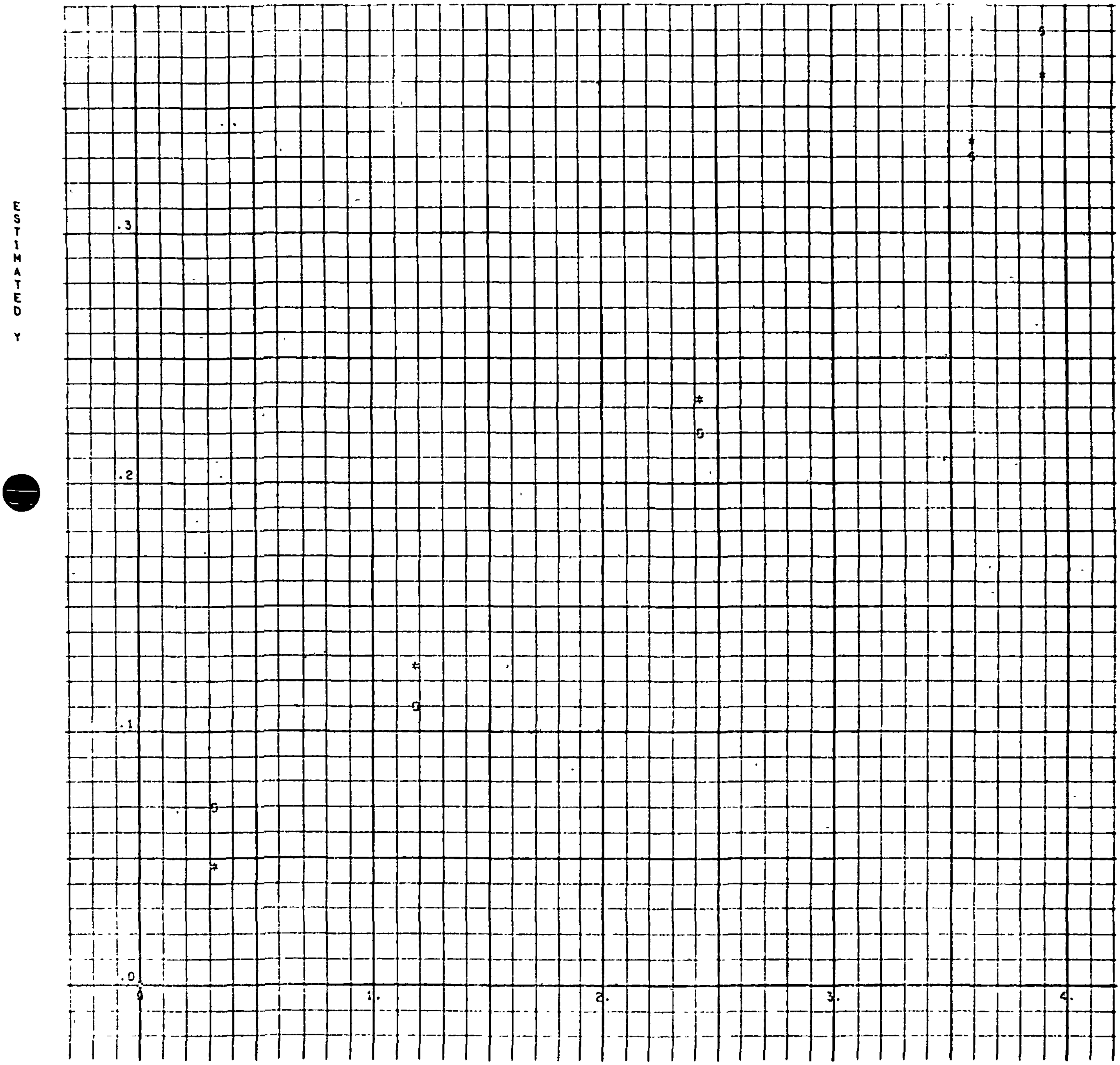

Test 3-14 Char D = .005

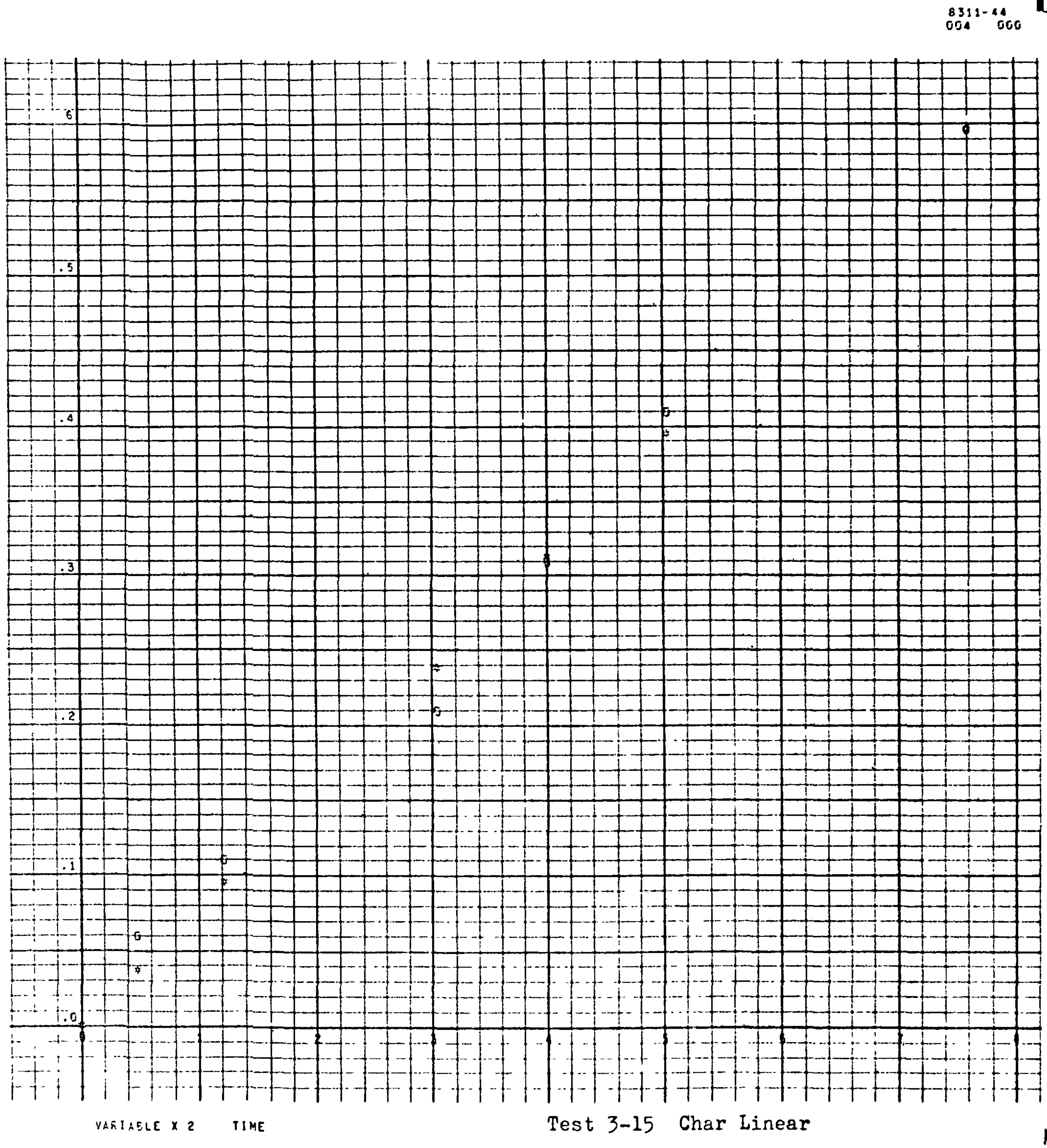

Test 3-15 Char Linear

8311-44
005 000

Test 3-16 Char Linear

R-6215

8311-46
004 000

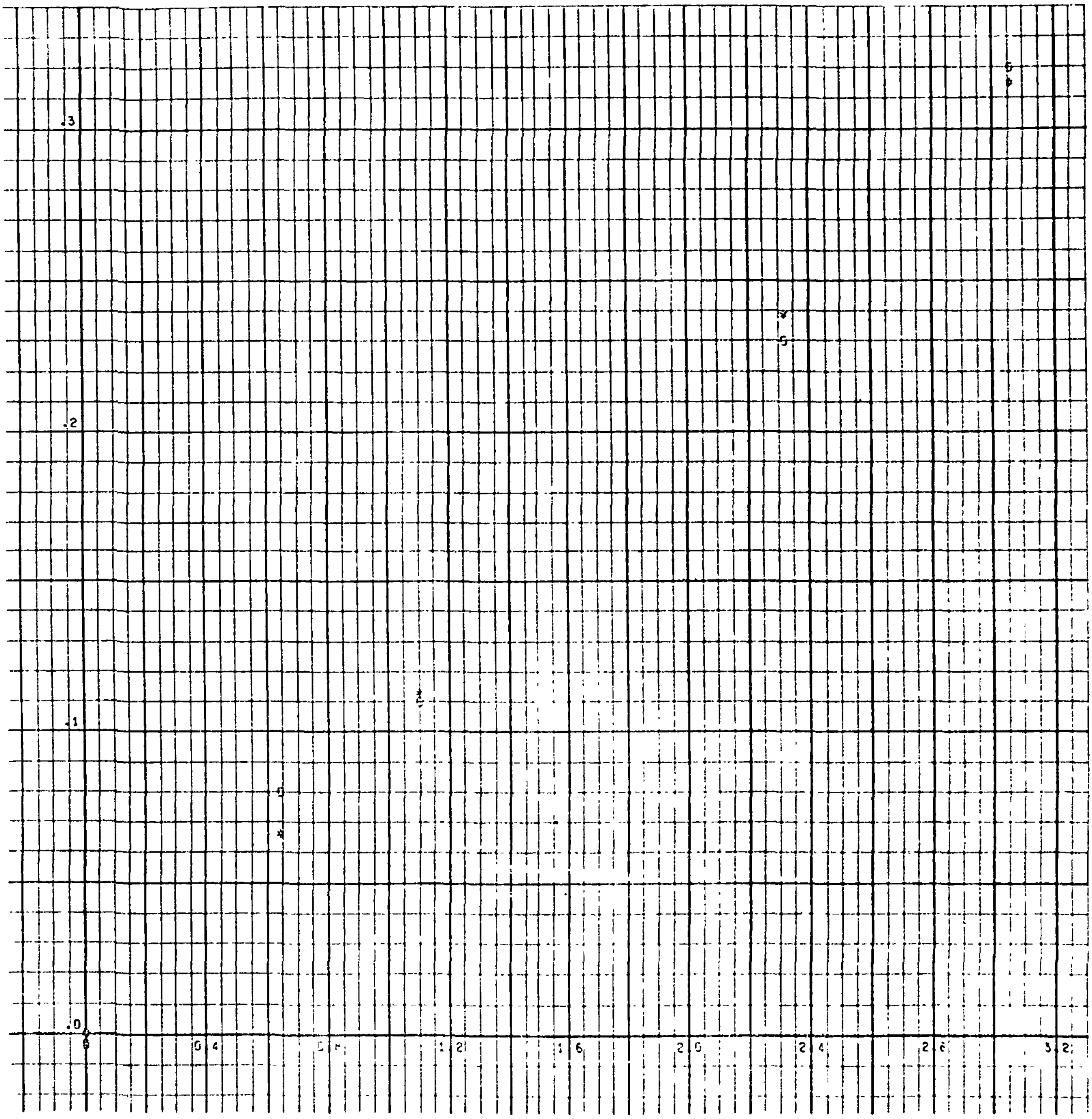

VARIABLE X 2 TIME

Test 3-17 Char Linear

8311-42
021 000

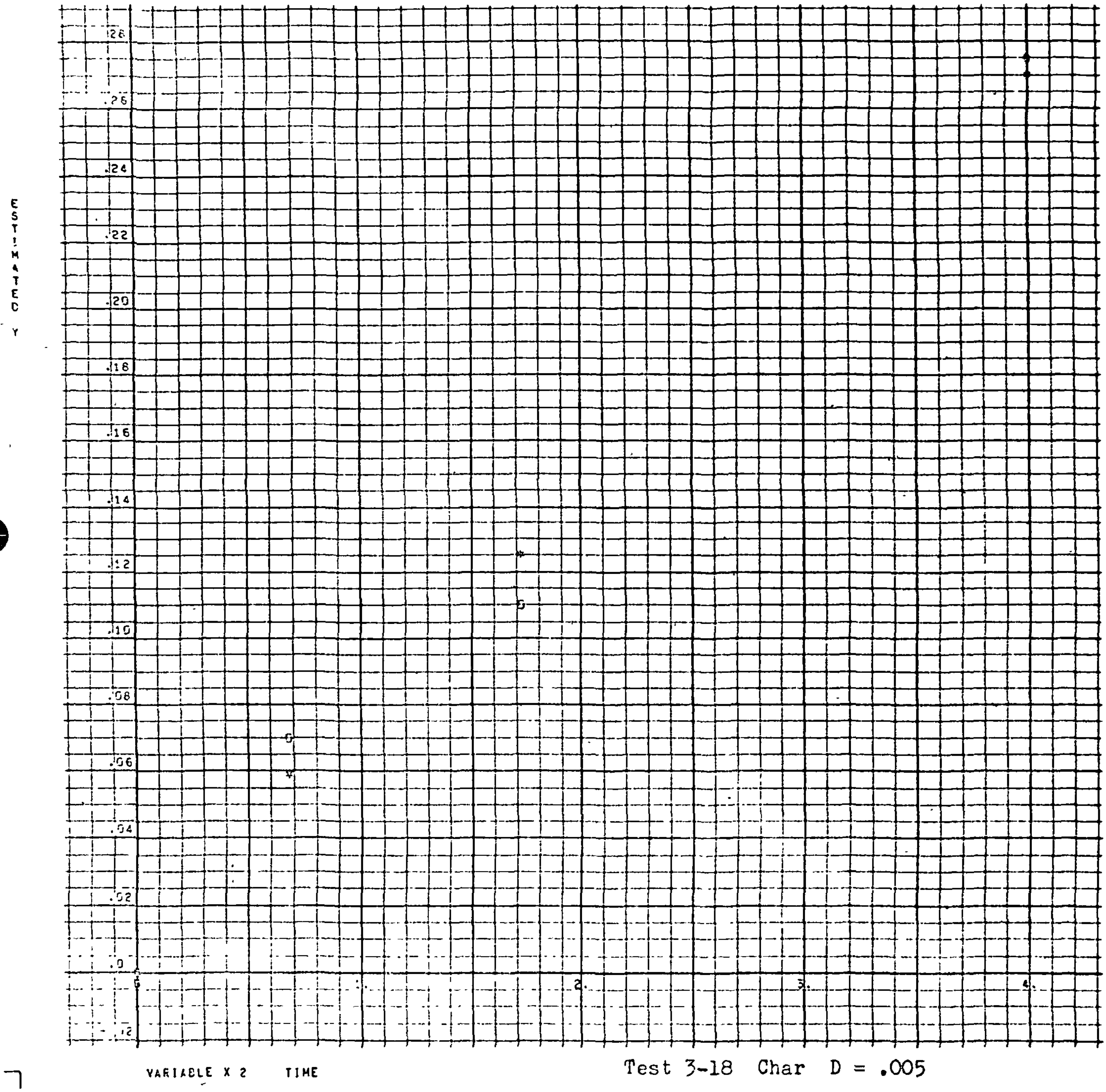

Test 3-18 Char D = .005

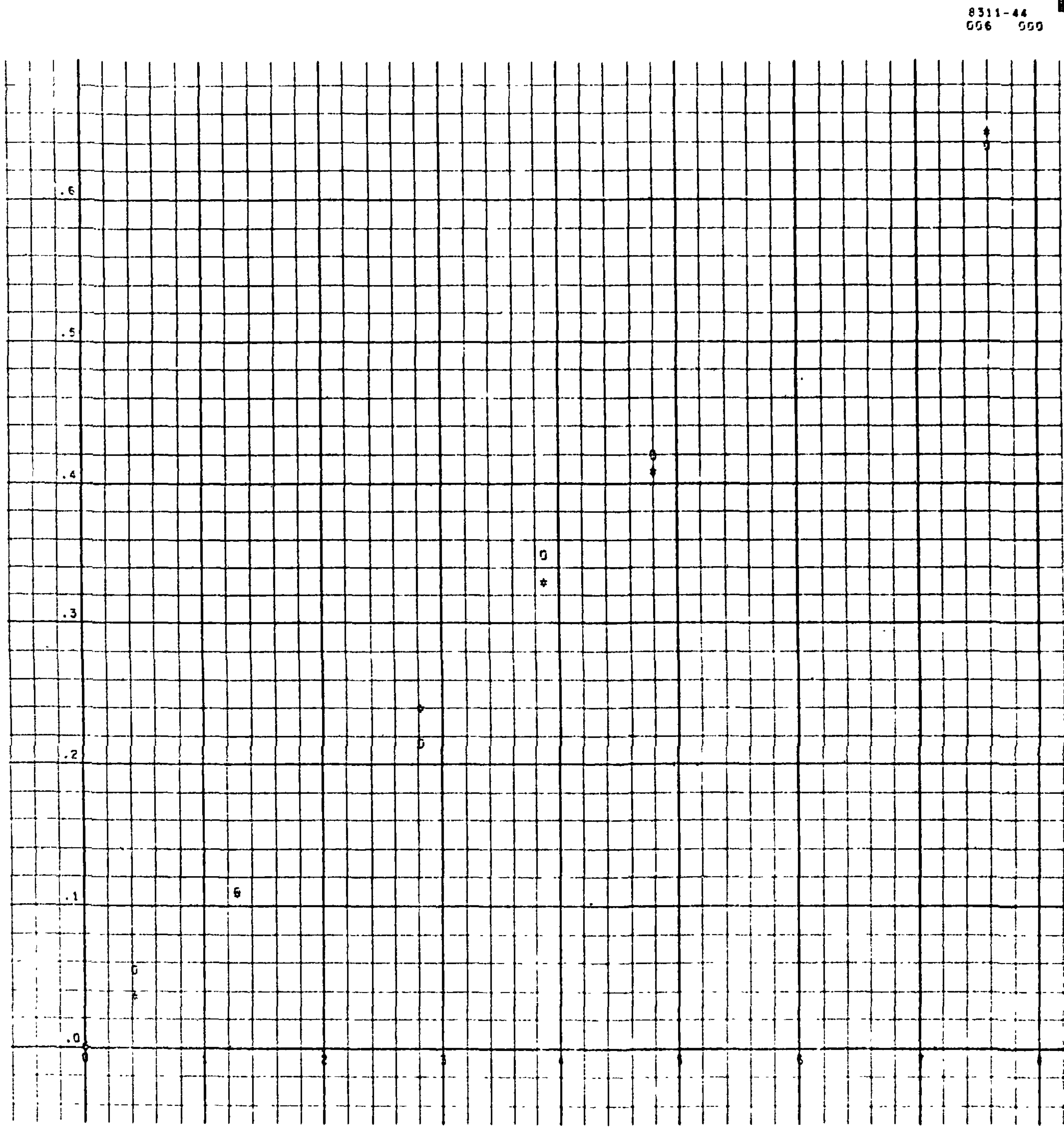

Test 3-19 Char Linear

8311-36
100 000

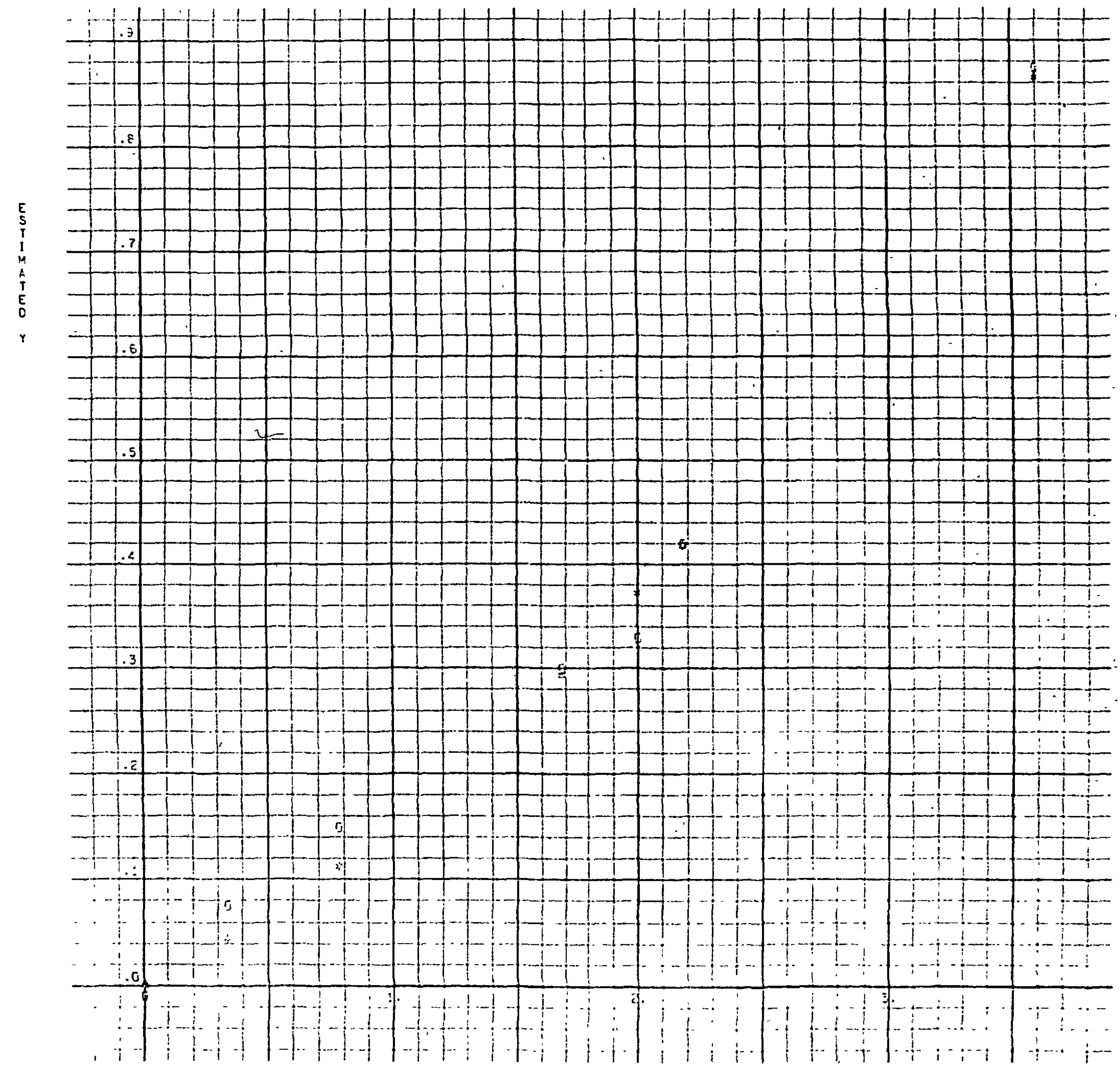

Test 3-20 Char D = .999

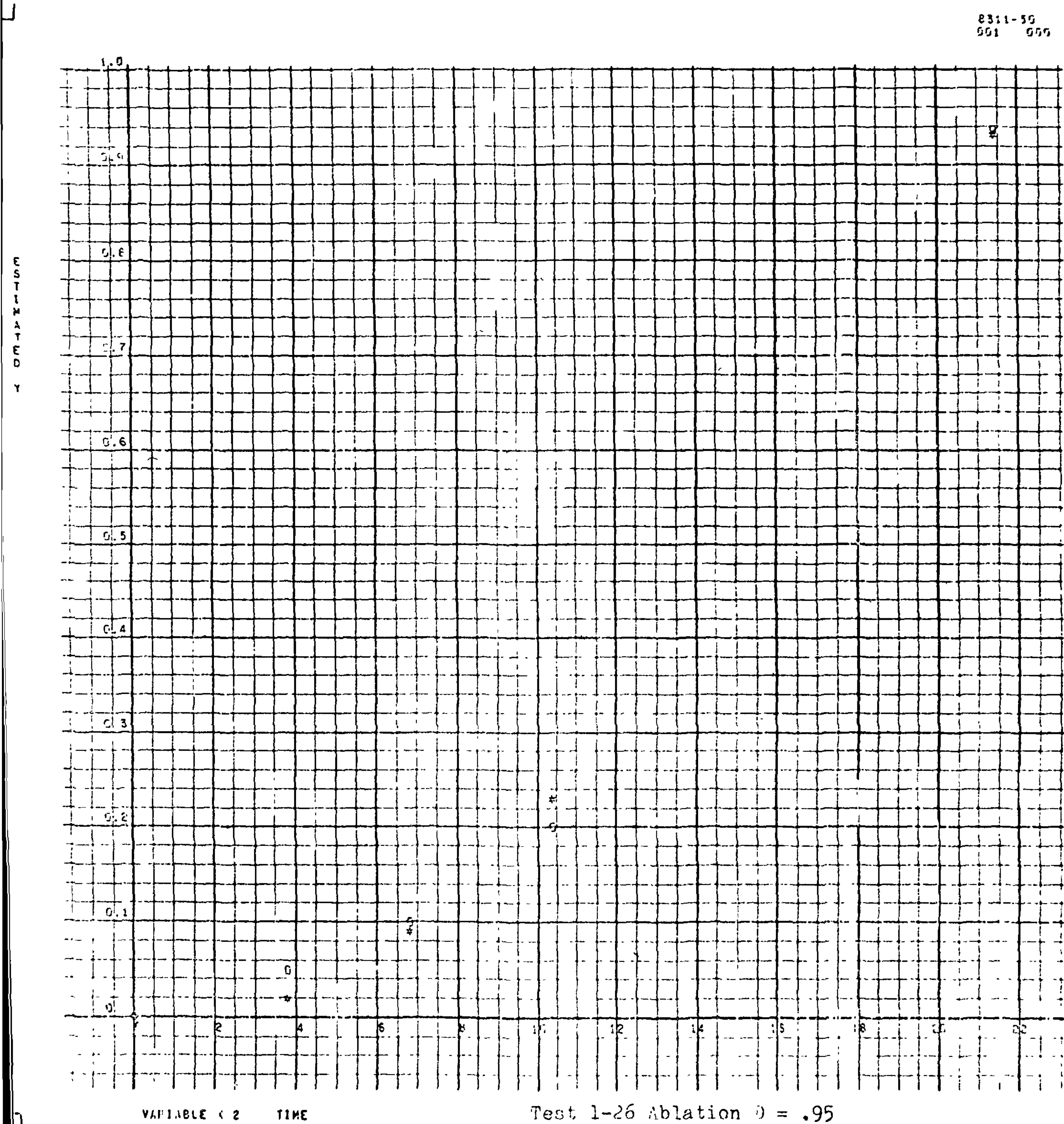

Test 1-26 Ablation θ = .95

Test 1-27 Ablation D = .95

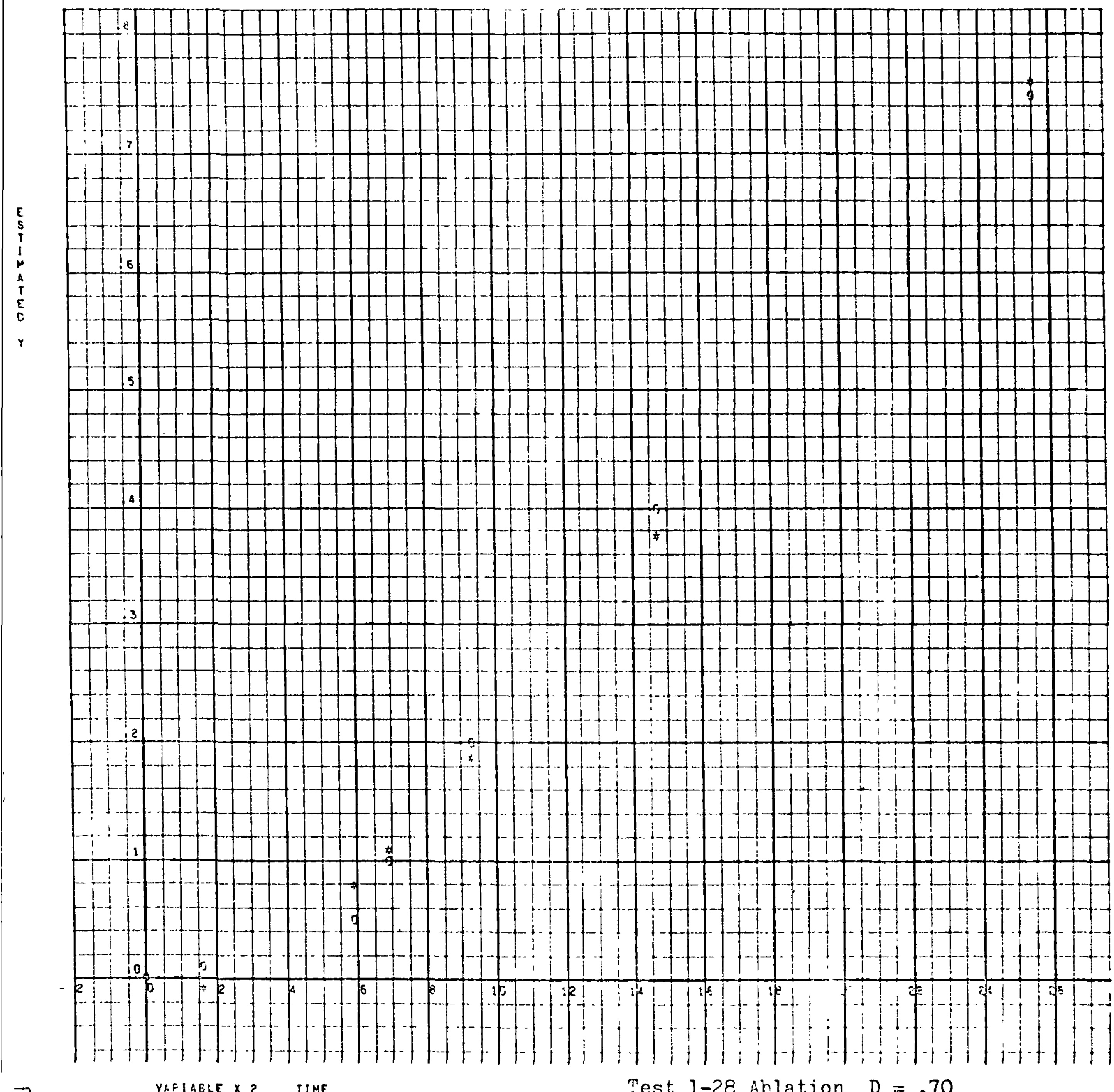

Test 1-28 Ablation D = .70

8311-49
021 000

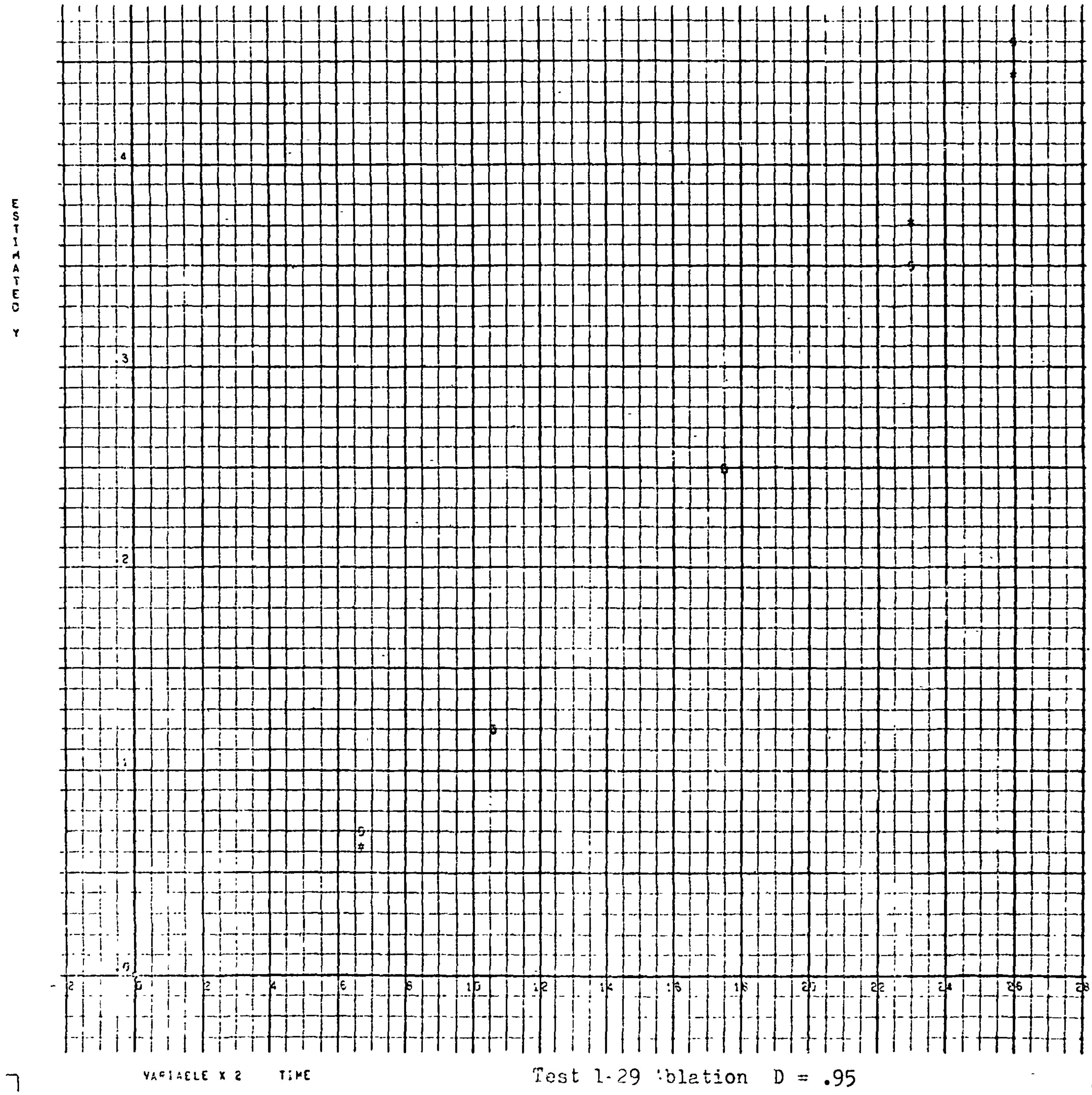

Test 1-29 Ablation D = .95

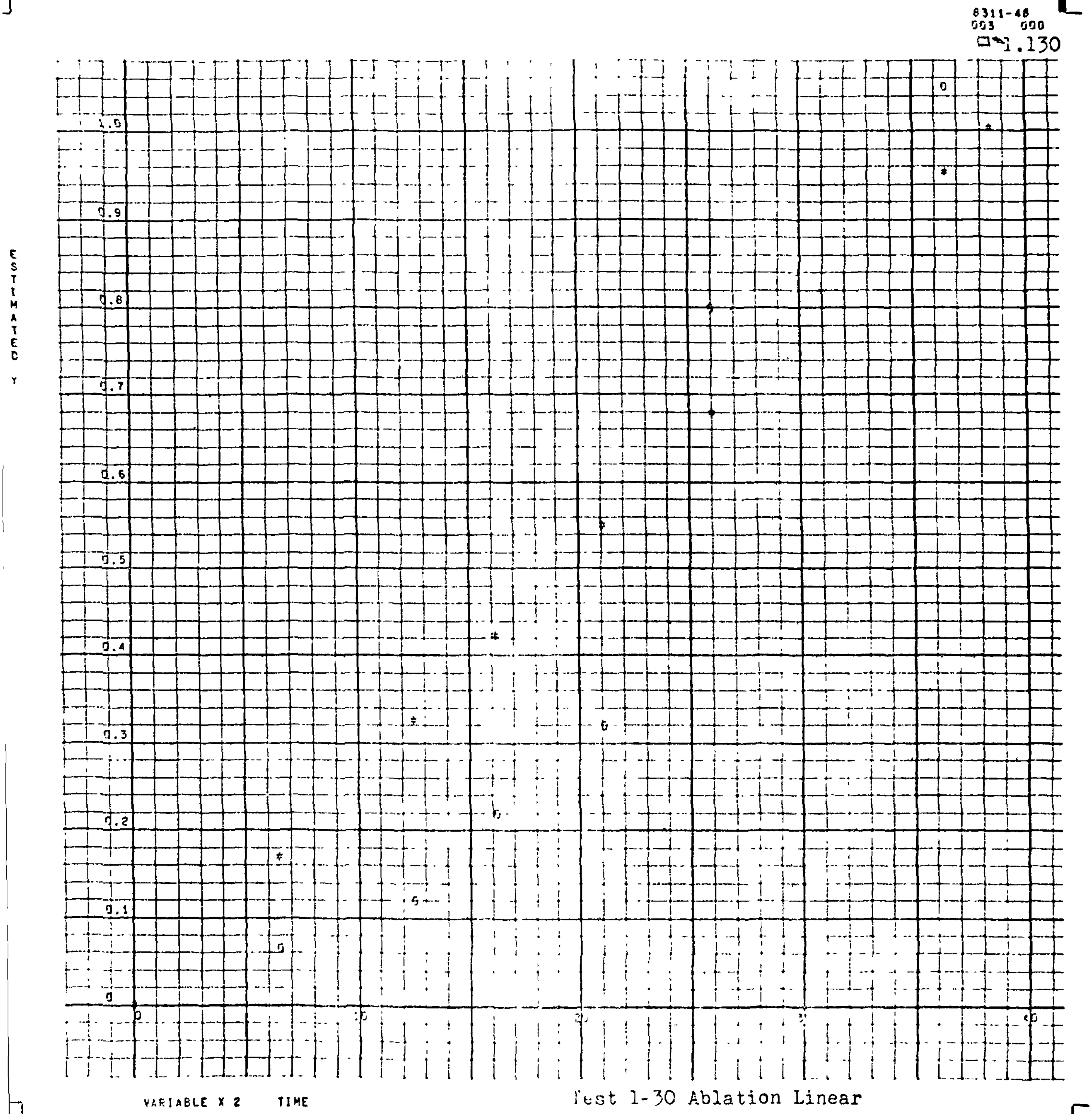

Test 1-30 Ablation Linear

0311-50
C93 000

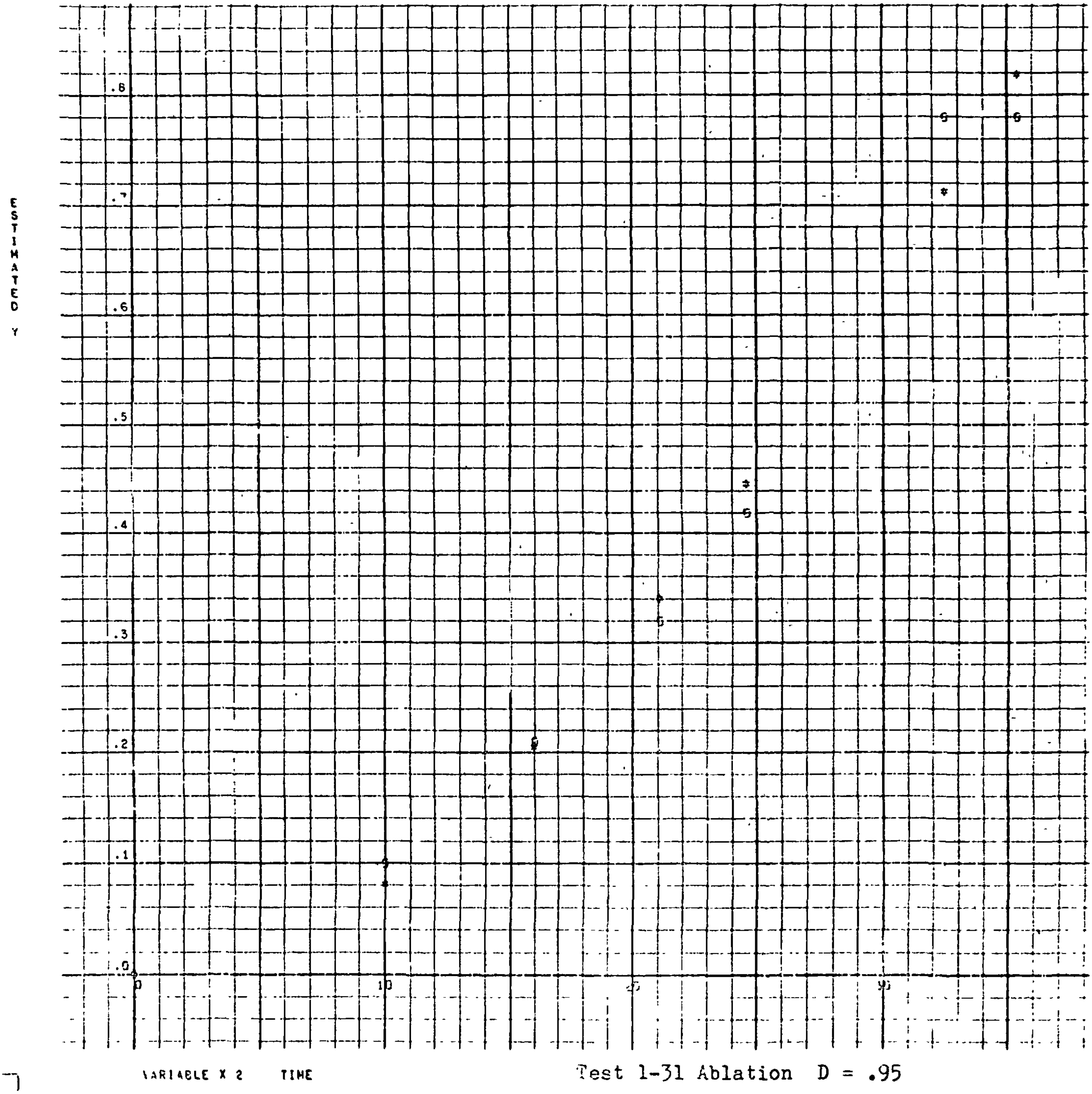

Test 1-31 Ablation D = .95

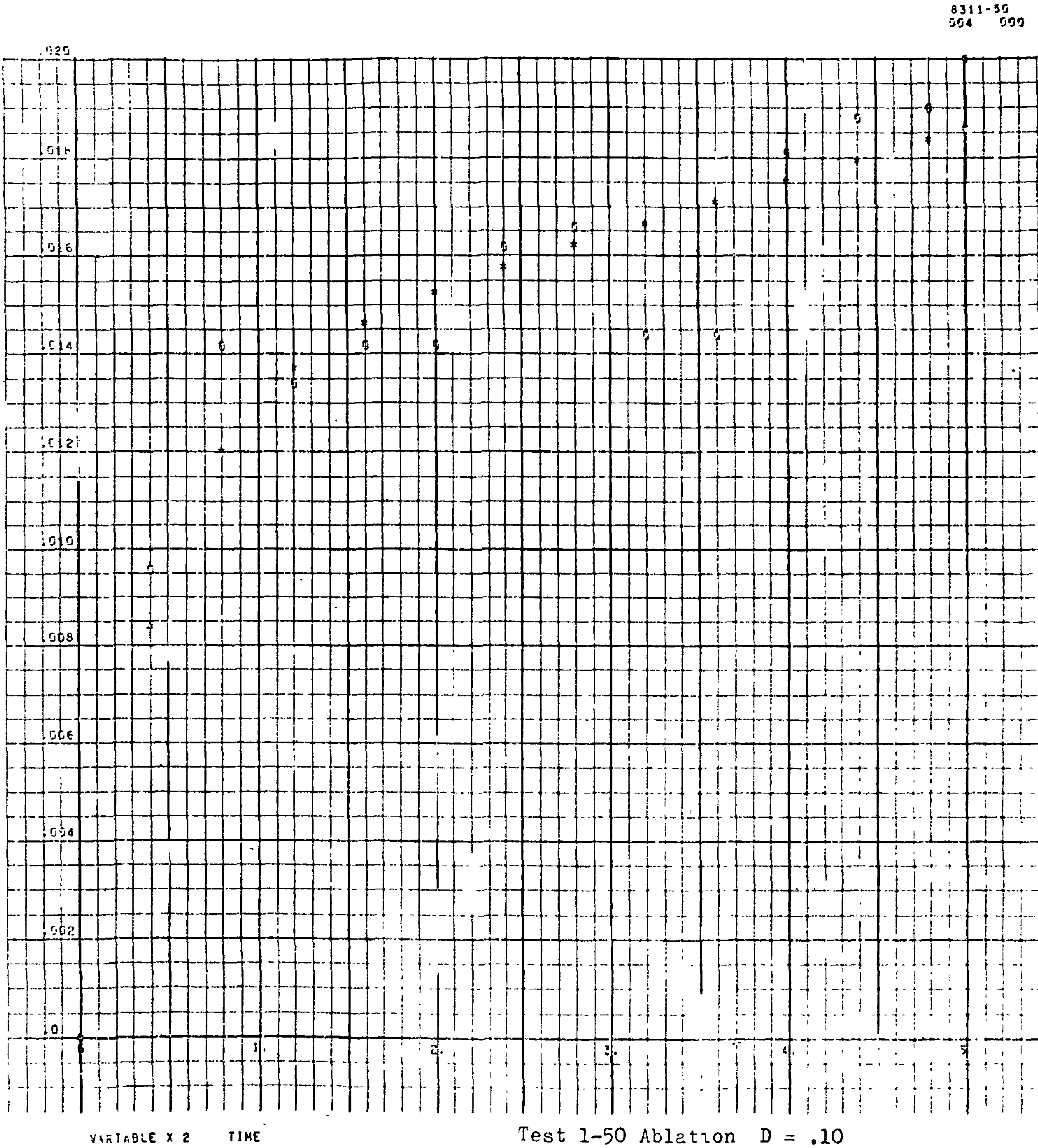

Test 1-50 Ablation D = .10

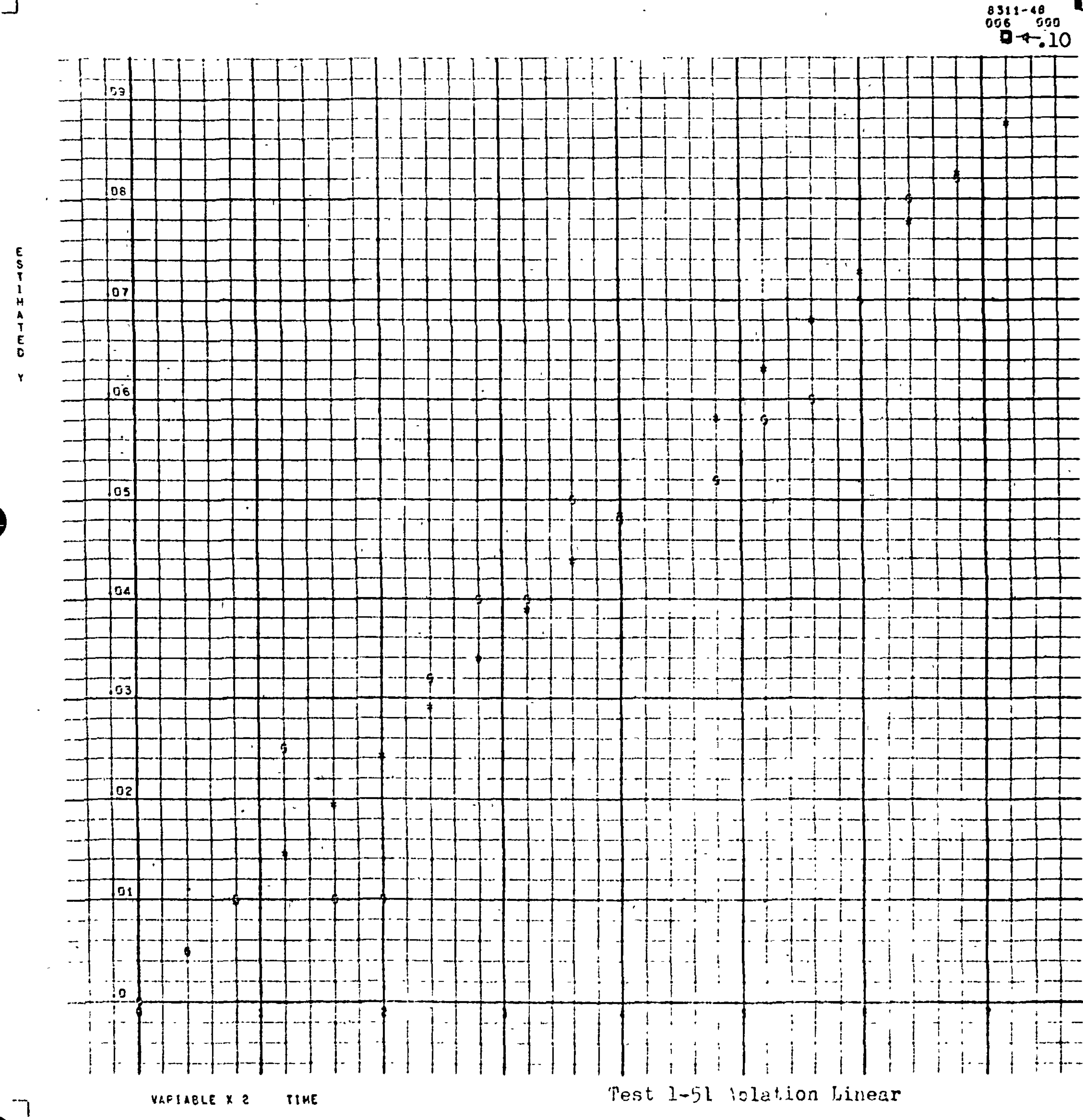

Test 1-51 Wolation Linear

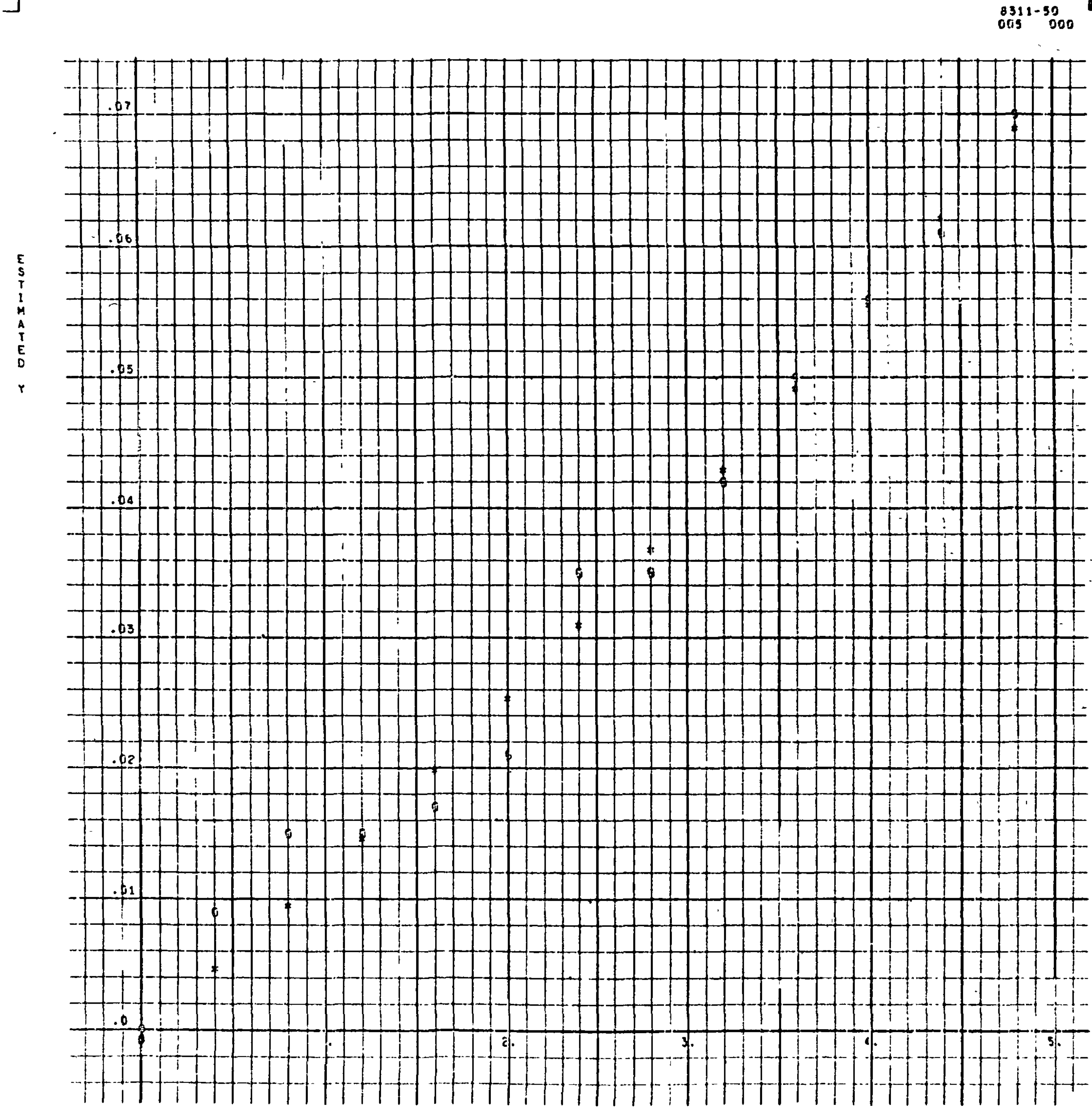

Test 1-52 Ablation D = .95

8111-50
519 000
□← .076

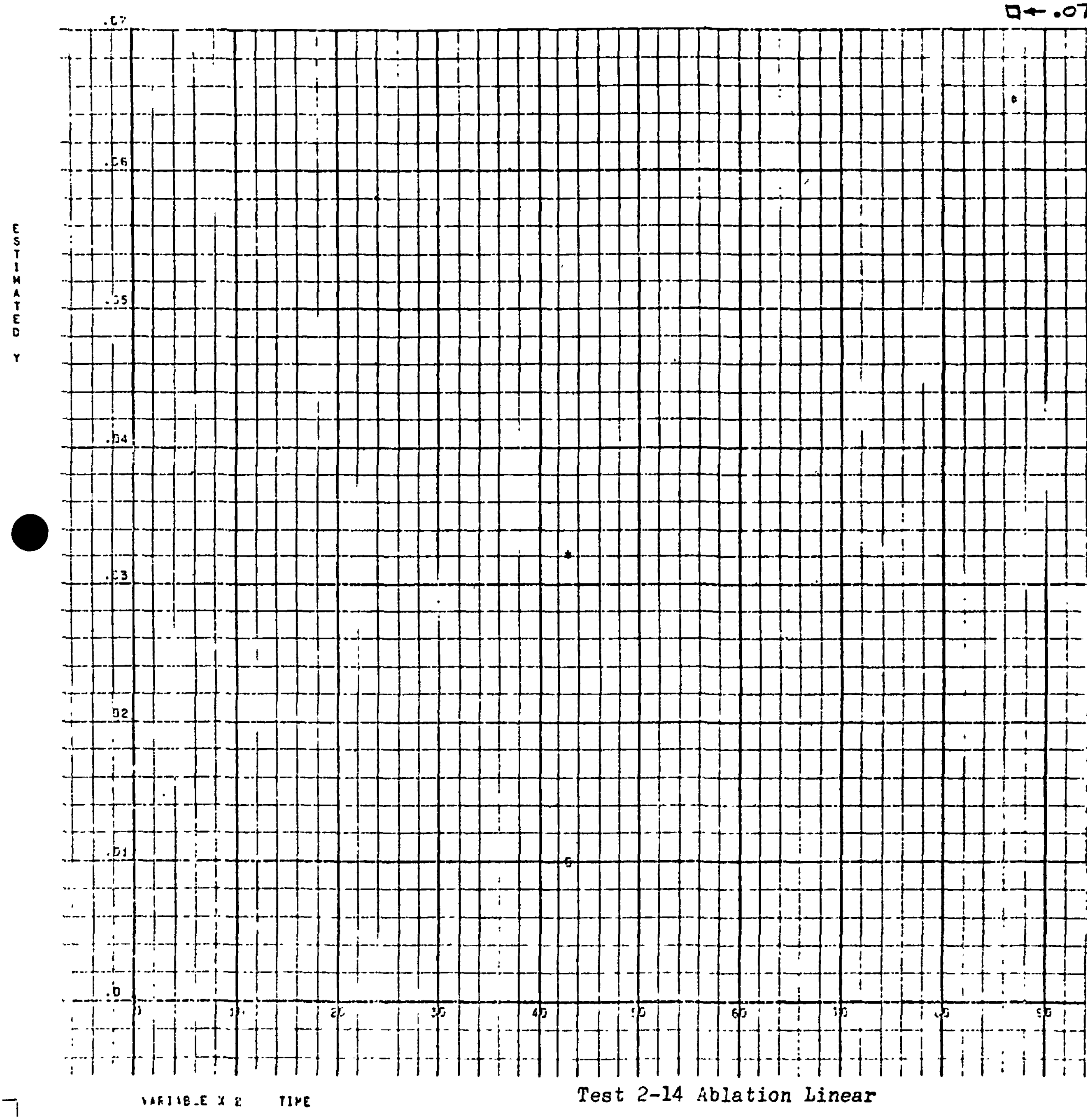

Test 2-14 Ablation Linear

8311-50
008 000

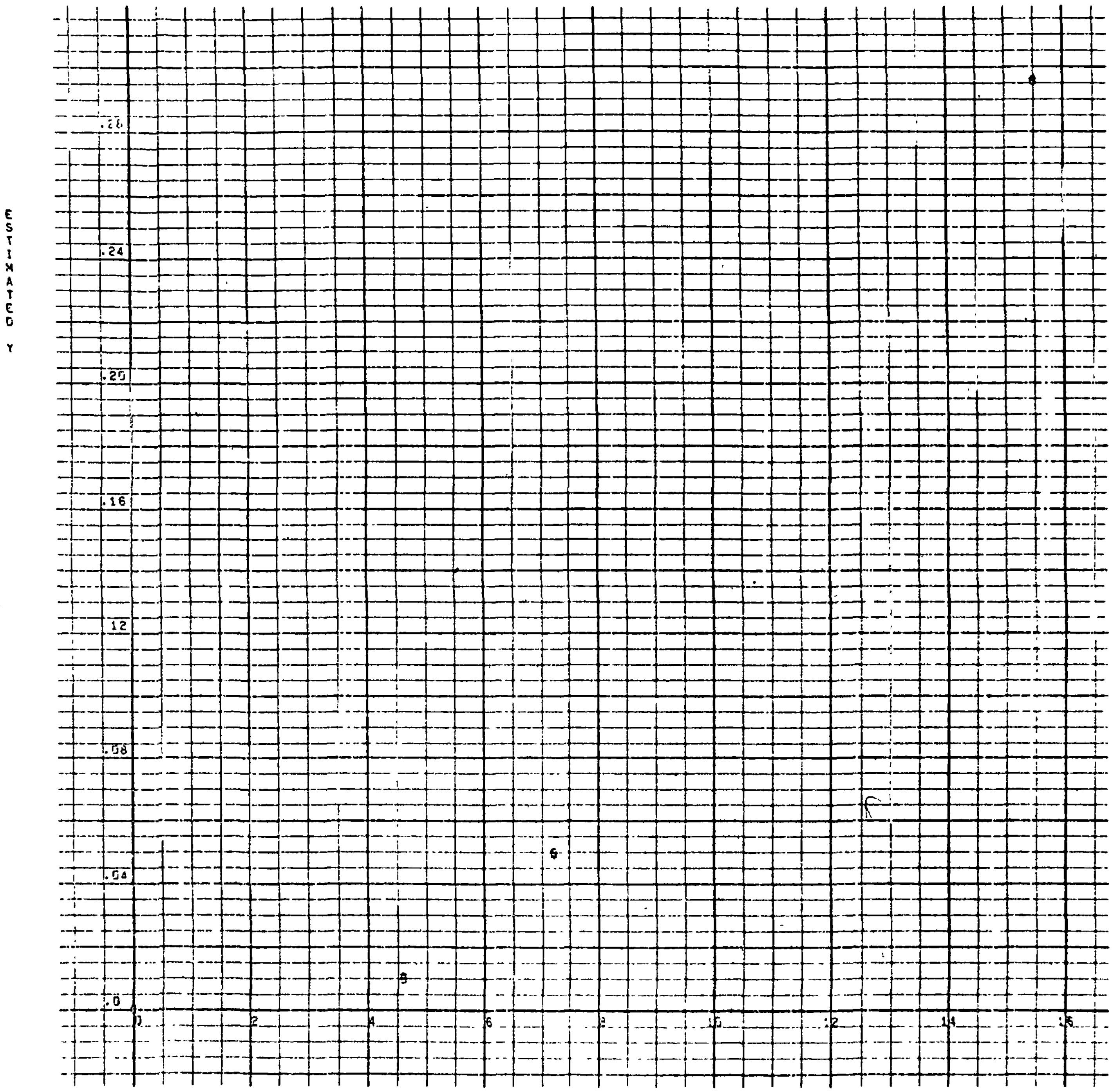

VARIABLE X 2 TIME

Test 2-21 Ablation D = .95

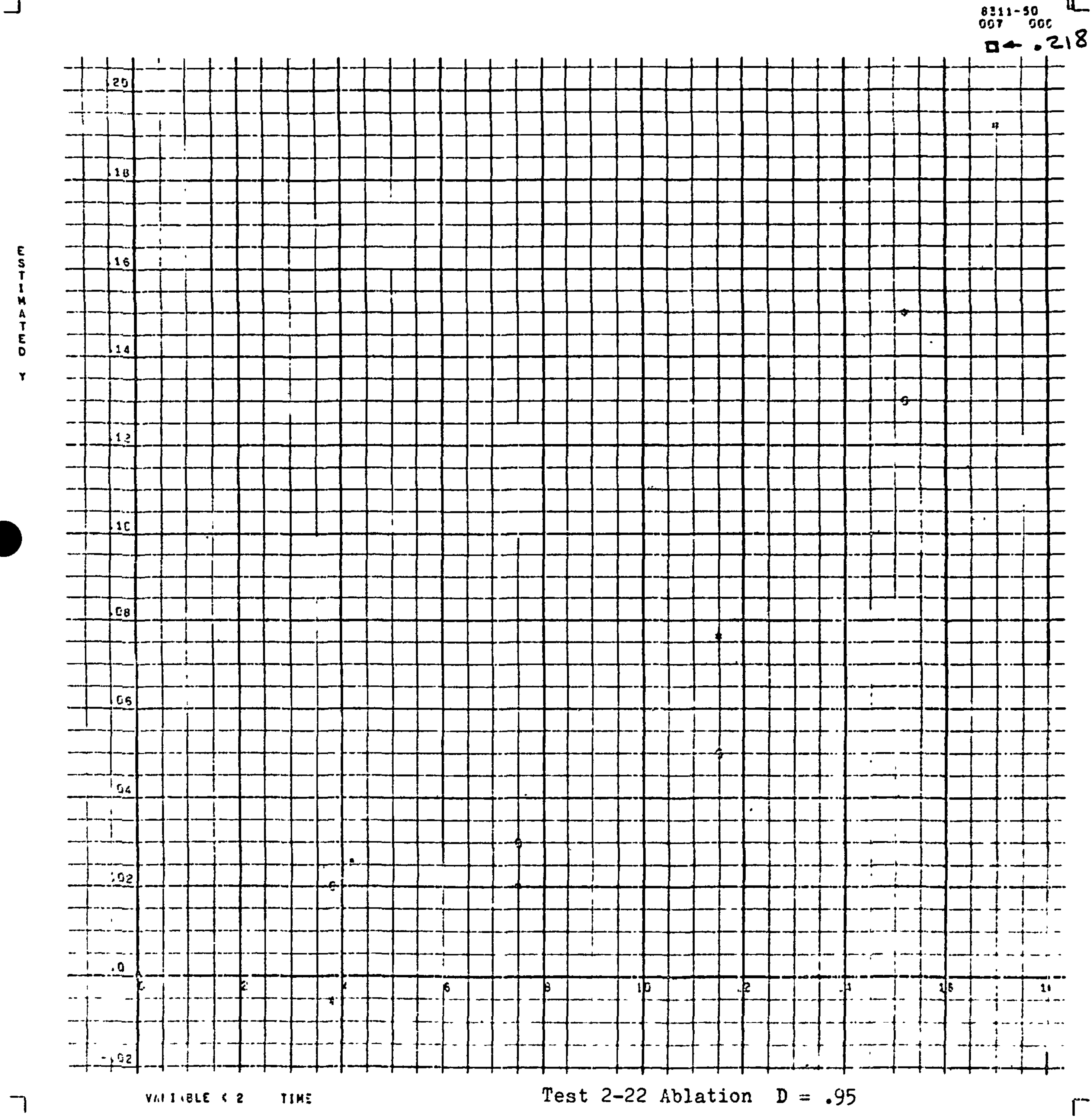

Test 2-22 Ablation D = .95

8311-50
008 000

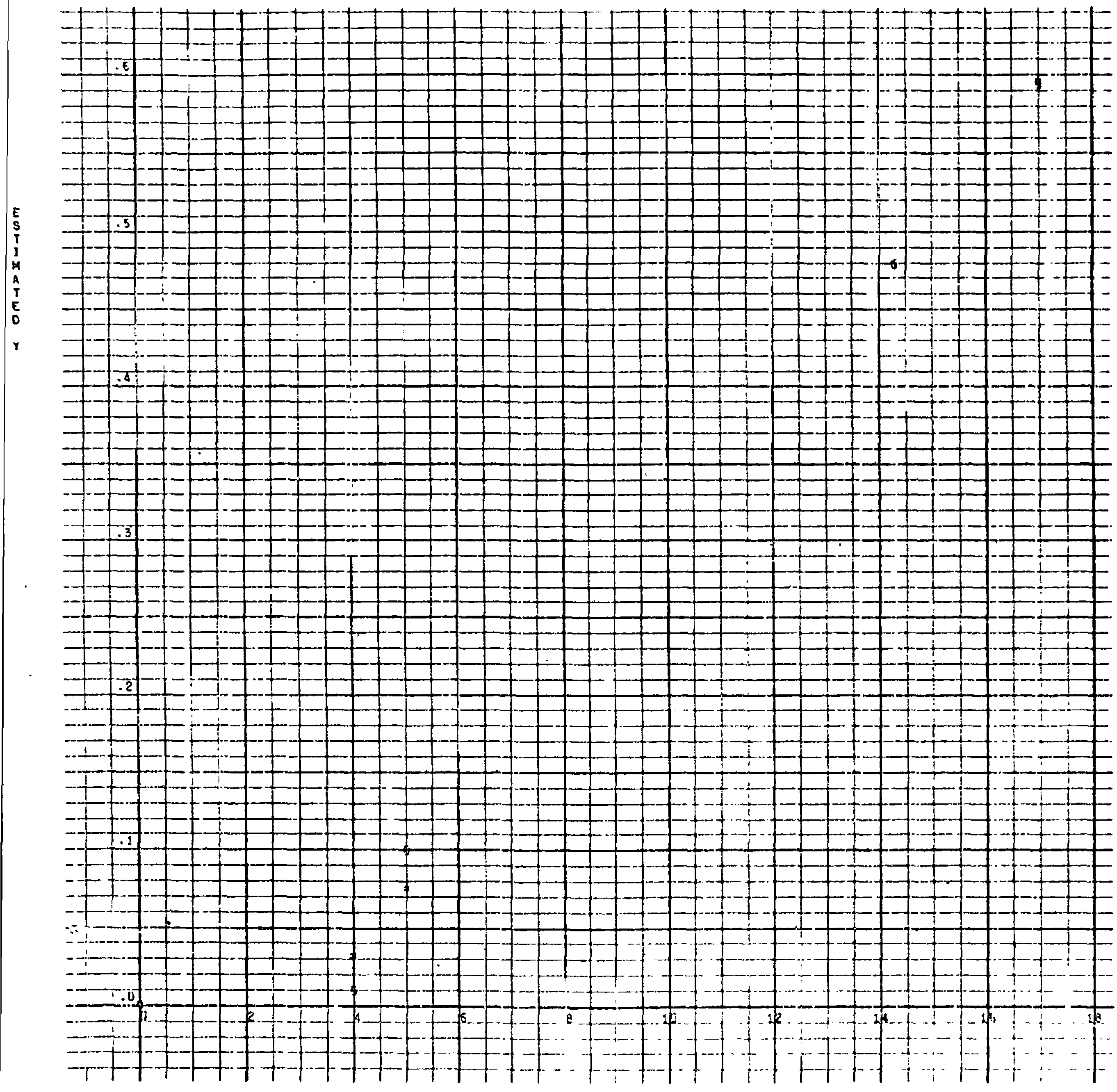

Test 2-23 Ablation D = .05

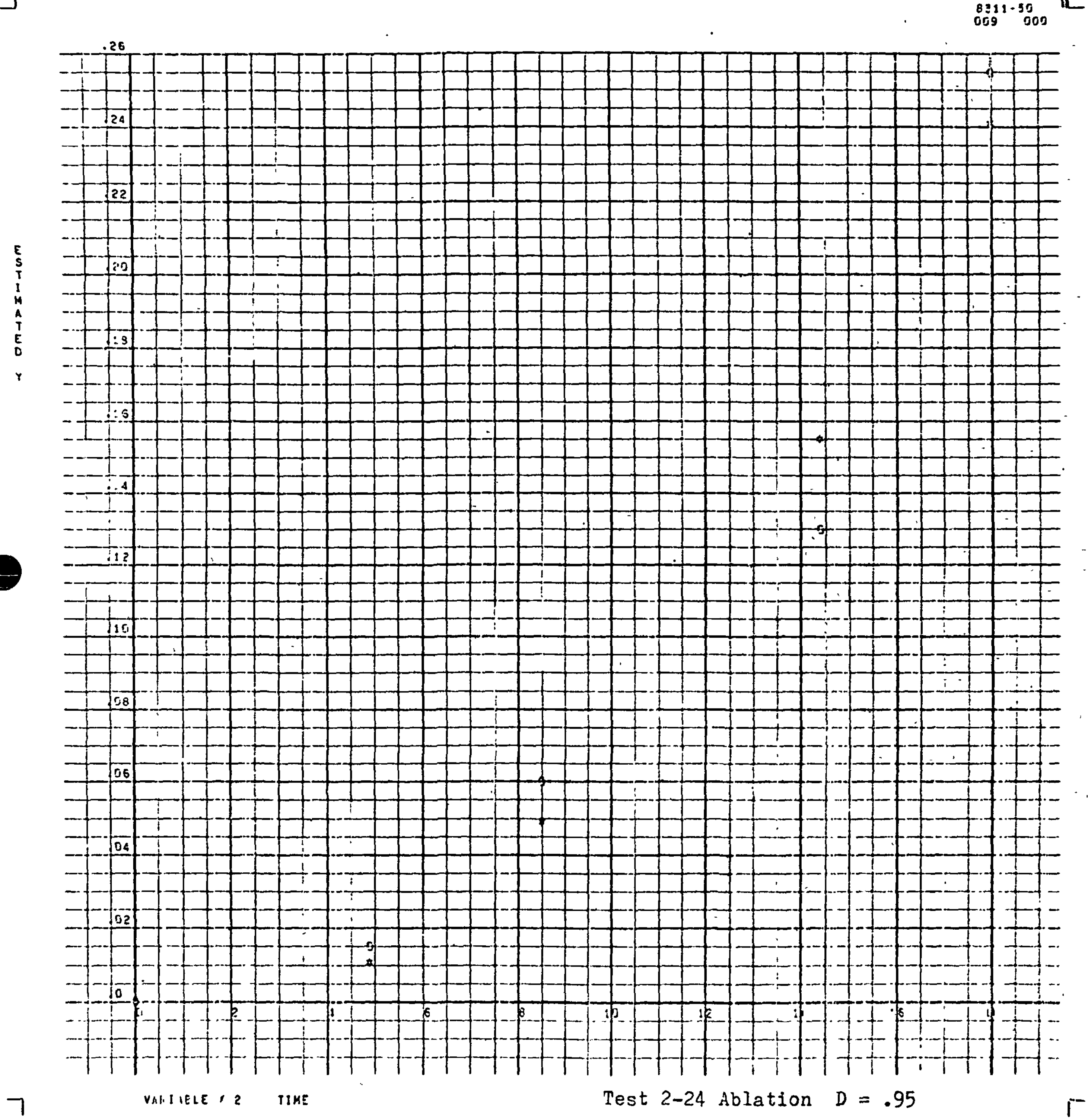

Test 2-24 Ablation D = .95

8311-50
0:5 000

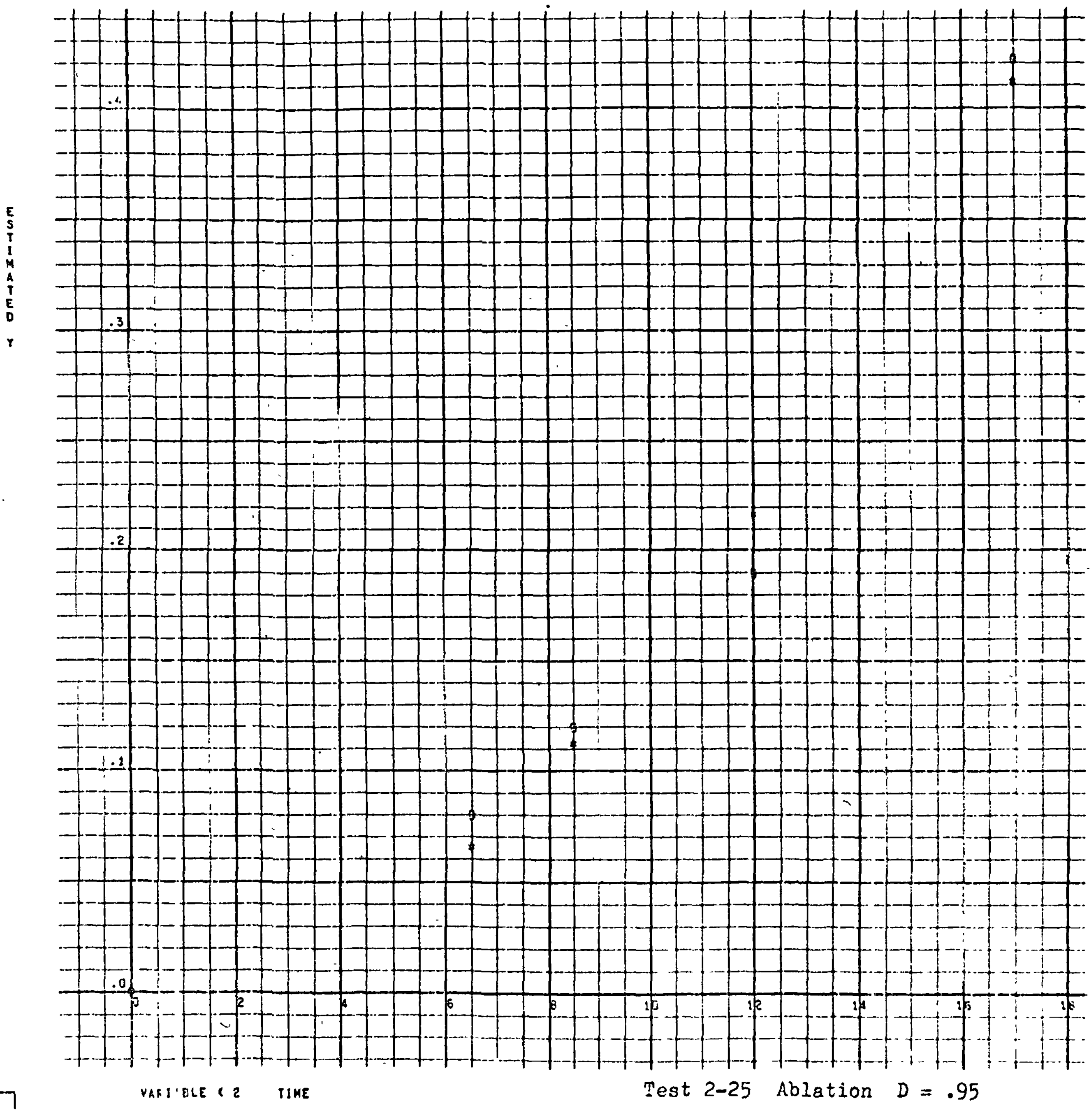

Test 2-25 Ablation D = .95

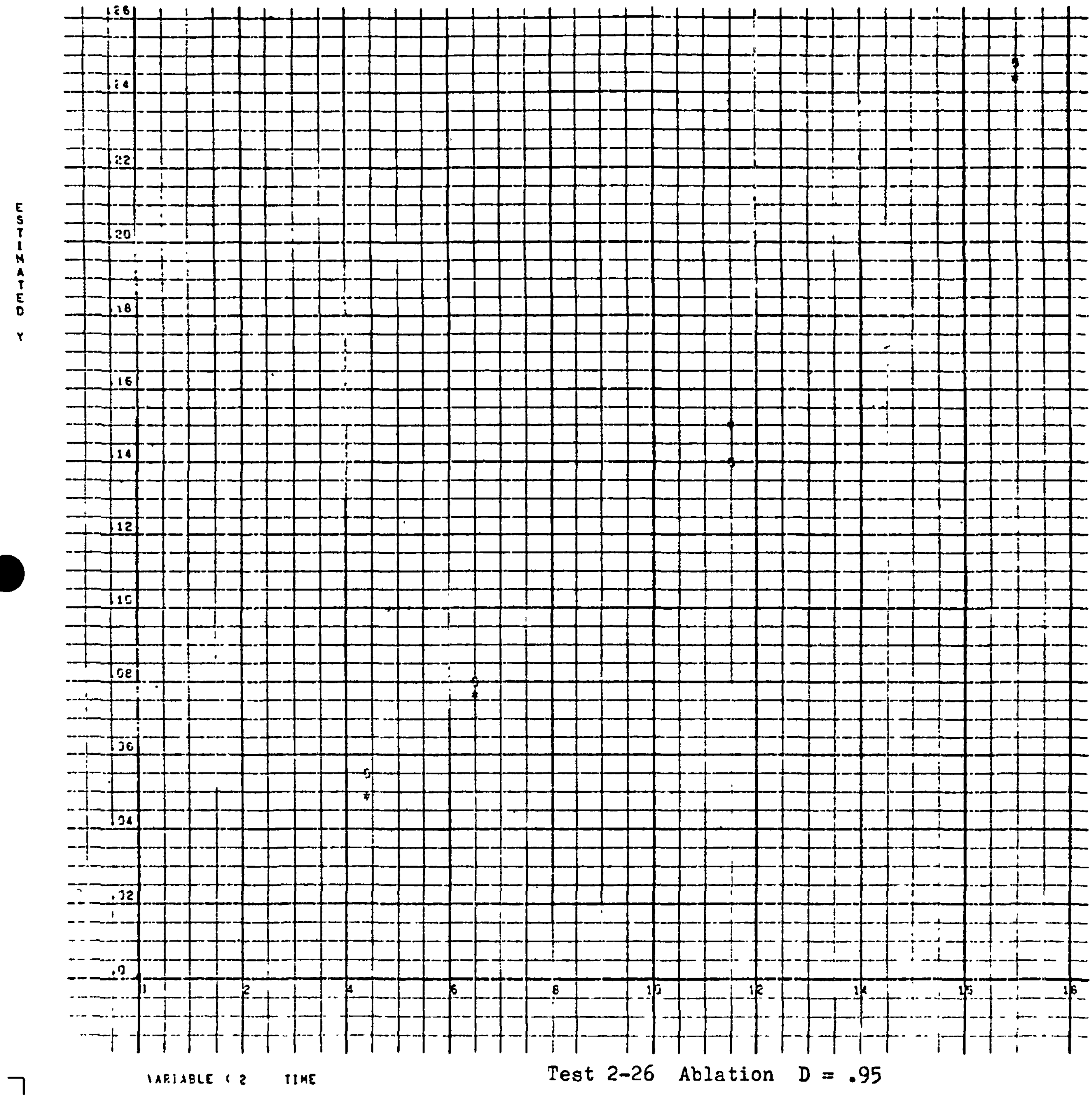

Test 2-26 Ablation D = .95

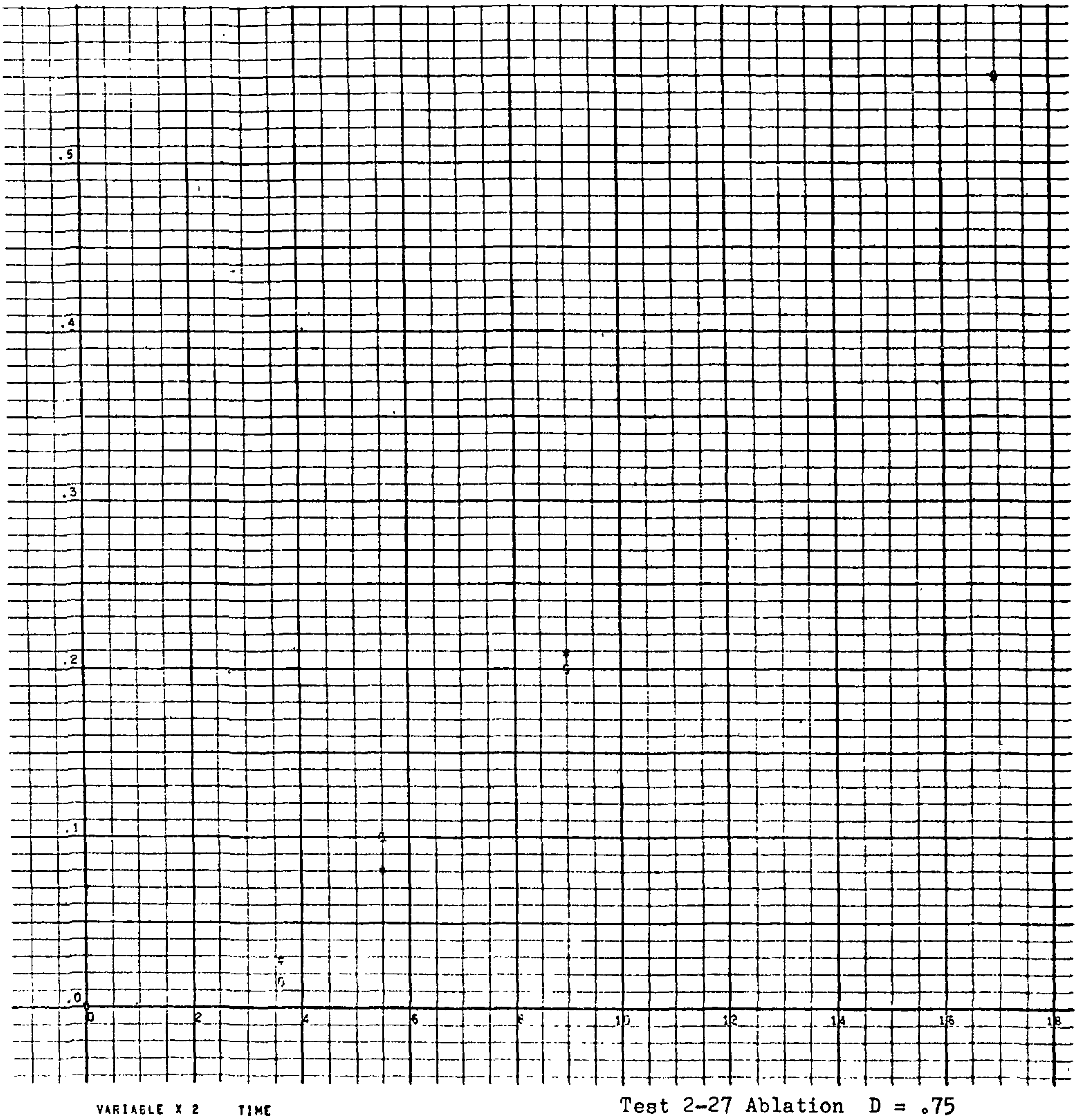

Test 2-27 Ablation D = .75

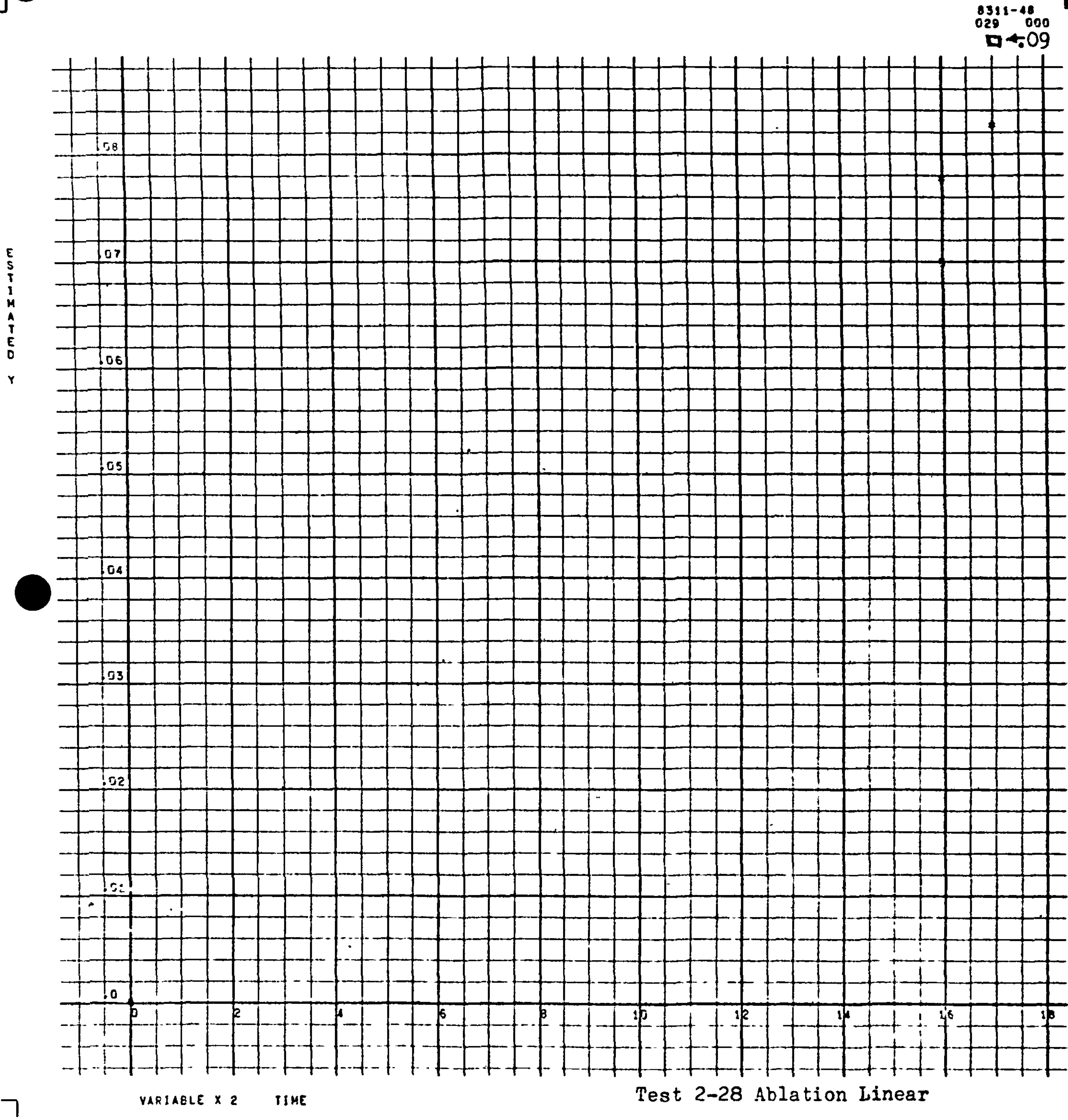

Test 2-28 Ablation Linear

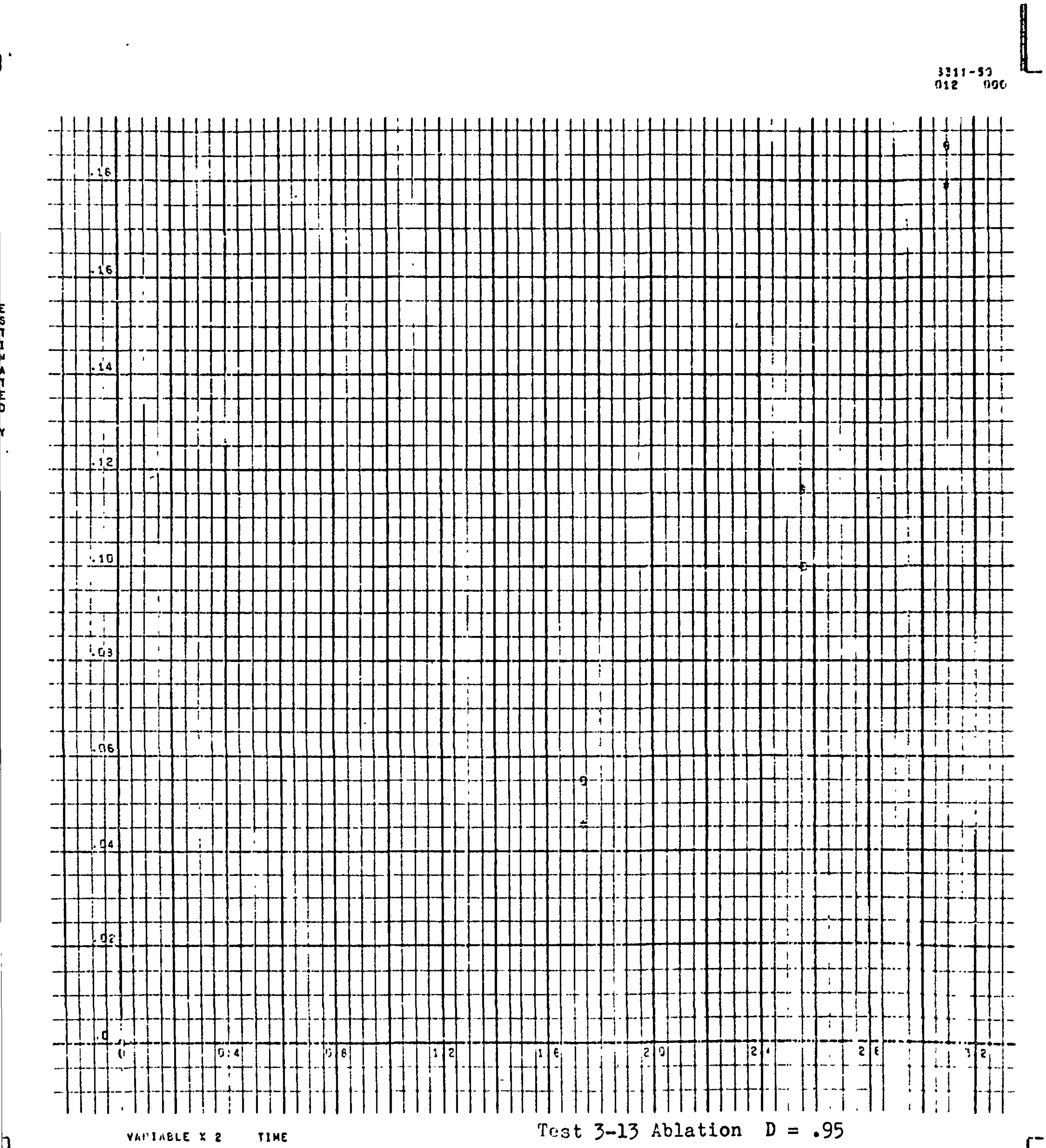

Test 3-13 Ablation D = .95

8311-48
015 000

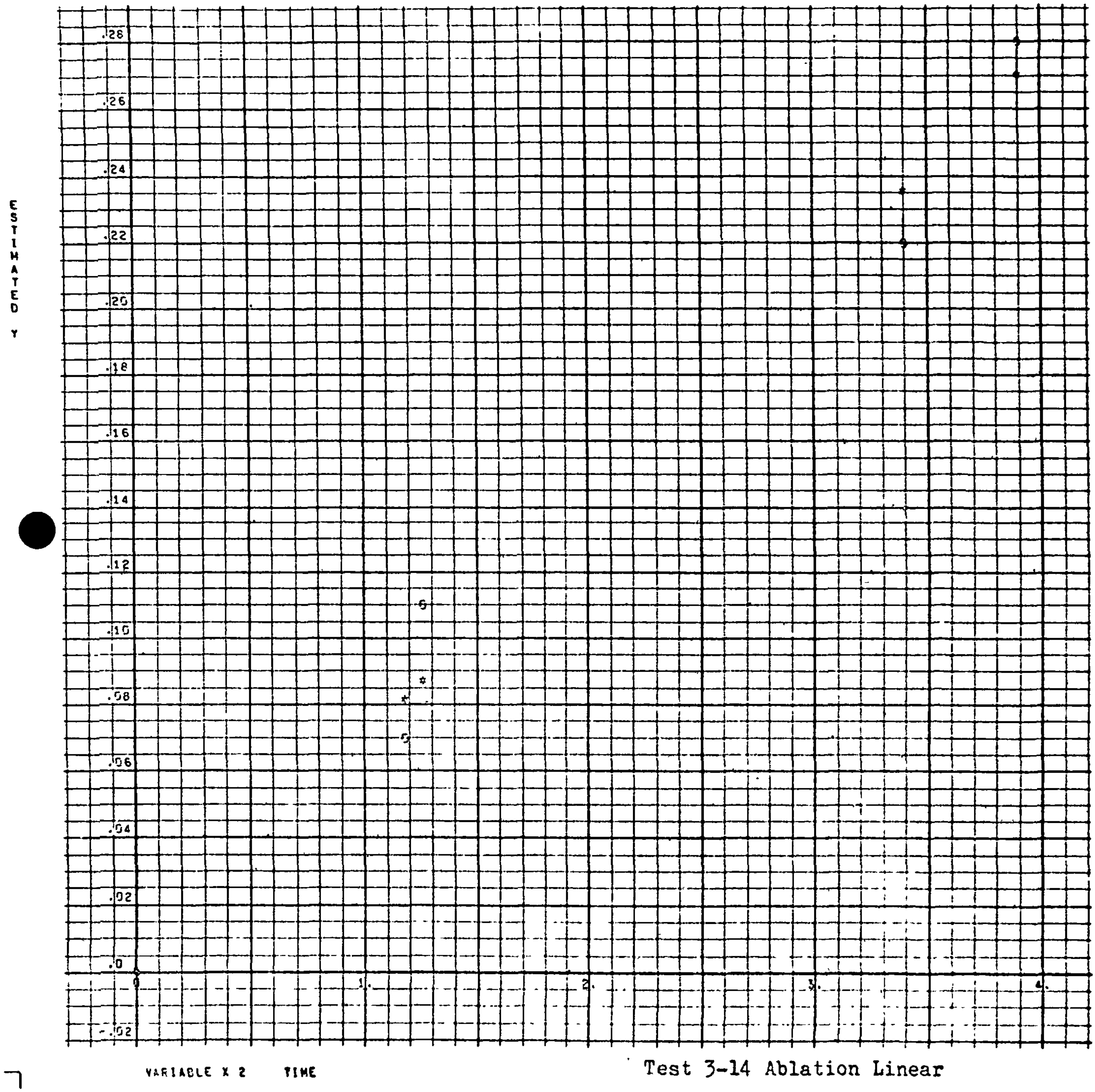

Test 3-14 Ablation Linear

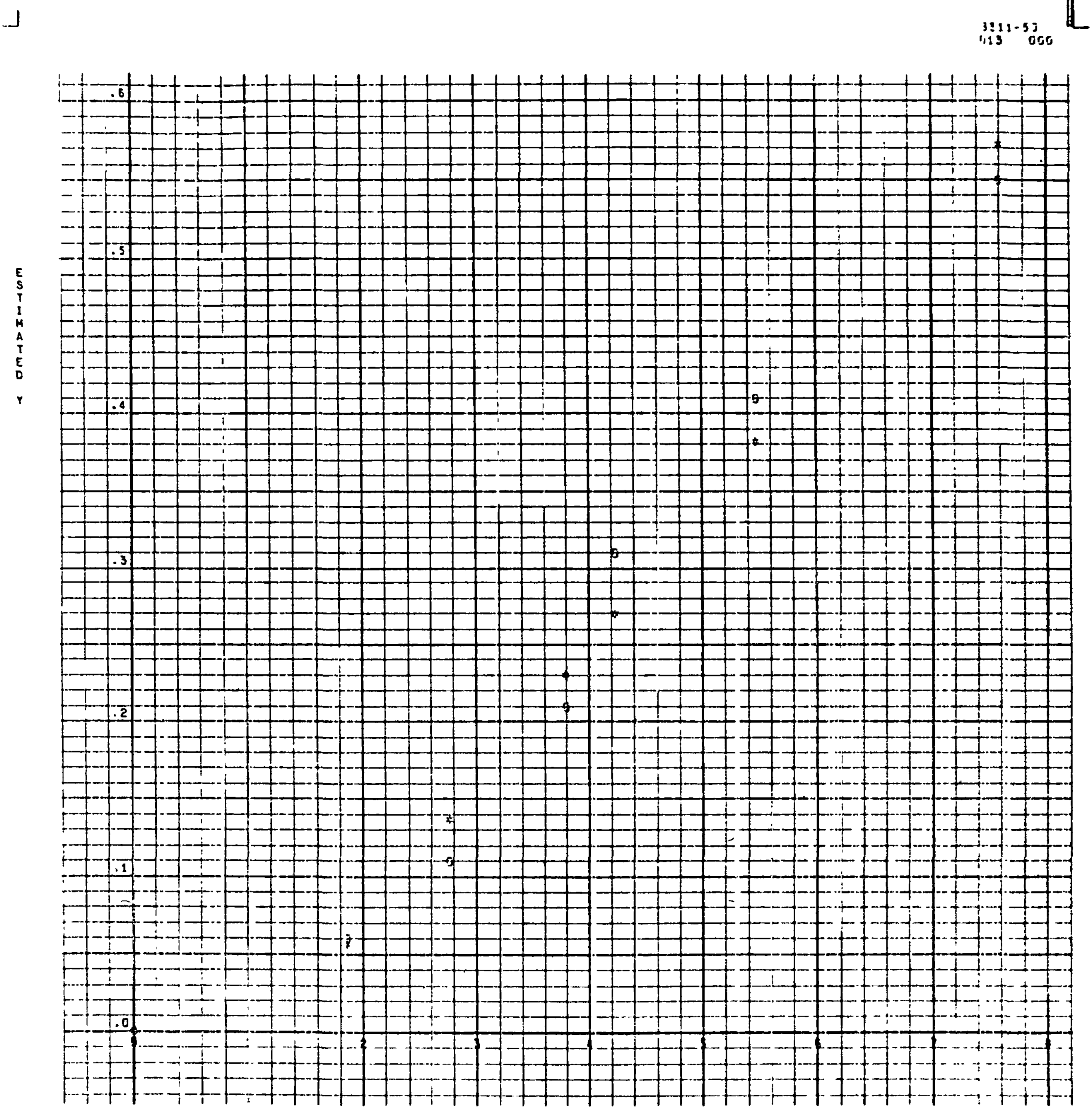

Test 3-15 Ablation D = .05

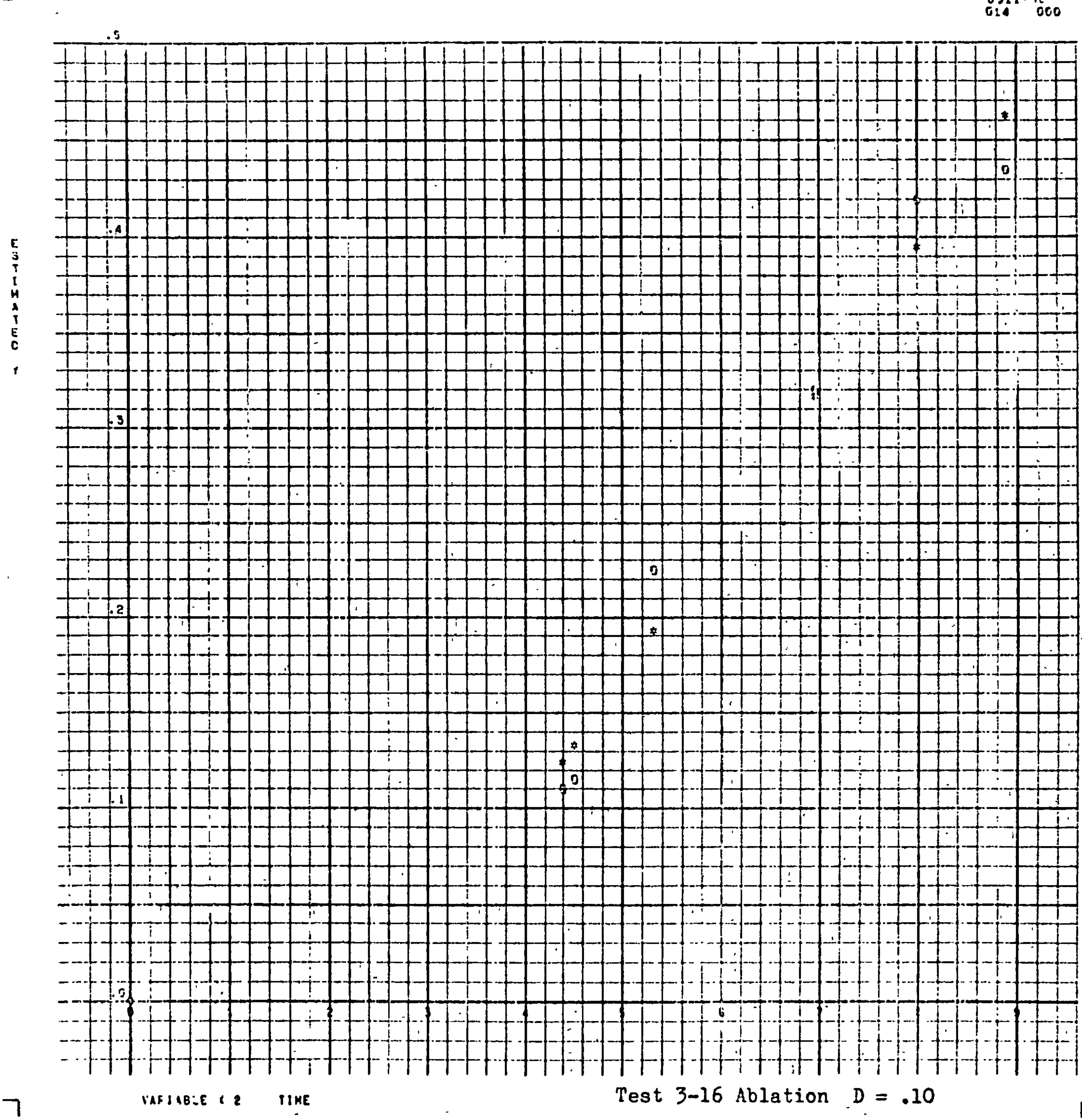

Test 3-16 Ablation D = .10

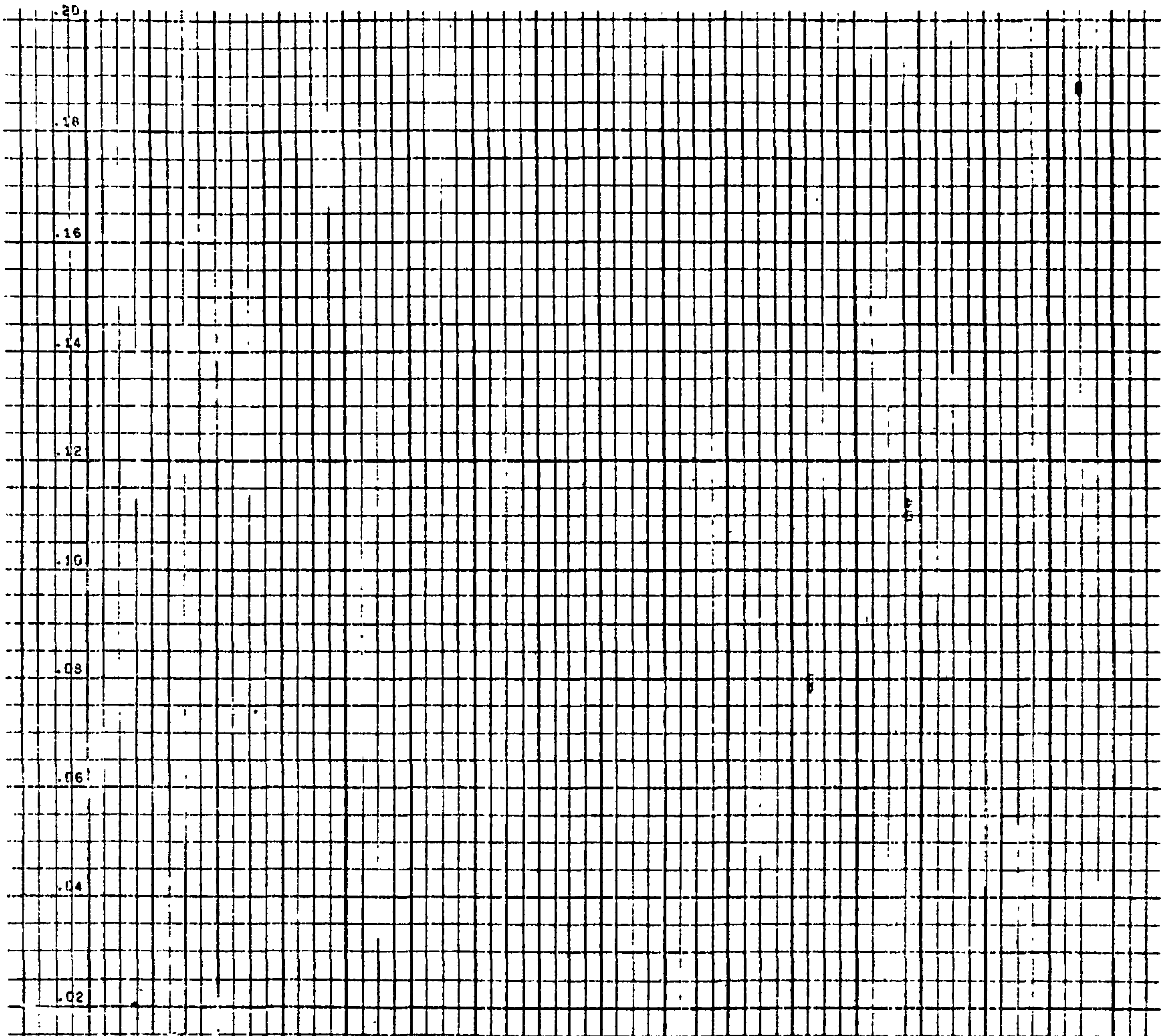

VARIABLE (2 TIME

Test 3-17 Ablation D = .95

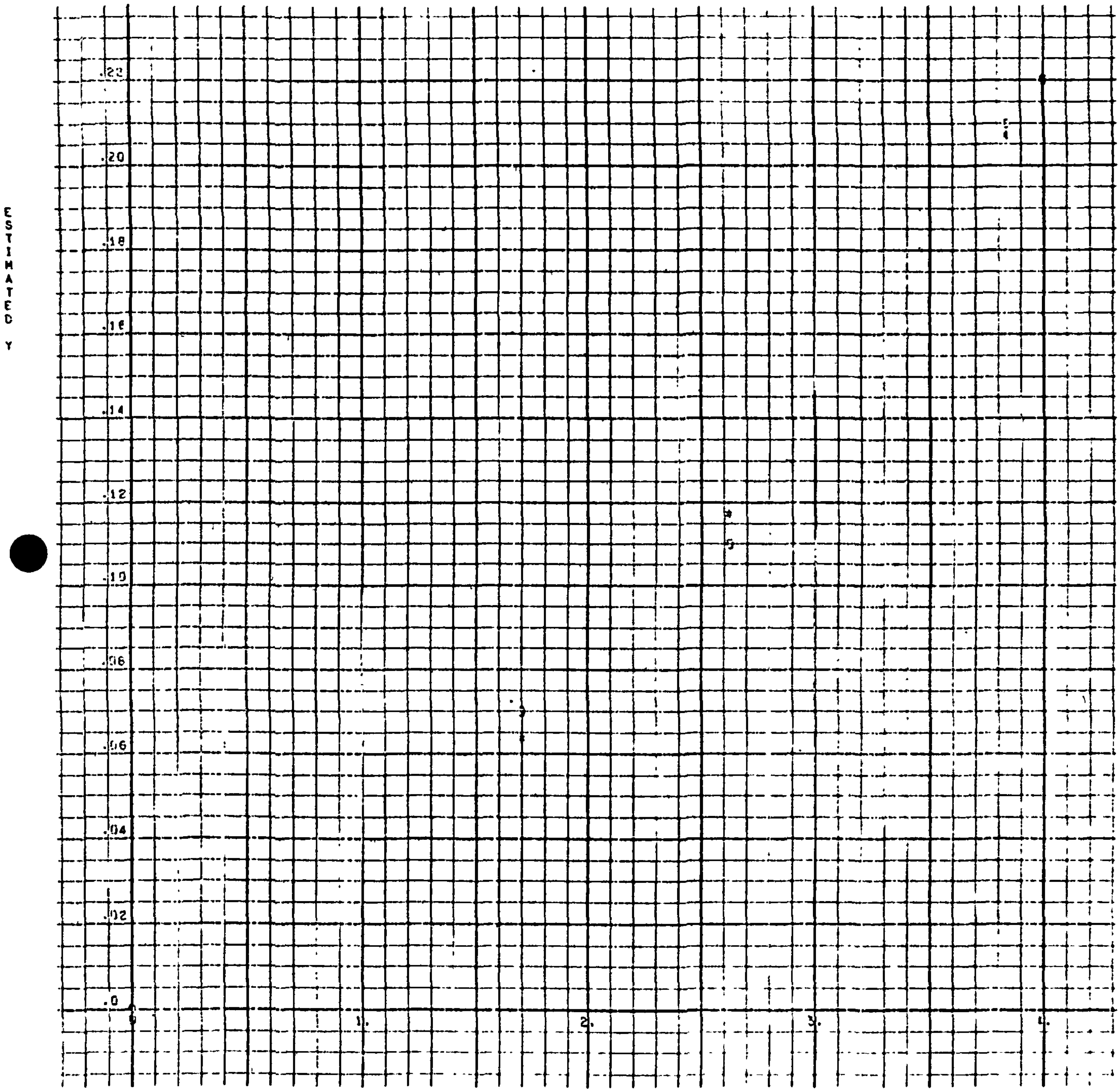

VARIABLE (2 TIME

Test 3-18 Ablation D = .95

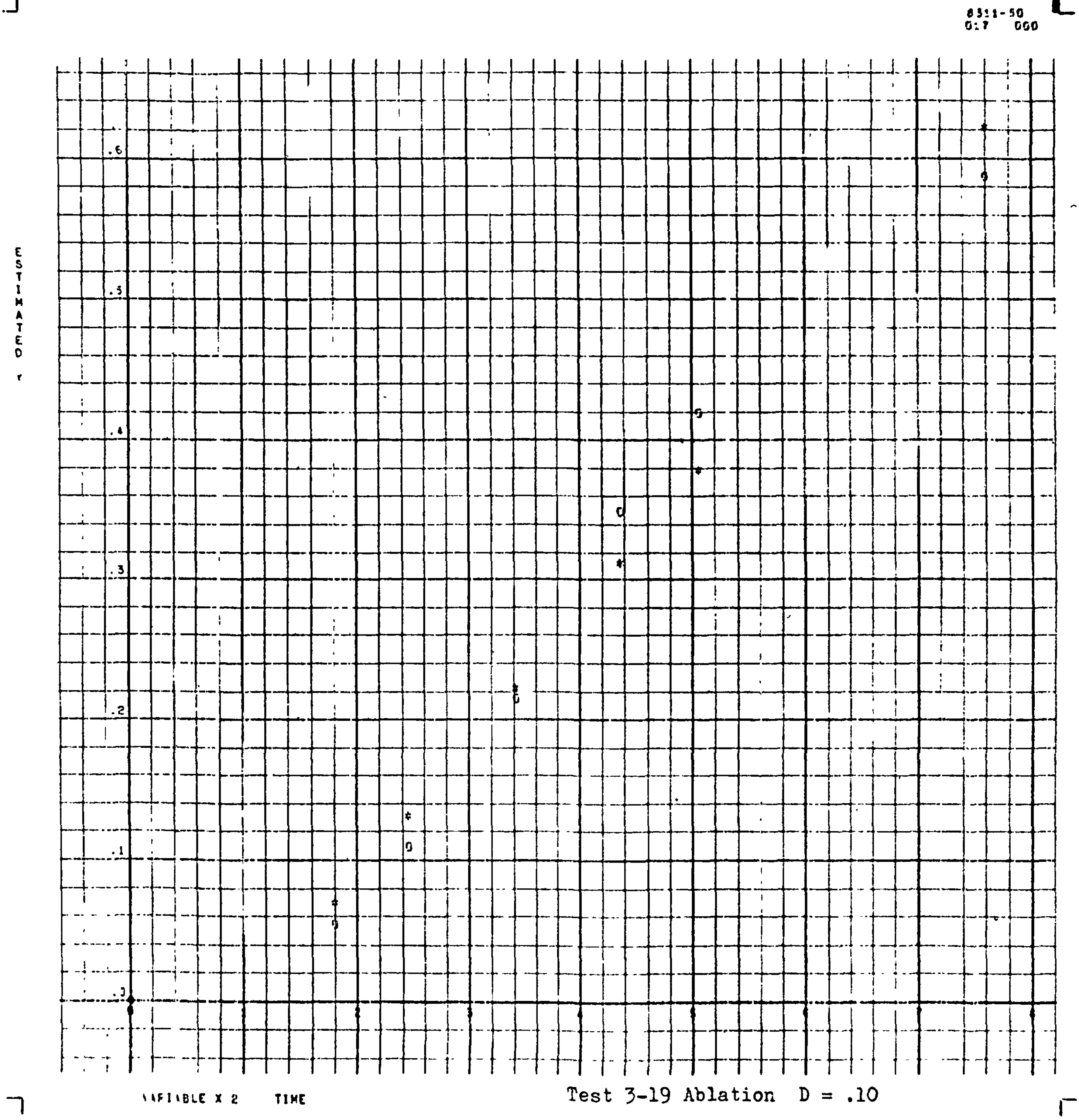

Test 3-19 Ablation D = .10

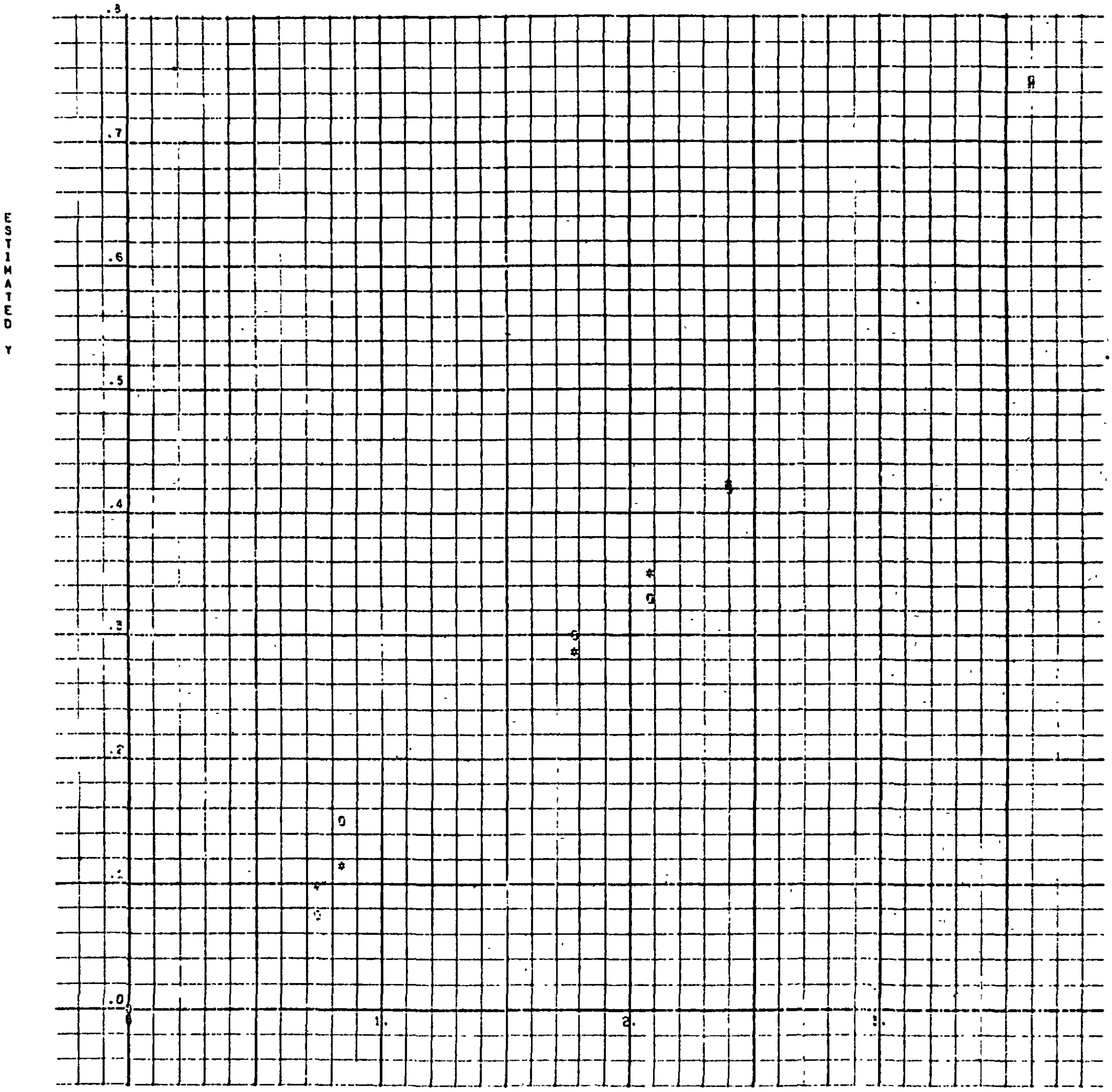

Test 3-20 Ablation D = .95